(NASA-CR-175856) JET FUEL INSTABILITY MECHANISMS Final Technical Report, 1 Aug. 1981 - 31 Mar. 1985 (Colorado School of Mines, Golden.) 104 p HC A06/MF A01
CSCL 21D G3/28

N85-28127

Unclas
21521

FINAL TECHNICAL REPORT

JET FUEL INSTABILITY MECHANISMS

by

S. R. Daniel

Colorado School of Mines

Department of Chemistry and Geochemistry

Golden, Colorado 80401

prepared for

National Aeronautics and Space Administration

Lewis Research Center

Grant NAG-3-197

1 August 1981 - 31 March 1985

CONTENTS

SUMMARY

The mechanisms of the formation of fuel-insoluble deposits were studied in several real fuels and in a model fuel consisting of tetralin in dodecane solution. The influence of addition to the fuels of small concentrations of various compounds on the quantities of deposits formed and on the formation and disappearance of oxygenated species in solution was assessed. The effect of temperature on deposit formation was also investigated over the range of 308-453°K.

Condensation reactions of oxidation products of 1-tetralone lead to solid deposits from the model fuel. These processes, as well as the reactions generating the oxidation products, are susceptible to catalysis by Lewis bases and Lewis acids (metal ions). That the catalysts persist in the fuel phase following deposition was definitely established in some cases. In others, catalytic effects on solution-phase composition persisted after the catalyst had been depleted in the liquid phase. Organosulfur compounds influence stability via base catalysis of condensation reactions, stabilization of soluble deposit precursors, or both. Metals influence via dissolution and alteration of condensation reactions through complexation of oxygenated intermediates by the metal ions. Solvent effects (dielectric constant, O_2 uptake) are important in the deposit-forming processes.

The deposits from the model fuel are complex solids containing carbonyl, alcohol, and acidic functional groups. The average molecular weight of deposits in solution corresponds

approximately to trimerization of tetralone monomeric units. The linkages in the deposit are cleaved by hydride. While the exact nature of the deposits changes over the temperature range studied, no changes in solution phase species are observed.

Many similarities in the deposition process, and in the effects of added compounds on deposition, in the real fuels to that in the model fuel were observed. An HPLC method for relating deposition to solution-phase composition was developed. Thereby, some added compounds were shown to alter deposition rates via alteration of the rates of oxidation of fuel hydrocarbons, and others by changing the rates of conversion of oxidation products to insoluble deposits. Some added compounds affect deposition in more than one mode.

INTRODUCTION

The mechanisms of jet fuel instability were investigated under grant NAG-3-197. Degradation reactions of several real fuels, of a model fuel consisting of tetralin + dodecane, and of the pure compound, α-tetralone, were studied. The objective was elucidation of mechanisms in the formation of non-volatile components (deposits) in jet fuels.

While fuel stability has been the subject of many investigations, the basic chemistry involved remains incompletely defined. Early studies of gasoline storage stability lead to identification of autoxidation of fuel hydrocarbons as the initial step in formation of "gums" (ref. 1-2). While subsequent reactions of the hydroperoxides resulting from autoxidation were assumed responsible (ref. 3), the mechanistic details are not known. The extent of deposit formation was found to parallel peroxide concentration but to be independent of concentrations of acids and aldehydes (ref. 4-6), which result from peroxide decomposition.

The presence of easily oxidized hydrocarbons (alkylaromatics, olefins) was found to decrease stability (ref. 7-8). Trace heteroatomic components were also found to exert strong influence (ref. 8). Elemental sulfur, H_2S, thiols, sulfides, and disulfides were depleted in gasoline during storage; however, thiophenes and residual sulfur compounds were not. Substantial quantities of sulfur and nitrogen were found in the gums (ref. 9).

In distillate fuels, where heteroatom content is generally

higher, even greater influence has been attributed to these constituents. Direct autoxidation of the heteroatomic species as well as condensation reactions of the heteroatomics with products of hydrocarbon autoxidation have been suggested as the processes leading to formation of deposits (ref. 7, 10-12). Taylor and Frankenfeld have identified polymeric oxidation products of 2,5-dimethylpyrrole in deposits formed from distillate fuels to which high concentrations of 2,5-dimethylpyrrole were added (ref. 13,14). However, previous studies in our laboratory have shown that at lower concentrations, pyrroles have little influence on stability (ref. 15-16). Metal surfaces in contact with the fuel have also been reported to influence stability (ref. 17-18).

Thermal instability, the formation of non-volatile deposits on heated surfaces in an operating engine, has been even less systematically treated. Dukek (ref. 19) has suggested that autoxidation of hydrocarbons remains the process responsible for instability. Similarities in elemental composition of storage and thermal deposits (ref. 20) and in their appearance (ref. 21) have been noted. Sulfur compounds (ref. 22-23), soluble metal compounds and metals surfaces (ref. 24), olefins (ref. 25), and peroxides and dissolved oxygen (ref. 19) have been identified as contributing to thermal instability. These generally correspond to factors leading to poor storage stability as well. However, antioxidants which effect improvement in storage stability generally have no beneficial influence on thermal stability (ref. 26-28) and lack of any correlation of measurements of thermal stability with those used to evaluate storage stability has been

reported (ref. 18).

Therefore, despite the accumulation of a substantial body of observations on the factors which influence stability, delineation of specific chemical processes has not been achieved. Analysis of storage and thermal deposits has produced only rudimentary information concerning the nature of these products of the deposition reactions (ref. 29) and attempts to identify specific reactant species in the complex mixture present in a real fuel have been unsuccessful. Clearly, mechanisms must be sought in less-complex model systems and then be extended to real fuels.

In earlier work in our laboratory (ref. 29) a model fuel was developed which mimics many of the stability characteristics of jet fuels. A 1:10 (V/V) solution of tetralin in n-dodecane forms deposits very similar in compostion and properties to those obtained from jet fuels under identical conditions. Additions of low concentrations of various compounds (Figures 1 and 2) were found to influence deposition in this model fuel in fashion analogous to that found for a Jet A fuel (ref. 15,29). Autoxidation of tetralin is a facile process which has been prevously studied in various media (ref. 30) and some decomposition products of the hydroperoxide have been identified (ref. 31-33). Preliminary results in that project suggested the importance of base-catalyzed condensation reactions of α-tetralone and α-tetralin hydroperoxide in deposit formation in this model system (ref. 29).

In this study, additional information on the mechanism(s) of the formation of deposit in the model fuel was sought. In

addition, parallelisms and departures between the model fuel and real fuels were explored. The following specific investigations were performed:

1. Development of a method for estimating basicity of organosulfur compounds to enable investigation of the relationship between influence of a sulfur compound on fuel stability and its basicity.
2. Determination of the effects of cupric and ferrous laurates and the metals on deposition rates in Jet A and in the model fuel.
3. Determination of the effects of Cu, Fe, and their laurates on the rates of formation and consumption of soluble deposit precursors in the model fuel.
4. Study of ERBS instability with the fuel in contact with copper plates maintained at potential difference of 10-50 volts.
5. Testing of an HPLC method for quantifying instability in real fuels.
6. Comparision of degradation of a Jet A and of a shale-derived JP5 at 353°K, 393°K, and 453°K.
7. Determination of the effect of repeated stressing (deposit removed via filtration) on stability of Jet A and shale JP5.
8. Evaluation of the stability of blends of Jet A and ERBS fuels.
9. Analysis of the fuel phase of various fuels and pure compounds which had been previously stressed in a JFTOT.
10. Study of the degradation of tetralin in a perfluoroalkane

medium at 393°K.

11. Evaluation of the influence of 4 nitrogen and 2 sulfur compounds on the stability of Jet A, shale JP5, and model fuel. The fate of the added heteroatomic compounds during fuel stressing was monitored via GC/MS.
12. Determination of the effect of added tetralone on deposition in Jet A.
13. Study of the influ nce of free-radical initiators and inhibitors on deposiion in the model fuel.
14. Investigation of the reaction of tetralone with tetralin hydroperoxide under a CO_2 atmosphere.
15. Study of the behavior of 1,2- and 1,4-naphthoquinones in dodecane medium.
16. Study of tetralone autoxidation in dodecane and neat.
17. Analysis of tetralone autoxidation products.
18. Comparison of model deposits with solids formed in tetralone/dodecane oxidation.
19. Derivatization of model and tetralone oxidation products via diazomethane, methanol/HCl, and $LiAlH_4$ treatments.
20. Preliminary study of deposit formation in tetralin and indane solutions in several normal alkanes.
21. Pyrolysis/mass spectrometry comparison of deposits from different fuels and different conditions via pattern recognition methods.
22. Characterization of model and real fuel deposits via instrumental (GPC, HPLC, IR, NMR, GC/MS, Py/MS, elemental analysis) and wet chemical methods.

EXPERIMENTAL WORK

All experimental work described was conducted in the laboratories of the Department of Chemistry and Geochemistry at the Colorado School of Mines. Solid-state NMR analyses were provided by the NSF Regional NMR Center at Colorado State University. Solution phase ^{13}C-NMR analyses were performed by Dr. Calvin Curtis at the Solar Energy Research Institute. Some of the quantitative Cu analyses were provided by Natural Resources Laboratory of Lakewood, Colorado.

Chemicals and Materials

Fuels. Jet A, ERBS, and shale-derived JP5 fuels were obtained from the Lewis Research Center. The Jet A was a commercial, petroleum-derived product containing 14.0% H and boiling over the range 411-531°K. The hydrocarbon composition of this fuel was 83% paraffinic, 17% aromatic, and 0.3 olefinic. The ERBS fuel contained 13% H and boiled over the range 435-601°K. The hydrocarbon content was 34% aromatic, 61% paraffinic, and <.1% olefinic (ref. 34). The JP5 fuel was refined by Sohio from Paraho II shale oil. It contains 78.3% saturates, 21.3% aromatics, and 0.4% olefins and essentially no nitrogen or sulfur (ref. 35).

The "model fuel" consisted of a 1/10 (v/v) solution of tetralin in n-dodecane. The n-dodecane was washed with concentrated H_2SO_4 until the acid layer was colorless, then once with dilute aqueous NaOH, then repeatedly with deionized water. The washed dodecane was then distilled; the purity was verified

by GC and UV spectrophotometry. This procedure was used for purification of the other n-alkanes as well. Tetralin was distilled and then passed through activated (400°C for 24 hours) silica gel immediately prior to preparing the model fuel. Indane was purified in the same manner.

Reagents. Pyrrole was purchased from Matheson, Coleman, and Bell; 2,6-dimethylquinoline, benzoyl peroxide, azobisisobutyronitrile (ABIN), chloroform, isooctane, and all the organosulfur compounds from Eastman Organic Chemicals; THF and acetonitrile from Waters Associates; tetralin, α-tetralone, indane, nonane, decane, dodecane, tetradecane, hexadecane, and the remaining organic nitrogen compounds from Aldrich Chemical Company. HPLC grade hexane, isooctane, tetrahydrofuran (THF), and chloroform were purchased from Fisher Scientific Company. The ethanol stabilizer was removed by passing the chloroform through activated silica gel prior to use. Deuterated chloroform and dimethylsulfoxide were obtained from Norell Chemical Company. Dichloromethane and semicarbazide hydrochloride were purchased from Matheson, Coleman, and Bell; hydroxylamine hydrochloride from Allied Chemical.

1-Tetralin hydroperoxide was prepared by the method of Knight and Swern (ref. 36). The product was recrystallized repeatedly from toluene at dry ice temperature until free from tetralone (HPLC analysis). 1-Tetralone was converted to the semicarbazone; the semicarbazone was separated by filtration and then hydrolyzed to regenerate the tetralone which was then

distilled. The absence of tetralol was verified via HPLC. α-Tetralol was prepared as previously described (ref. 29).

Cupric acetylacetonate and ferric acetylacetonate were synthesized according to Fernelius and Bryant (1957). Both were recrystallized from acetone. Copper metal foil (.002 in., Sargent Welch) and iron wire (.009 in., J.T. Baker) were used without treatment. Cupric laurate was prepared by the method of Whitmore and Lauro (ref. 37). Ferrous laurate was synthesized from lauric acid (titrated with aqueous NaOH to phenolphthalein end point) and $FeSO_4.7H_2O$ under N_2. A small amount of $Na_2S_2O_4$ was added to prevent formation of ferric salts. The white ferrous laurate was washed with deoxygenated water and dried under nitrogen. Analysis via dichromate titration gave 12.22% Fe (12.29% Fe theoretical).

Tetralin-1,4-diol (a gift from Marathon Oil Company) was purified by recrystallization twice from denatured ethanol (observed mp. 411-412°K). 1,2-naphthoquinone (Eastman Organic Chemicals) and 1,4-naphthoquinone (Aldrich Chemical Co.) were recrystallized from acetone.

Analytical Methods

Gas chromatography (GC) was performed using a Varian 3700 gas chromatograph with flame ionization detector. Capillary GC was performed using a Hewlett-Packard Model 5840 chromatograph equipped with flame ionization detectors and a 15m x .25 mm DB-5 bonded phase column (J and W Scientific).

A Waters Associates liquid chromatograph with Model 6000

pumps, U6K injector, 440 UV detector (254 nm), and R401 refractometer was used for high-performance liquid chromatographic (HPLC) analyses. Normal phase separations were performed on an IBM 250 mm Silica column; reverse phase separations on a Waters Associates μC-18 column; and gel-permeation chromatography (GPC) on a Waters Associates Ultra-Styragel 100A column. Polystyrene standards (Waters Associates) and reagent-grade aromatic compounds were used to obtain a calibration of retention time with molecular weight. Dual Hewlett-Packard 3390 integrators received signals from the two detectors.

Infrared spectra were recorded using a Perkin-Elmer 521 Spectrophotometer. Multiple internal reflectance (MIR) spectra were obtained using a Wilks Model 9 MIR attachment. UV spectral measurements were made using Cary 219 and Beckman DU-2 spectrophotometers.

Elemental analyses were obtained using a Carlo Erba 1104 Elemental Analyzer. Weight measurements were performed with a Cahn 4700 Electrobalance.

Proton nuclear magnetic resonance (^{1}H NMR) measurements were made with a Varian EM360A spectrometer. Dr. Calvin Curtis of Solar Energy Research Institute performed solution-phase ^{13}C NMR measurements. Solid-state cross-polarization/magic angle spinning (CP/MAS) ^{13}C NMR spectra were provided by the NSF Regional NMR Center at Colorado State University.

Gas chromatography/mass spectrometry (GC/MS) results were obtained using an Extranuclear Laboratories Simulscan spectrometer. Pyrolysis/mass spectrometry (py/MS) spectra were

recorded using an Extranuclear Laboratories SpectrEL spectrometer. Data reduction and pattern recognition computations were performed using a PDP-10 mainframe system.

Open column chromatographic fractionation of deposits was performed using Bond Elute columns from Analytichem International. The deposit was placed atop a Bond Elute cyanopropyl (CN) column which was connected above a Bond Elute unbonded silica gel column. The columns were conditioned with 6 ml hexane, then eluted with 6 ml benzene to obtain an aromatic fraction. The two columns were then disconnected and eluted separately with 4 ml 3/1 (v/v) benzene/chloroform (moderately polar aromatics). The CN column was then eluted with 6 ml chloroform (polar fraction) and, finally, with 6 ml methanol (highly polar fraction). Solvent was evaporated from each fraction under a stream of N_2 gas.

Stability Tests

Fuels were stressed in 147-ml, Flint-glass jars as previously described (ref. 15,29). In some cases, an alternative method was used. One-half mL samples of fuel (with additives in some experiments) were sealed in 10-mL glass ampules (Kimax). Following stressing for the desired time in an oven, the glass ampule was broken open. Deposit weights were, in some cases, then obtained by decanting the fuel from the ampule, washing the adhering deposit with hexane, weighing, dissolving the deposit from the ampule with an equivolume toluene-methanol-acetone mixture, and reweighing.

Derivatizations

Model deposits and tetralone oxidation products were derivatized for purposes of functional group identification and increased volatility for GC/MS analysis.

Methylation. Model deposits or tetralone oxidation products were methylated via treatment with excess CH_3OH in the presence of catalytic amounts of concentrated HCl at 353°K for 24 hours. Solvent was then evaporated under vacuum at ambient temperature. Alternatively, the methylation was effected with diazomethane by the method of Fales, Jaouni, and Babashak (ref.38). Typically, 0.12 ml of oxidized tetralone was derivatized using 0.132 g N-methyl-N-nitrosourea to generate the diazomethane. Product was obtained by evaporation of the ether at ambient temperature and pressure.

Carbonyl derivatization. Model deposit was treated with hydroxylamine hydrochloride to produce oximes and with semicarbazide hydrochloride to yield semicarbazones by standard procedures (ref. 39).

Hydride reduction. Model deposit (.08 g) was dissolved in 1 ml THF and added to 1.9 g $LiAlH_4$ in 50 ml THF in a round-bottom flask. The solution was refluxed for 24 hours; 100 ml water + 20 ml 2 N H_2SO_4 were slowly added to decompose excess $LiAlH_4$; and the aqueous phase was extracted with 200 ml diethyl ether. After washing of the organic layer with dilute $NaHCO_3$ and water, the ether was allowed to evaporate.

Peroxide cleavage. Model deposit was heated in contact with tetralin under an N_2 atmosphere for several days at 473°K in an attempt to cleave any peroxide linkages present. Tetralin was expected to function as H donor under these conditions.

RESULTS AND DISCUSSION

Effects of Sulfur Compounds in Jet A

Previous work in our laboratory demonstrated a correlation between amount of deposit produced in a Jet A fuel (168 hr at 394°K) and the basicity of added nitrogen heterocycles (5 ppm N). Effects on deposition of similar concentrations of added organosulfur compound were also determined (ref. 29). However, test of the analogous correlation was not made due to lack of basicity data for the sulfur compounds. Therefore, basicities of these compounds were estimated as proportional to the change in NMR chemical shift of the H atoms adjacent to the S atom when the compound was complexed with excess I_2 (ref. 40-41).

Using this basicity parameter, correlations for individual classes of compounds (sulfides, disulfides, thiols) similar to those for nitrogen heterocycles were obtained (Figure 3). The strong steric dependence of basicity as estimated in this way is consistent with evidence of steric inhibition of the base catalysis of deposition by nitrogen heterocycles (ref. 15,16). The effects of organosulfur compounds on deposition appear to involve base catalysis and complexation or decomposition of deposit precursors. The net effect of a given compound (ref. 29) depends on these two competing influences.

Effects of Metals and Metal Salts

Jet A. The formation of insoluble deposits in Jet A fuel aged in contract with air at 394°K for 7 days is significantly

accelerated by copper metal but not by iron metal. The amount of deposit formed increases with the surface area of copper metal in contact with the fuel although deposition does not occur preferentially on the metal surface. Copper content of the fuel phase is not significantly higher at the end of the test period than in the unaged fuel (1.3×10^{-6} vs 0.9×10^{-6}M).

Addition of cupric acetylacetonate, cupric laurate, and ferrous laurate to Jet A (3-8 ppm metal) significantly increased deposition after 7 days at 394°K. In the case of ferrous laurate, the solids were abnormally non-adherent to glass surfaces. Lauric acid (added at comparable concentration) slightly decreased deposition.

Table 1. EFFECTS OF METALS AND SALTS ON JET A DEPOSIT FORMATION

Metal or Salt Added	Δ in Deposit Weight relative to neat Jet A (μg/coverslip)
$3.2 cm^3$ Cu metal	+100 ± 20
$3.8 cm^3$ Fe metal	-52 ± 17
7.7×10^{-5}M $Cu(acac)_2$	+47 ± 13
5.0×10^{-4}M Cu laurate	+193 ± 20
1.4×10^{-4}M Fe laurate	-8 ± 17
1.0×10^{-4}M lauric acid	-21 ± 25

Model Fuel. As previously discussed (ref. 29) deposition in the model fuel is preceded by formation of α-tetralin hydroperoxide and decomposition of the hydroperoxide to α-tetralone and

α-tetralol:

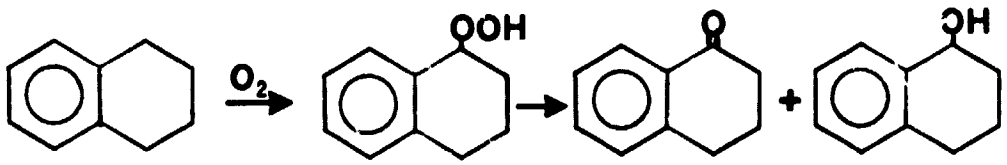

With the onset of deposit formation, the concentrations (monitored by HPLC) of α-tetralone and of α-tetralin hydroperoxide decrease dramatically. Copper metal, cupric laurate, and ferrous laurate all increase the initial formation rate of α-tetralone, depress the hydroperoxide concentration throughout the test period, and hasten the decrease in concentration of α-tetralone in the deposition phase of the process. Thus both formation of deposit precursors and their subsequent reactions to form deposits are promoted. Iron metal had essentially no effect on the precursor concentrations or on the rate of deposition. See Figure 4 and Table 2. Platinum metal was also found to in-

Table 2. EFFECTS OF METALS AND SALTS ON MODEL DEPOSIT FORMATION

Metal or Salt Added	Δ Deposit weight relative to neat model fuel (g)
6.5cm^3 Cu metal	+.085 ±.04
~.3cm^3 Fe metal	-.006 ± .01
1.0x10^{-5}M Cu laurate	-.027 ± .002
1.7x10^{-4}M Cu laurate	+.097 ± .04
1.5x10^{-4}M Fe laurate	+.093 ± .01
3.2x10^{-4}M lauric acid	+.001 ± .01

crease the rate of tetralin hydroperoxide decomposition.

In the case of addition of cupric laurate to the model fuel, the influence on deposition rate was unexpectedly concentration dependent. At 10 ppm Cu added, deposition was significantly increased while at 2 ppm Cu added a slight decrease in the amount of deposit formed was observed. In both cases the effects on precursor concentrations were as shown in Figure 4. Addition of α-tetralol to the model system decreases the amount of deposit formed while addition of either α-tetralone or of the hydroperoxide increases deposition (ref. 29). Hence, one role of the cupric laurate may be complexation of α-tetralol (incompletely in the case of low concentrations of added cupric salt) and thereby prevention of the inhibition process. Similarly, cupric acetylacetonate did not significantly increase deposition in Jet A when added at concentrations below approximately 1 ppm Cu (ref. 29).

The soluble copper content of the fuels spiked with cupric laurate decreased significantly during the test period. However, the total weight of deposit formed was much greater than the weight of copper salt added. Despite loss of soluble copper from the fuel phase, the effect on deposition appears to be catalysis of oxidative condensation reactions of the deposit precursors and interference with the inhibitory action of components such as tetralol.

ERBS. The mechanism by which metals influence instability of fuels in contact with the metal surface is open to speculation. Surface catalysis of reactions producing deposits from soluble precursors would be expected to lead to deposits

primarily on the metal surfaces. However, as previously reported (ref. 29), while Cu metal increases rates of deposition from Jet A, the deposits do not form on the Cu surface but on glass surfaces of the reaction vessel. Surface catalysis of autoxidation or other reactions leading to deposit precursors could produce the observed effects assuming glass surfaces provide more active sites for nucleation of deposits. However, the catalysis by Cu metal could also arise from solubilization of the metal to provide low concentrations of soluble Cu salts or complexes resulting in homogeneous catalysis. When ERBS fuel was stressed at 393°K in contact with Cu plates maintained at a potential difference of 50 volt, no significant difference in the amounts of deposit produced in the two cell compartments was observed. A similar amount of deposit was produced in a second container of fuel in contact with a single, isolated Cu plate. While no current flow through the electrochemical cell was expected, differences in the electrical double layers at the surface of the two charged Cu plates would be expected to alter the activity of the surfaces as heterogeneous catalysts. Certainly surface catalysis of oxidation reactions requiring oxidation state change of the Cu would be altered. On the other hand, dissolution of surface oxide or other salts via complexation or acid-base processes should be little affected by the potential gradient. This result is therefore consistent with homogeneous catalysis of deposition in this fuel as indicated in the experiments with soluble salts in the model fuel.

HPLC Method for Monitoring Instability

During stressing of Jet A fuel at 394°K, the concentration of polar species in the fuel phase continues to increase as deposit is formed (ref. 29). Using an HPLC method developed for studying the model fuel (ref. 42), these polar species (presumably autoxidation products) can be separated from the fuel hydrocarbons. This method has now been applied to the shale-derived JP5, the ERBS fuel, and to blends of Jet A and ERBS fuels.

The total area of peaks corresponding to polar components (e.g. Figure 5) as determined by the 254nm UV detector was normalized with respect to the total response of the RI detector (quantifying the major non-polar components). This normalized HPLC parameter correlates well with deposit weight as determined via the coverslip method (ref. 29). A similar correlation can also be obtained selecting a single polar component peak as a measure of degradation (Figure 6). The HPLC method is much more rapid and precise than the coverslip method for comparison of relative instability of closely-related fuel samples and for comparisons of fuel samples stressed at different temperatures. The HPLC method supplanted the coverslip method in most subsequent experiments.

Temperature Effects on Deposition Mechanisms

The widespread use of accelerated storage stability tests has been based on the reported correlation of results of such methods with actual storage behavior in some studies (ref. 43)

and on expediency. However, at some elevated temperature, pyrolysis processes will clearly begin to occur as well. Concern that changes in mechanism of instability may occur at or below temperatures employed in accelerated storage tests has been expressed (ref. 44). HPLC analyses of Jet A samples stressed at temperatures from 308°K to 453°K (Figure 7) demonstrate that the fuel phase contains essentially the same polar components in all cases. The concentrations of polar species is different in the various samples reflecting differences in extent of degradation over the actual stressing times involved. However, no departure in the nature of soluble reaction products is evident. The shale-derived JP5 similarly shows no change in liquid phase products with temperature (e.g. Figure 5). Differences in the processes by which these precursors are converted to deposits or the conversion of other fuel components to deposits would, of course, not be revealed by this analysis.

The deposits resulting from stressing of Jet A and shale JP5 fuels at 393°K and at 453°K were compared by pyrolysis/mass spectrometry (py/MS). While direct visual comparison of spectra of such complexity (Figure 8) is not generally instructive, pattern recognition techniques provide useful information. In the samples stressed for the purposes of this comparison, extensive deposition was obtained by continuing the process for up to two weeks. As a result, some of the deposit formed was suspended in the liquid phase rather than adhering to the glass surfaces. The adherent and suspended deposits were analyzed separately. The dendogram in Figure 9 is a simple graphical

representation of the similarities observed in the py/MS results for these samples. Clearly, the variance within the triplicates for each different deposit is significantly smaller than the variance between deposits. An alternative presentation of these data is the nonlinear map of Figure 10. Significant compositional differences between the various samples are indicated.

Effect of Prior Deposit Formation on Fuel Stability

The debate over which fuel components are involved in the formation of deposits centers on whether the involvement of trace constituents in the deposition process is stoichiometric or catalytic. A sample of Jet A was repeatedly stressed at 453°K. The fuel was filtered and transferred to a cleaned container ten times. While the rate of deposit production visibly decreased during the study, deposition continued throughout. No significant differences in the nature of the deposit with time were noted. In view of the amounts of deposit produced stoichiometric involvement of trace components was certainly not responsible for continued deposit formation beyond the initial stage.

While concentrations of polar species in the fuel phase increased throughout (via HPLC), no new species were observed. GC/MS analysis of the fuel phase revealed loss of volatiles and some changes in the relative areas of some chromatographic peaks which may reflect preferential reactivity. However, these differences are small and incomplete resolution limits

interpretation. In the example of Figure 11, component B which is depleted relative to component A is aromatic while A is aliphatic (Figure 12). In view of the closeness of the retention times of the two components, differential volatility does not seem a likely explanation of the relative depletion.

The analogous experiments with shale-derived JP5 produced comparable results. Deposit formation continued throughout at somewhat diminished rates.

Stability of Jet A/ERBS Blends

ERBS fuel is definitely less stable than Jet A when stressed at 394°K. HPLC anaylses of the two fuels reveal considerable compositional difference. Degradation of the fuels and of four blends of the two were followed via HPLC and deposit weights were determined by the coverslip method. Linear regression of the deposit weights and HPLC parameter (normalized concentration of polars) yields r^2=0.939. The individual results show considerable scatter irrespective of which analytical method is selected.

Blending the ERBS and Jet A fuels does not produce fuels with stability corresponding to the weighted average for the constituents. Rather, substantial quantities of ERBS can be added to Jet A with only slight destabilization of the blend (Table 3). The explanation may lie in the presence of antioxidants or other stabilizing components in the Jet A in quantities sufficient to stabilize significant amounts of added ERBS. In a longer test period, this stabilizing influence may

disappear as the stabilizers are consumed. Differences in the solvation properties of the two fuels for deposits and precursors may also be important.

Table 3. STABILTY OF JET A/ERBS BLENDS (394°K, 168 hours)

Fuel	mg deposit	HPLC area*
Jet A	.095	.0024
	.043	.00078
	.205	.00551
Jet A ave.	.114	.0029
84% Jet A	.154	.00421
	.146	.00436
	.225	.0142
84% Jet A ave	.175	.0076
66% Jet A	.130	.00588
	.271	.00942
	.191	.00538
66% Jet A ave	.197	.0069
50% Jet A	.217	.0189
	.160	.0079
	.190	.0293
50% Jet A ave	.189	.0187
30% Jet A	.248	.0327
	.149	.0168
	.236	.0169
30% Jet A ave	.211	.0221
ERBS	1.452	.228
	1.901	.264
	2.039	.197
ERBS ave	1.797	.230

* HPLC area is the summed peak area for all UV peaks after 3.5 minutes divided by the total RI peak area.

Effects of JFTOT Stressing on the Fuel Phase

Analyses via HPLC of several fuels and pure hydrocarbons before and after stressing in the JFTOT, show essentially no differences. No significant concentrations of products of degradation processes are found in the liquid phase. Only polar degradation products would be detectable by this method; products of non-oxidative pyrolysis processes would elute with fuel hydrocarbons. These results may be interpreted in terms of a very steep temperature gradient at the heater tube interface resulting in significant reaction only at the surface, of rapid and efficient adsorption of degradation products from solution onto the heater tube surface, or of degradation reactions producing non-polar products. These observations are consistent with the conclusions of Kim and Bittker (ref. 45) that cracking rather than autoxidation reactions are important in JFTOT stressing.

Effect of Medium on Tetralin Oxidation

The role of dodecane in the formation of deposits in the model fuel (tetralin/dodecane) is not clear. When neat tetralin is stressed in air at 393°K, tetralin hydroperoxide and its decomposition products are formed in the liquid phase. However, no solids separate. When dodecane is added to the stressed tetralin, no precipitation occurs; nor are model fuel deposits completely soluble in tetralin. Hence a role other than strictly that of solvent is suggested for dodecane. Analysis of the

liquid phase of the model fuel during stressing via GC/MS yields evidence of low concentrations of dodecane derivatives early in the process. However, these compounds are not found at later stages (Figure 13). Upon formation of deposits, oxygenated derivatives of dodecane may be adsorbed on the polar surfaces of the deposits. In the washing of adsorbed fuel from the deposits prior to analysis (with hexane) the dodecane derivatives may be removed.

Perfluoroalkanes offer an interesting substitute for dodecane in the model fuel. They have low dielectric constants and dissolve large concentrations of oxygen. However, the strength of the C-F bonds precludes autoxidation of the perfluoroalkane itself. Unfortunately, quantitative evaluation of the stressing of tetralin in the perfluoroalkane solvent FC77 was complicated by the low solubility of tetralin in this solvent. Nonetheless, deposits similar to those from tetralin/dodecane were produced within five days at 394°K. Thus, the perfluoroalkane provides an appropriate solvent for oxygen uptake and occurrence of deposit forming reactions without oxidation of the perfluoroalkane. An analogous role is postulated for dodecane in the model fuel with autoxidation of the dodecane itself incidental to deposit formation. Condensation reactions producing deposits from soluble precursors evidently require media of low dielectric constant and are irreversible.

The Role of Heteroatomics in Instability

Jet A. The contention that nitrogen and sulfur compounds catalyze deposit formation in Jet A (ref. 15,16,40) was based on inference. The fate of added heteroatomics was not directly determined in those studies. The effects on deposition of addition of six heteroatomic compounds (Figure 14) to Jet A are shown in Figure 15. In each case, the weight of added heteroatomic (10-40 ppm heteroatom in the fuel phase initially) was less than 5% of the weight change observed. The fuel phase changes in the various samples during stressing were monitored via HPLC (Figures 16,17). Except for dipentylsulfide, these heteroatomics increased deposit weights in Jet A via promotion of the formation of soluble polar precursors. Dipentylsulfide promotes instead the conversion of precursors to deposits.

The persistence of benzoquinoline in the fuel phase throughout stressing is easily observed in HPLC of these samples (Figure 17). The abnormally large absorptivity of benzoquinoline at 254 nm provides high sensitivity for detection of this compound in the fuel matrix. Less sensitivity is afforded for the other heteroatomics and their fates are not obvious from the HPLC data. GC/MS data for these samples similarly do not provide unequivocal evidence of whether the heteroatomics remain in the fuel phase after deposition.

Shale-derived JP5. Results rather different than those in the petroleum-derived Jet A were obtained with this fuel (Figure 18). In general the effects of the heteroatomics on stability

were smaller. Dibenzothiophene which promoted deposition in Jet A inhibits it in this fuel. 2,6-Dimethylpyridine has little effect on this fuel while strongly promoting deposition in Jet A. On the other hand, indole promotes deposition in both fuels but by different mechanisms: in Jet A, the formation of precursors is accelerated while in the JP5 conversion to deposits is catalyzed. The danger of extrapolating the observed influence of a certain additive on a given fuel to other fuels is plainly illustrated here.

Model Fuel. The influence of the added heteroatomics on the concentrations of individual compounds can be followed in the model fuel and compared to the resulting effect on deposit weights (Figure 19). Indole and dipentylsulfide decrease the tetralone concentration; this leads to greater deposition with indole and suppressed deposition with dipentylsulfide. The liquid phase in the dipentylsulfide-containing sample is essentially devoid of oxidation products. The primary autoxidation process has been inhibited. With indole, by contrast, conversion of tetralone to other products, including deposits, is accelerated (Figure 20).

Dimethylpyrrole, dibenzothiophene, and benzoquinoline suppress deposition in dissimilar ways (Figure 21). Dimethylpyrrole slows conversion of tetralone; dibenzothiophene suppresses all oxidation, and benzoquinoline has little effect on the tetralone concentration, reflecting influence at more than one point in the process. The presence of benzoquinoline in the liquid phase after deposition is again apparent in the HPLC.

Dimethylquinoline increases conversion of tetralone to deposits.

The fate of the added heteroatomic was followed by GC/MS analysis of the liquid phase throughout the stressing process. The presence of benzoquinoline in the liquid phase, as indicated in the HPLC results, is confirmed here. The molecular ion and first fragment peak are readily apparent (Figure 22). Dibenzothiophene also survives in the fuel following deposition (Figure 23). This fact was not apparent in HPLC due to simultaneous elution of dibenzothiophene and tetralin.

Dimethylpyridine is evident in the fuel for about three days but is absent when visible deposition occurs (Figure 24). However, the increased rate of conversion of tetralone to deposits in these samples continues after depletion of dimethylpyridine in the fuel phase. Similarly, dimethylpyrrole disappears from the liquid phase after about one day (Figure 25) but continues to influence liquid phase composition thereafter.

Dipentylsulfide is depleted in the liquid phase very quickly; it is absent after one day. It rapidly deposits on the container walls as a dark solid insoluble in organic solvents. However, the liquid phase remains devoid of oxidation products throughout stressing. Indeed, replenishing the air and restressing does not result in oxidation in the liquid phase or in deposit formation. Very effective trapping by the deposited dipenylsulfide of radicals needed to initiate autoxidation of tetralin may be responsible.

An interesting, but perplexing, aspect of stabililty research was illustrated in these studies. One of five

replicates of the model fuel spiked with 2,6-dimethylpyridine generated an amount of deposit at least ten-fold that in the other four. HPLC analyses (Figure 26) showed abnormally large concentrations of naphthalene derivatives (from tetralin autoxidation) and low amounts of the long-retention-time species which is formed late in the stressing process. In this regard, the abnormal replicate ressembled a sample subject to oxygen replenishment and restressing. No satisfactory explanation of this abnormality is apparent. The analogous occurrence of an occasional sample which produced very large amounts of deposits was observed in studies of the effects of Cu metal on Jet A stability.

HPLC analyses of the deposits from the heteroatomic-spiked model fuels exhibit significant differences (Figures 27 and 28). Although the deposits were repeatedly washed with hexane before being dissolved in the mobile phase for analysis, evidence of the adsorbed heteroatomic compound is found in some cases.

Effect of Added Tetralone on Deposition in Jet A

The addition of low concentrations (6.1×10^{-5}M) of tetralone to Jet A was previously reported to lead to increased rates of deposit formation (ref. 29). The addition of much higher concentrations of tetralone (Table 4) do not produce additional increases in rate. However, the deposit produced is no longer adherent (as is the rule with deposits formed at 394°K from Jet A and from the model fuel) to glass surfaces. The overall

deposition rate is controlled by oxygen availability with tetralone effectively present in excess. At these concentrations, tetralone dominates the deposition reactions relative to the natural Jet A components. Deposit weight determinations in this case were subject to abnormally large scatter due to suspended deposits.

TABLE 4. EFFECT OF TETRALONE ON JET A STABILITY

Added Tetralone Molarity	Average mg deposit/coverslip		
	24 hours	48 hours	192 hours
.010	.084	.163	.315
.020	.075	.145	.219
.100	.059	.136	.330

Effect of Radical Initiators on Model Fuel Stability

Although autoxidation, a free-radical process, is generally agreed to be the starting point for instability, the addition of standard free-radical initiators to Jet A does not increase the rate of deposition at 394°K (ref. 29). Indeed, benzoyl peroxide causes a decrease in deposition weights; presumably, promoting other processes which do not generate deposits. Addition of these initiators to the model fuel yields generally similar effects on deposit weights (Table 5).

TABLE 5. Effects of Radical Initiators and Inhibitors

Compound Added	Average Total Deposit Weight (mg) 5 days	10 days	13 days
none	1.72	2.62	3.36
Benzoyl peroxide	1.86	2.29	2.48
Azobisisobutyronitrile	2.36	1.91	3.29
1,4-Naphthoquinone	1.40	1.67	2.60
1,2-Naphthoquinone	0.39	0.41	0.51
1,4-Tetralindiol	0.41	1.58	4.26

Compounds were added at 0.010M, fuel stressed at 394°K in glass

The effects of addition of 1,4-naphthoquinone and 1,2-naphthoquinone are interesting. The 1,2-isomer produces the sort of inhibition characteristic of free-radical trapping; the 1,4-isomer does not. Inasmuch as the two isomers should both function as free radical traps, the observed behavior is indicative of some other mechanism of influence. The results for addition of 1,4-tetralindiol demonstrate another type of influence. In the early stages, this compound delays deposition by preferentially consuming oxygen relative to other components. In late stages of the process, however, the oxidation products of the diol contribute to increased deposition.

Tetralone/Tetralin Hydroperoxide Condensation Reactions

Molecular weight estimations for deposits from both real and model fuels (ref. 29) range from about 400 to 1000. The

deposition process must involve reactions linking small numbers of monomeric components. The earlier observation that addition of both tetralone and tetralin hydroperoxide to Jet A leads to large increases in deposition rate which are further increased by base catalysis lead to the postulation (ref. 41) that condensation reactions of these two molecules form deposits in the model fuel. This was tested by studying the reaction of the two pure compounds in dodecane solution under an inert atmosphere.

HPLC of the reaction mixture as it was stressed at 394°K for a period of several weeks, demonstrated (Figure 29) that the hydroperoxide underwent the usual decomposition. However, no deposit separated from the liquid phase. Introduction of air and restressing produced deposits within a few days. Thus, while tetralone and the hydroperoxide are involved in reactions leading to deposits, additional oxidation is required.

Since tetralin hydroperoxide decomposes fairly rapidly at 394°K, further study of model reactions were directed toward oxidation of tetralone. In addition, no evidence of cleavage of peroxide linkages by heating model deposit in the presence of excess tetralin was found. The other primary decomposition product, tetralol, functions as an inhibitor of deposition (ref. 29).

Tetralone Oxidation

The autoxidation of tetralone has received only modest

attention in the literature (ref. 31-33,46,47). Several oxidation products have been reported (Figure 30); however, the formation of insoluble phases has not been mentioned.

While the naphthoquinones have not been reported among the oxidation products of tetralone, their elemental compositions (75.9%C, 3.8%H, and 20.2%O) are quite similar to that of the deposits from the model fuel. Derivatization of model deposit with hydroxylamine and with semicarbazide hydrochloride produces an oxime and semicarbazone, respectively, with melting points (Table 6) similar to those of the naphthoquinones (and different than that for 1-tetralone).

TABLE 6. Derivatives of the Carbonyl Function in Deposits

COMPOUND	mp of Oxime (°K)	mp of Semicarbazone
1-Tetralone	376	490
2-Tetralone	361	477
1,2-Naphthoquinone	442	457
1,4-Naphthoquinone	-	520
Model deposit	423-425	518-523

Data from reference 48

Therefore, the possible involvement of 1,4- or 1,2-naphthoquinone in model deposit formation was studied by stressing each in dodecane solution under air for several weeks. These compounds exhibit limited solubility in dodecane at room temperature but greater solubility at 394°K. Analysis of the reaction mixtures via HPLC demonstrated the lack of any significant oxidation or

degradation over a two-week test period. No deposit corresponding to model deposit was formed in these solutions. The naphthoquinones apparently do not represent precursors to model deposits.

The oxidation of carefully purified tetralone as a neat liquid, leads to a bewildering array of products (Figure 31). No insoluble deposits separate from the liquid phase even after prolonged stressing. Evaporation of the remaining tetralone after stressing does, however, produce a material similar in appearance to model deposit. Stressing of tetralone in dodecane under air also generates a deposit ressembling the model fuel deposit.

Analysis of oxidized neat tetralone via GPC (Figure 32) indicates primarily unreacted tetralone and other monomers but a small amount of higher molecular weight species. An additional small peak at longer retention time may correspond to highly polar species retarded by adsorption on the gel surface. Reverse-phase HPLC analysis of oxidized tetralone results in very poor resolution of peaks with short retention times, consistent with the suggestion that polar products arise. This oxidation mixture and the fractions obtained by repetitious normal-phase HPLC separation and fraction collection (Figure 31) produced few peaks in GC/MS (Figure 33). In view of the indicated molecular weight distribution, high polarity of the components is indicated.

The solid resulting from distillation of unreacted tetralone from the oxidation mixture was fractionated via extraction with

aqueous NaOH. Acidification of the resulting NaOH solution caused precipitation of a brown solid which is soluble in chloroform and dimethylsulfoxide. The MIR infrared spectrum (Figure 34) of this material reveals the presence of OH, aromatic CH, and carbonyl functional groups. The NMR spectrum (Figure 35) in dimethylsulfoxide solution gives no evidence of carboxylic acid or phenol functional groups; however,the solubility may be insufficient to permit detection of these groups if only one is present per molecule. Alternatively, the base-solubility may be associated with enolate anion formation. Only very low intensity peaks are obtained in the GC/MS analysis of this material. Among the species tentatively identified are compounds VII and IX in Figure 30.

Derivatization of the oxidation products with diazomethane or with methanol/HCl only slightly increased the volatilization of the sample in the GC/MS (Figure 36). Several oxidation products (Compounds V,VI,VIII, and X in Figure 30) were identified (e.g. Figure 37 is the mass spectrum of dimethyl phthalate produced by methylation of X in Figure 30). However, no compounds corresponding to oligomers were identified. Either derivatization results in cleavage of oligomers, or leaves them insufficiently volatile for elution into the mass spectrometer.

Characterization of Deposits

The solids produced from fuels upon stressing pose a challenging problem in structural characterization. Limited solubility, strong adhesion to surfaces, and low volatility

complicate the analyses. While the deposits from the model fuel are more tractable, they are far from simple.

Deposits produced from the various fuels over the temperature range 308-453°K with addition of low concentrations of sulfur and nitrogen compounds differ little in elemental composition (Table 7). Certainly, the added heteroatomics exert

TABLE 7. Elemental Composition of Deposits

Fuel(Deposition T, °K)	%C	%H	%N	%O(Diff)
Jet A (393)	73.7	5.69	0.22	20.7
Jet A + 5ppmN pyrrole (393)	72.5	4.99	0.27	22.2
Model	72.5	5.57	-	21.9
Model + 10ppmN quinoline (393)	73.4	6.45	0.28	19.9
Model + 10ppmN indole (393)	73.1	6.30	0.31	20.3
Shale JP5 (393)	71.7	6.68	0.19	21.4
Shale JP5 (353)	70.0	6.34	0.23	23.4
Shale JP5 (453)	74.6	6.21	-	19.2
Shale JP5 + 20ppmN DMP (393)	69.0	6.43	0.27	24.3

an influence on deposition rates without dominating the stoichiometry of the deposit, although compositional change does occur. The elemental composition data for the JP5 fuel illustrate the compositional changes associated with different deposition temperatures.

Despite similarities in chemical composition, deposits from the various fuels differ considerably in other properties. The deposits from the shale-derived fuel are much lighter in color and are more soluble in organic solvents than are those from petroleum-derived Jet A or ERBS. Both IR (Figure 38) and ^{1}H NMR (Figure 39) spectra demonstrate that this deposit is much more

aliphatic in character than are those from the petroleum-derived Jet A (ref. 29) despite the fact that the fuel itself contains a higher fraction of aromatics than does the Jet A. Clearly, different chemistry is involved in deposit formation in these two fuels.

Because the model deposit is generally more soluble in organic solvents and was expected to have less complex composition, structural characterization effort was concentrated on this material. The IR spectral characteristics of the model and Jet A deposits are very similar (Figure 40). Solid-state ^{13}C NMR results for Jet A deposits (Figure 41) indicate greater relative aliphatic carbon content than for the model deposit (Figure 42). Assigning the integrals as indicated in the figures, the carbon ratios (carbonyl/aromatic/aliphatic) obtained are 1/11.2/4.7 for model deposit and 1/16.3/15.4 for Jet A deposit. These compare to 1/6/3 for tetralone, for example. The solution phase ^{13}C NMR spectrum for model deposit in deuterochlorform is very complex (Figure 43). Peaks corresponding closely to those observed in the spectrum of tetralone are present along with many others. In ^{1}H NMR (Figure 44), two distinct groups of peaks (aliphatic H at 0-3 ppm and aromatic H at 6.5-8 ppm) arise. An aliphatic H/aromatic H ratio of 1.36 was calculated for the model deposit. Combining this result with the solid-state ^{13}C data, an aromatic H/C of 0.67 and an aliphatic H/C of 1.34 may be caluclated. These low values indicate aromatic ring fusion and substitution at aliphatic carbons (e.g. by OH).

Normal-phase HPLC analysis of the model deposit clearly shows that it is a mixture, at least in solution (Figure 45). The range of retention times observed indicates considerable variation in component polarity. That peaks for these polar components are observed with the 254 nm detector but not with the RI detector indicates the presence of chromaphores such as carbonyl or aromatic rings. Based on these results, fractionation of the model deposit on the basis both of relative solubilities and open-column chromatographic elution was performed.

That fraction of model deposit soluble in benzene differs significantly from the fraction insoluble in benzene but souble in THF. The MIR infrared spectra (Figure 46) show several differences. In particular, aromatic CH is clearly evident in the benzene fraction (3050 cm^{-1} and 750 cm^{-1}) but not in the THF fraction (there may be some contribution from residual extraction solvent). The absorbances due to OH also seem depressed in the THF fraction relative to that in the benzene fraction, and changes in the carbonyl region are evident. The results of py/MS analysis of these two fractions more clearly demonstrate the differences (Figure 47). Major peaks at m/e = 146,131,118, and 90 are characteristic of the tetralone fragment. The peak at 78 indicates some residual benzene (extraction solvent) in the sample. In neither fraction are characteristic fragmentation patterns of normal alkyl species apparent.

The majority of the model deposit is soluble in dichloromethane. Not surprisingly, therefore, the MIR infrared

spectrum of the dichloromethane-soluble fraction (Figure 48) is quite similar to that of the unfractionated model deposit (Figure 40). The small amount of dichloromethane-insoluble material which can be dissolved in THF is not clearly differentiated from the other fraction in terms of the infrared spectrum; however, significant differences appear in the py/MS spectra (Figure 49). Again tetralone fragments are apparent; however, the 43,57,71,85, series for n-alkyl species may possibly be discerned in the spectrum of the dichloromethane-insoluble fraction.

Two major peaks are observed in the HPLC analysis of the model deposit (P2 and P3 in Figure 45). Via fraction collection in HPLC, MIR spectra of these two separate fractions were obtained (Figure 50). An interesting feature of both spectra is the sharp band at about 1260 cm^{-1}. This feature is buried in a broad absorbance in the spectrum of the unfractionated material; it may represent the C-O stretch associated with an alcohol or phenol; however, no clear indication of O-H stretch is seen in the 3600-3400 cm^{-1} region.

Fractionation of Jet A deposits into benzene-soluble and benzene-insoluble-THF-soluble fractions yields spectrally dissimilar materials. The benzene-soluble fraction contains less OH and carbonyl functionality than does the other fraction (Figure 51). The association of these with a more polar fraction is not surprising. Differences are also seen in py/MS; little structural information can be obtained from these complex spectra (Figure 52). Extraction with dichloromethane, alternatively, yields two fractions having very similar MIR spectra (Figure 53).

Open-column chromatographic fractionation of deposits produced results comparable to solvent extraction. No more definitive structural assignments were attained.

Treatment of the model deposit with $LiAlH_4$ drastically changes the material. A much larger number of components is found in both HPLC (Figure 54) and GC/MS (Figure 55) suggestive of nucleophilic cleavage of linkages such as ester and ether groups by the hydride. Identification of these components and reconstruction of their linkages in the deposit are goals of continuing research in our laboratory.

Despite the volume of chromatographic and spectral data we have obtained for deposits, no definitive structure can be assigned even to model deposits. Pattern recognition techniques hold the most promise for progress in this matter. Comparisons of py/MS spectra of deposits produced under different conditions identifies parameters which result in structural changes. For example, differences may be seen in the py/MS spectra (Figures 56 and 57) of deposits from JP5 to which the various heteroatomics had been added. These data may be combined with other analytical information (e.g. elemental composition, IR, NMR, etc.). Use of factor analysis permits association of the changes with specific features (masses in the mass spectrum, frequencies in the IR, etc.). Via this indirect route, work on delineation of structures of deposits continues in our laboratory. The structural changes found may then be related to mechanisms of deposition.

REFERENCES

1. B. Brooks, Ind. Eng. Chem., 18, 1198 (1926).
2. D. Yule and T. Wilson, Ind. Eng. Chem., 23, 1254 (1931).
3. J. Morrell, C. Dryer, C. Lowry and G. Egloff, Ind. Eng. Chem., 28, 465 (1936).
4. J. Morrell, C. Dryer, C. Lowry and G. Egloff, Ind. Eng. Chem., 26, 655 (1934).
5. J. Morrell, C. Dryer, C. Lowry and G. Egloff, Ind. Eng. Chem., 26, 497 (1934).
6. C. Dryer, C. Lowry, J. Morrell and G. Egloff, Ind. Eng. Chem., 26, 885 (1934).
7. T. Wallace, in Advances in Petroleum Chemistry and Refining, vol. 9, ed. J. McKetta, Interscience Publishers, New York, pp. 353-407, 1964.
8. F. Schwartz, M. Whisman, C. Allbright and C. Ward, Bur. Mines Bull., 626, 44 pp., 1964.
9. E. Walters, H. Minor and D. Yubroff, Ind. Eng. Chem., 41, 1723 (1949).
10. R. Thompson, L. Drudge and J. Chenicek, Ind. Eng. Chem., 41, 2715 (1949).
11. E. Elmquist, Symposium on Distillate Fuel Oils, ASTM STP, #244, Philadelphia, p. 26 (1959).
12. R. Offenhauer, J. Brennan and R. Miller, Ind. Eng. Chem., 49, 1265 (1957).

13. J. Frankenfeld and W. Taylor, First annual report, U.S. Department of Energy, DOE/BC/10045-12, Feb., 1981.

14. J. Frankenfeld and W. Taylor, Final report, U.S. Department of Energy, DOE/BC/10045-23, June, 1981.

15. J. Worstell and S. Daniel, Fuel, 60, 481 (1981).

16. J. Worstell, S. Daniel and G. Frauenhoff, Fuel, 60, 485 (1981).

17. E. White, Manual on Requirements, Handling, and Quality Control of Gas Turbine Fuels. ASTM STP, #531, Philadelphia, 32 pp. (1973).

18. C. Johnson, D. Finl and A. Nixon, Ind. Eng. Chem., 46, 2166 (1954).

19. W. Dukek, J. Inst. Pet., 50, 273 (1964).

20. A. Nixon, in Autoxidation and Antioxidants, ed. W. Lundberg, Interscience Publ., New York, p. 695, 1962.

21. J. Smith, Ind. Eng. Chem., Prod. Res. Devel., 8, 299 (1969).

22. W. Taylor and T. Wallace, Ind. Eng. Chem., Prod. Res. Devel., 6, 258 (1967).

23. W. Taylor, Ind. Eng. Chem., Prod. Res. Devel., 15, 64 (1976).

24. W. Taylor, J. Appl. Chem.,18, 251 (1968).

25. W. Taylor, Ind. Eng. Chem., Prod. Res. Devel., 8, 375 (1969).

26. B. Englin, V. Slitikova, R. Aliev and V. Sashevskii, Khim. Tekhnol. Topl. Masel, 20, 40 (1975).

27. A. Nixon and H. Minor, Ind. Eng. Chem., 48, 1909 (1956).

28. W. Taylor, J. Appl. Chem.,19, 222 (1969).

29. S. Daniel, "Studies of the Mechanisms of Turbine Fuel Instability", NASA Contractor Report 167963, Jan. 1983.

30. J. Bolland, Quart. Rev., 3, 1 (1949).

31. A. Robertson and W. Waters, J. Chem. Soc., 1574 (1948).

32. A. Robertson and W. Waters, J. Chem. Soc., 1578 (1948).

33. A. Robertson and W. Waters, J. Chem. Soc., 1585 (1948).

34. G. Prok and G. Seng, NASA Technical Memorandum 81440, 1980.

35. D. Bittker, Lewis Research Center, personal communication.

36. H. Knight and D. Swern, Org. Syn., 34, 90 (1954).

37. W. Whitmore and M. Lauro, Ind. Eng. Chem., 22, 646 (1930).

38. H. Fales, T. Jaouni, and J. Babashak, Anal. Chem.,45, 2302, 1973

39. R. Shriner, R. Fuson, and D. Curtin, The Systematic Identification of Organic Compounds, 5th ed., John Wiley, New York, pp. 227-305, 1964.

40. S. Daniel and F. Heneman, Fuel, 62, 1265 (1983).

41. S. Daniel, Colorado School of Mines Quarterly, 78, 47 (1983).

42. S. Daniel, J. Worstell, G. Strand and G. Frauenhoff, J. Liquid Chromatogr., 4, 539 (1981).

43. F. Schwartz, M. Whisman, C. Allbright and C. Ward, Bur. Mines Bull., 660, 58 pp., 1972.

44. L. Jones, R. Hazlett, N. Li, and J. Ge, Fuel, 63, 1152 (1984).

45. W. Kim, and D. Bittker, NASA Technical Memorandum 86874, 1984

46. A. Kammeva, and L. Muzychenko, Trudy Moskou Khim. Technol., 23, 61 (1956), CA53: 10142b.

47. M. Martan, J. Manassen, and D. Vofs, Tetrahedron, 26, 3815 (1970).

48. Z. Rappoport, editor, Handbook of Tables for Organic Compound Identification, 3rd ed., CRC Press, Cleveland, Ohio, pp. 161-185, 1967.

FIGURE 1

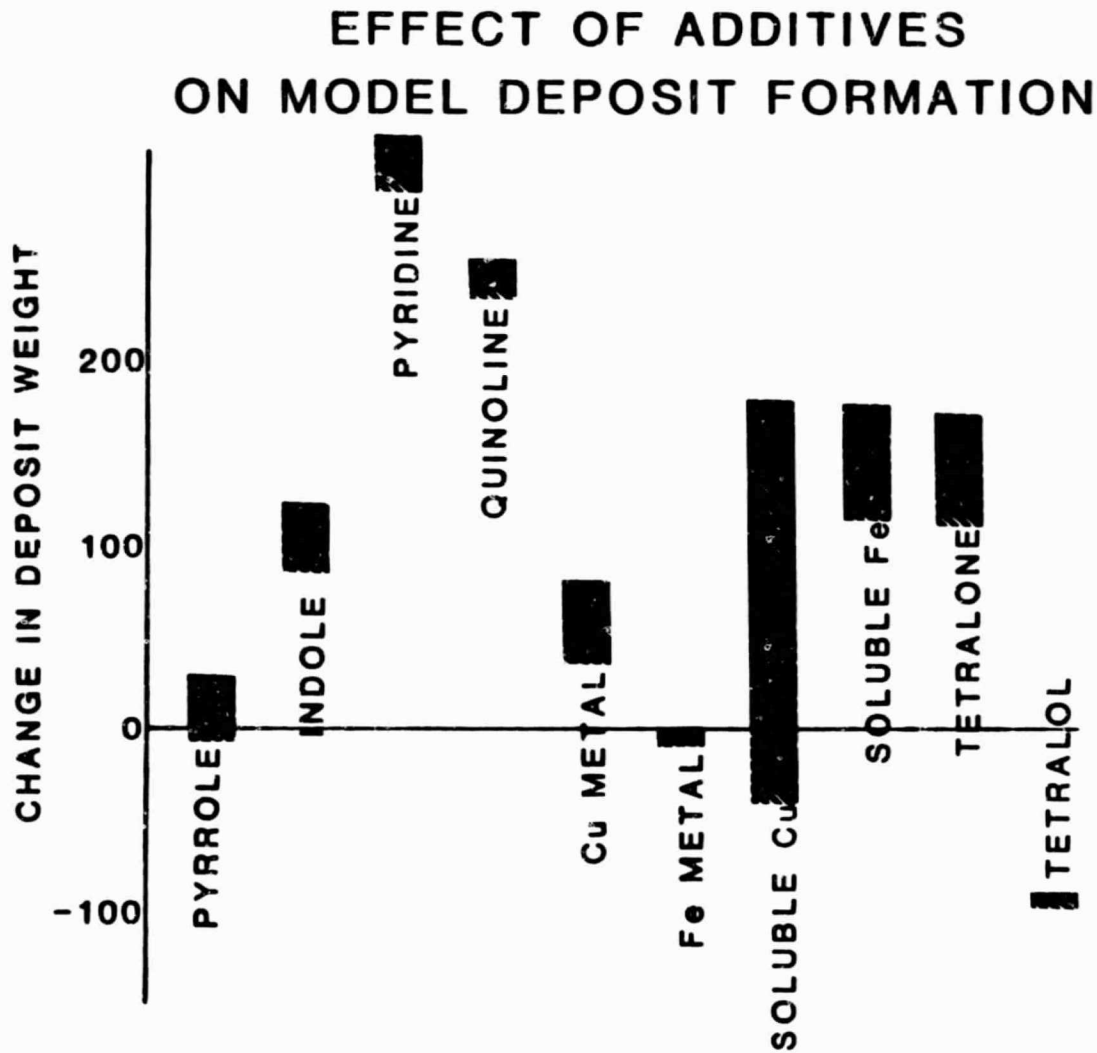
EFFECT OF ADDITIVES
ON MODEL DEPOSIT FORMATION
CHANGE IN DEPOSIT WEIGHT
200
100
0
-100
PYRROLE
INDOLE
PYRIDINE
QUINOLINE
Cu METAL
Fe METAL
SOLUBLE Cu
SOLUBLE Fe
TETRALONE
TETRALOL

FIGURE 2

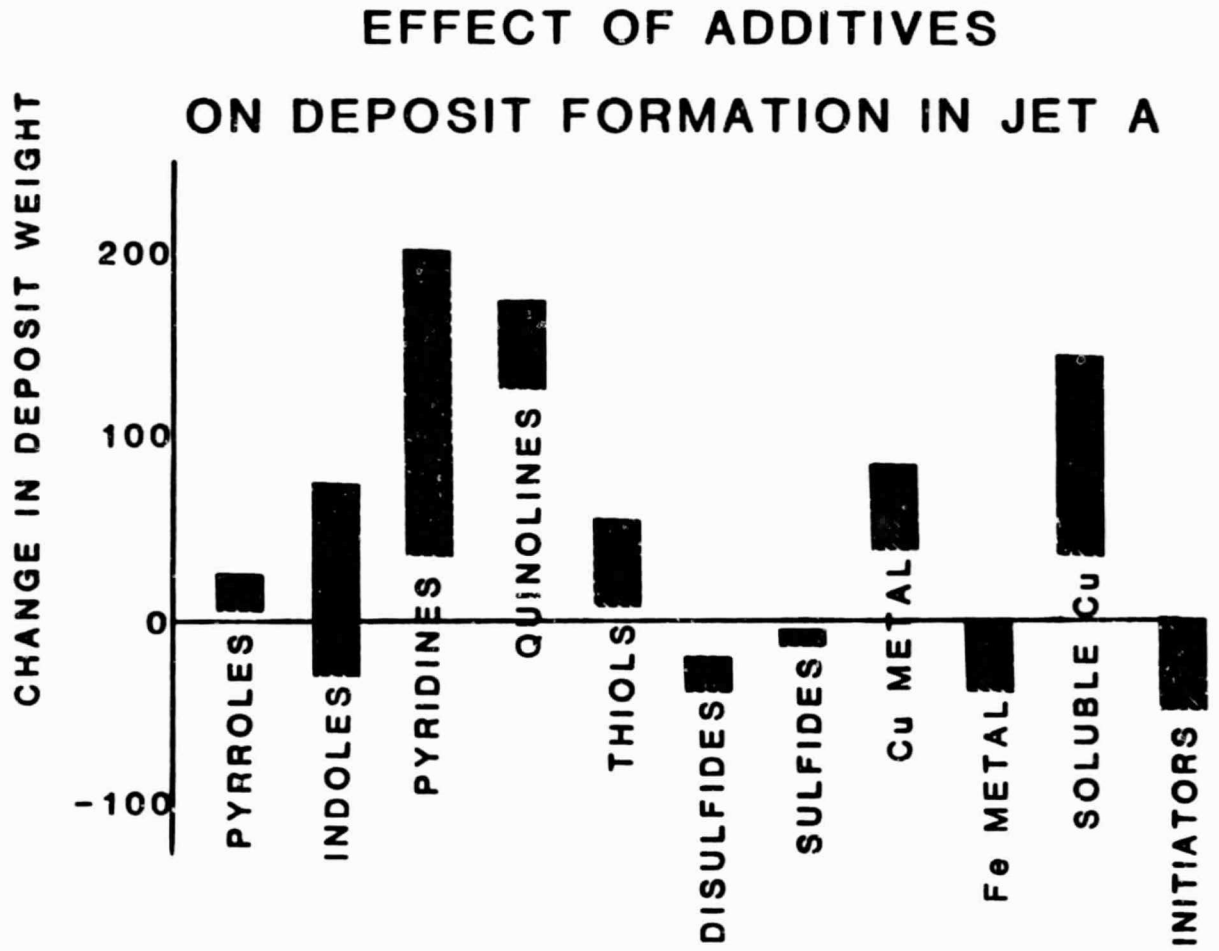
EFFECT OF ADDITIVES
ON DEPOSIT FORMATION IN JET A
CHANGE IN DEPOSIT WEIGHT
200
100
0
-100
PYRROLES
INDOLES
PYRIDINES
QUINOLINES
THIOLS
DISULFIDES
SULFIDES
Cu METAL
Fe METAL
SOLUBLE Cu
INITIATORS

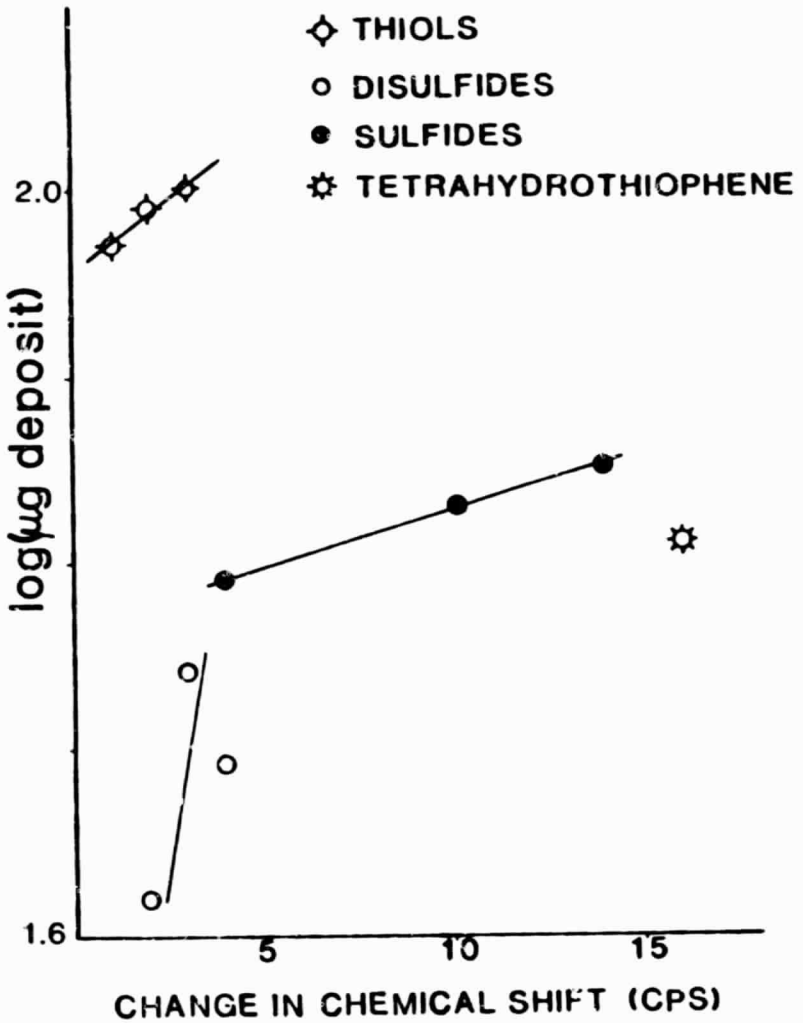

FIGURE 3. BASICITY AND PROMOTION OF DEPOSITION

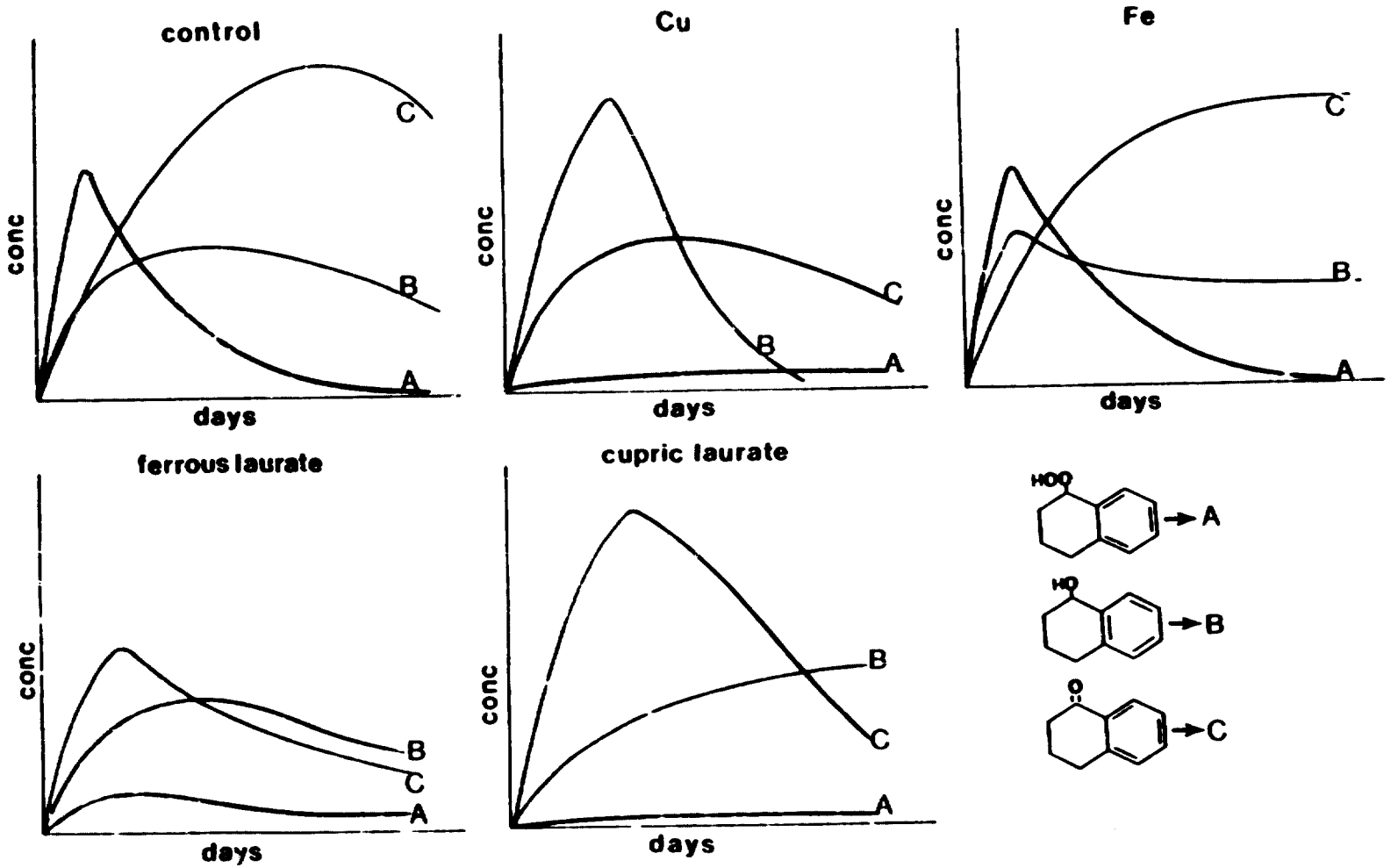

FIGURE 4. EFFECTS OF METALS AND SALTS ON MODEL DEPOSITION

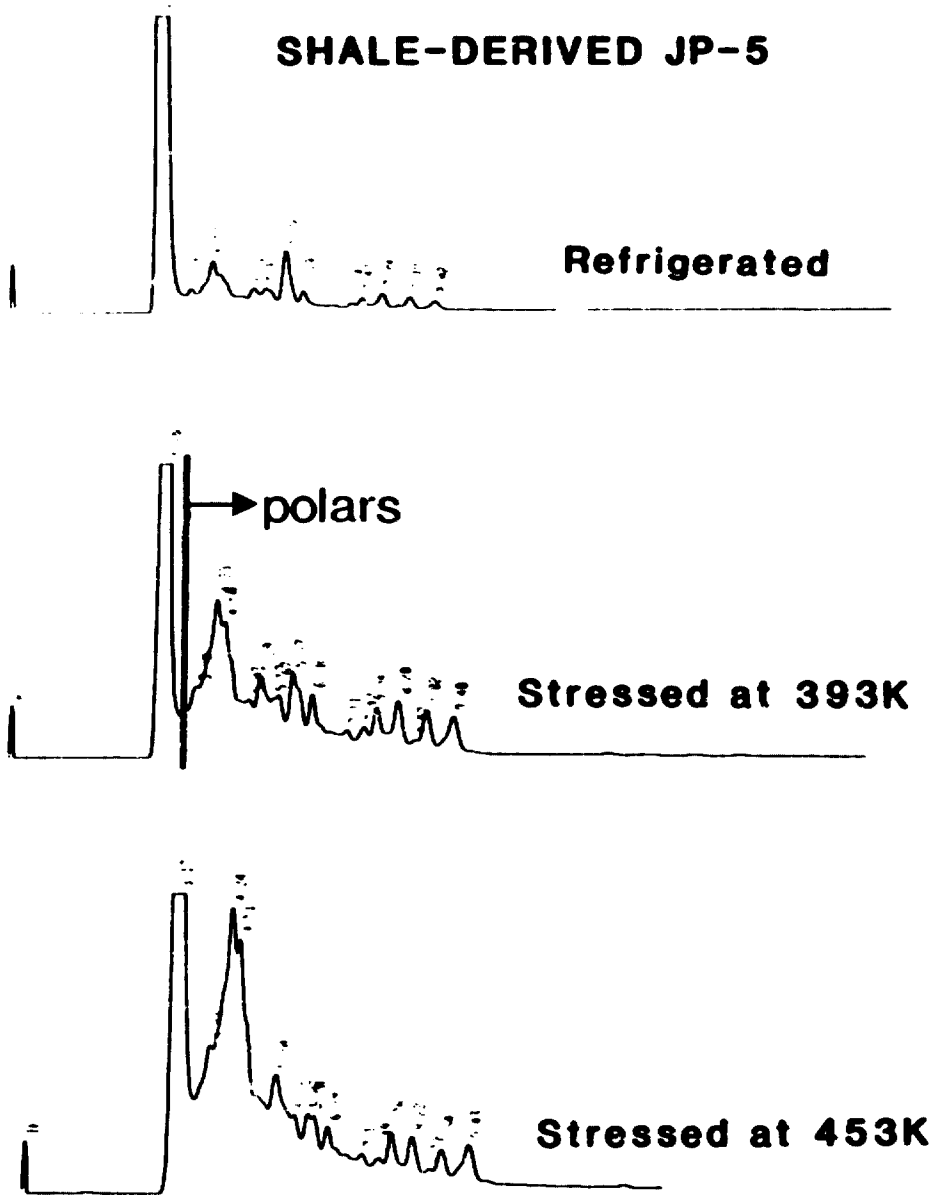

FIGURE 5. HPLC ANALYSIS OF STRESSED JP5

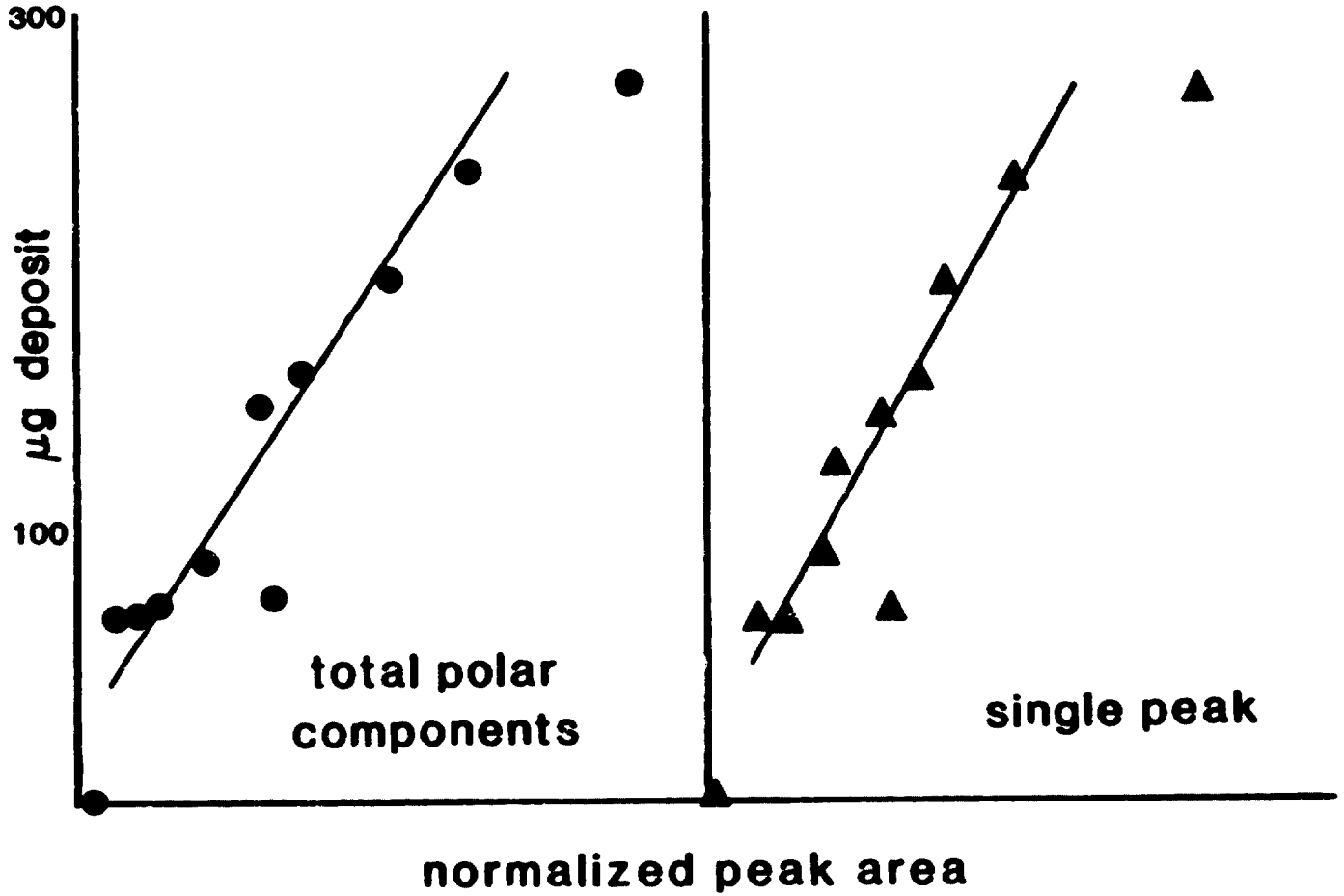

FIGURE 6. CORRELATION OF HPLC AND GRAVIMETRIC METHODS

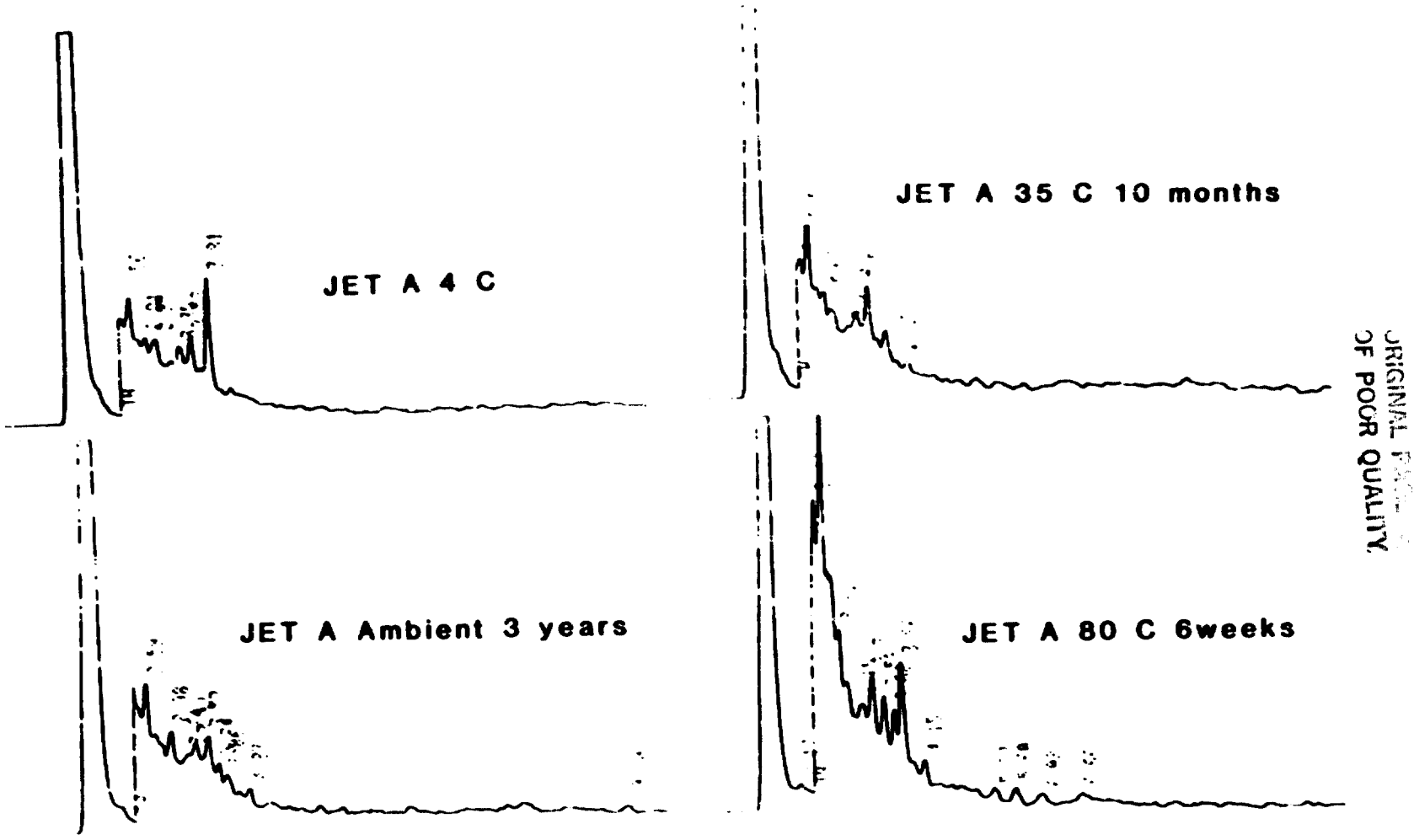

FIGURE 7. COMPARISON OF DEGRADATION AT DIFFERENT TEMPERATURES

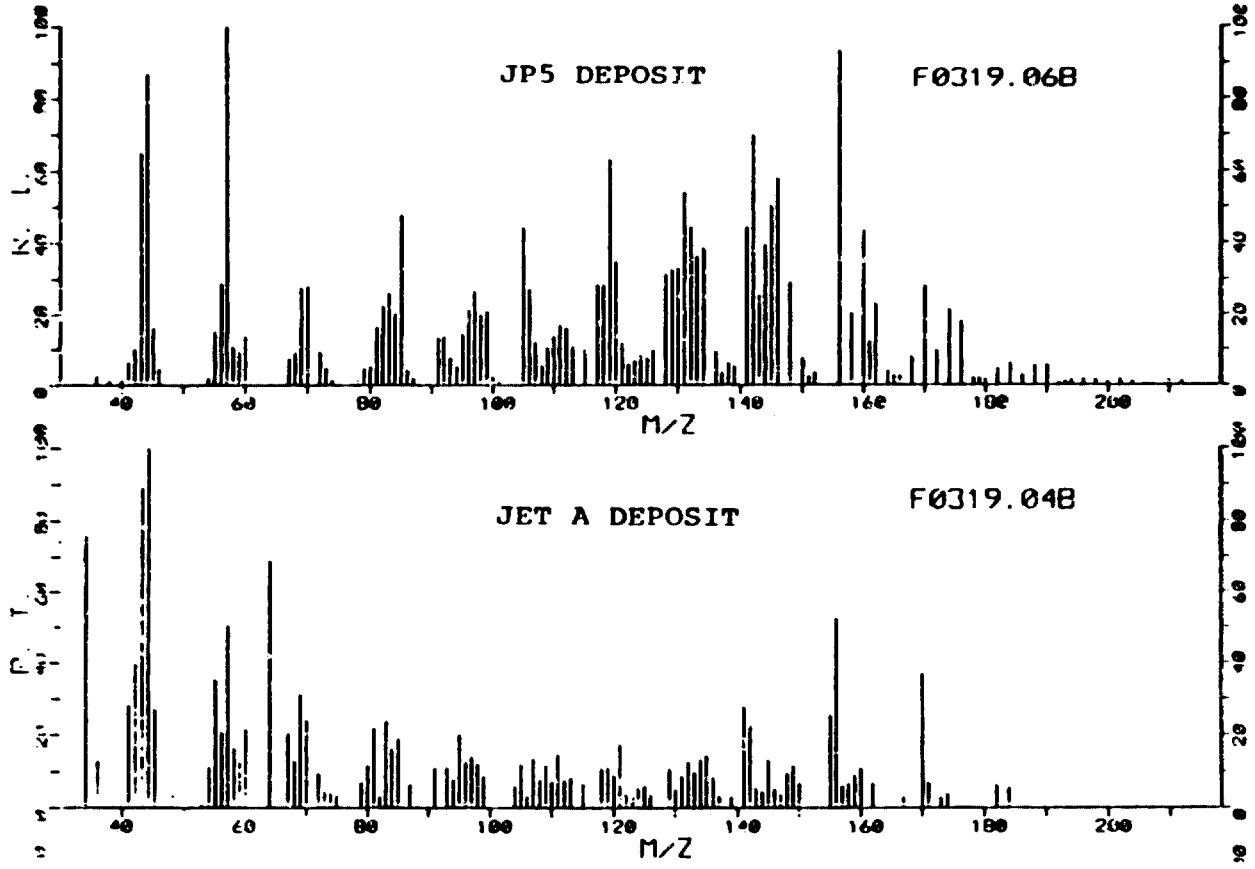

FIGURE 8. PYROLYSIS MASS SPECTRA OF FUEL DEPOSITS

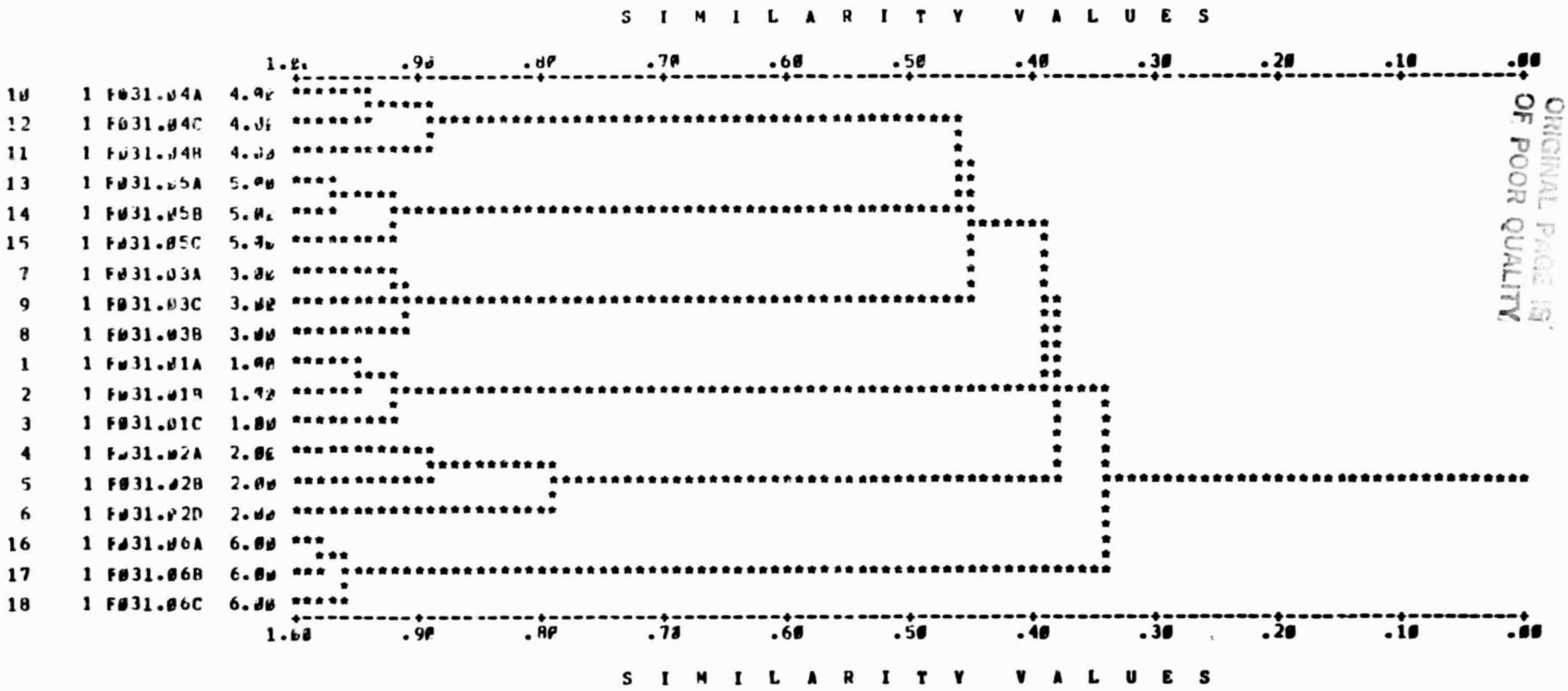

FIGURE 9. HIERARCHICAL DENDOGRAM - py/MS OF DEPOSITS

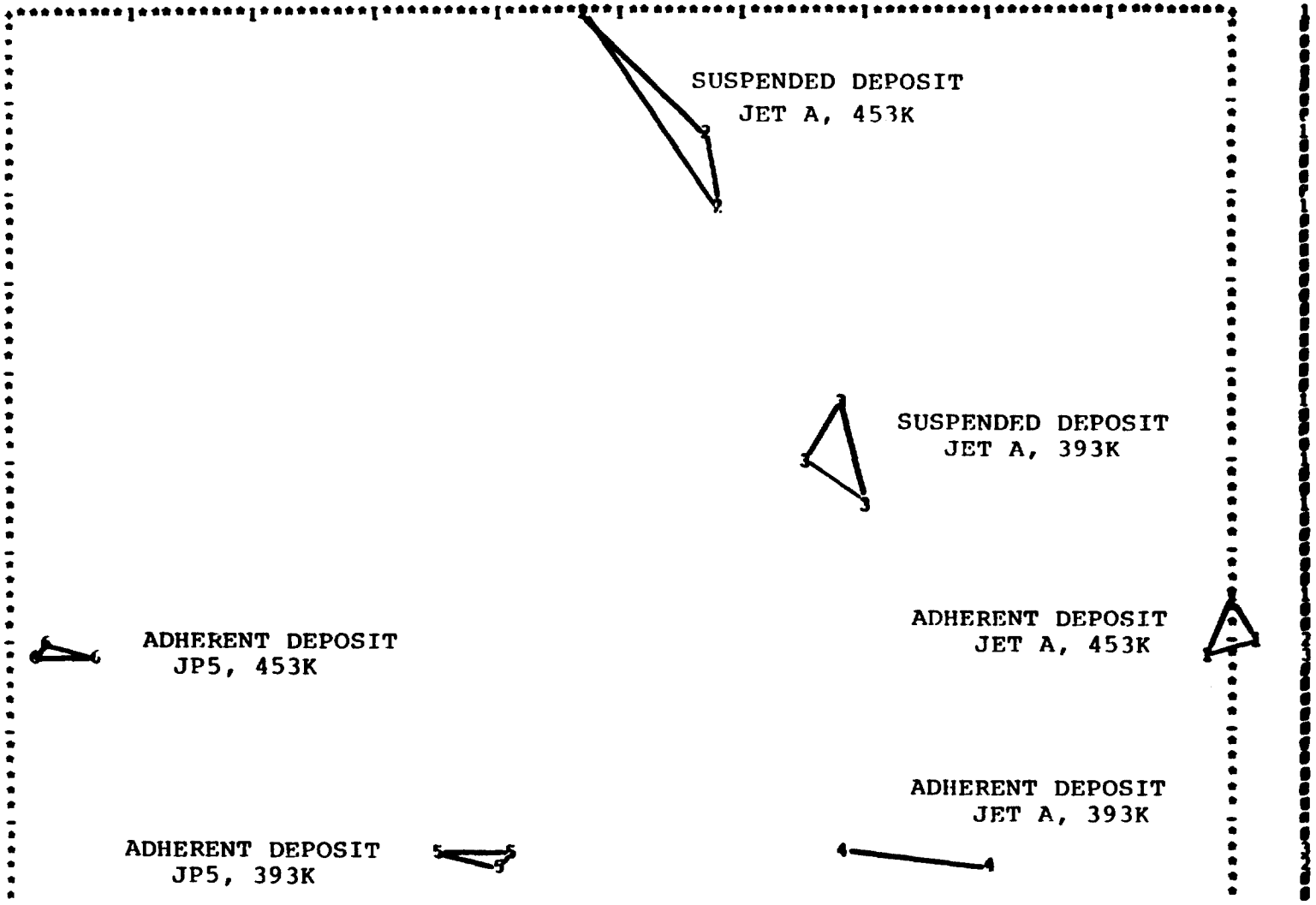

FIGURE 10. NON-LINEAR MAP - py/MS OF DEPOSITS

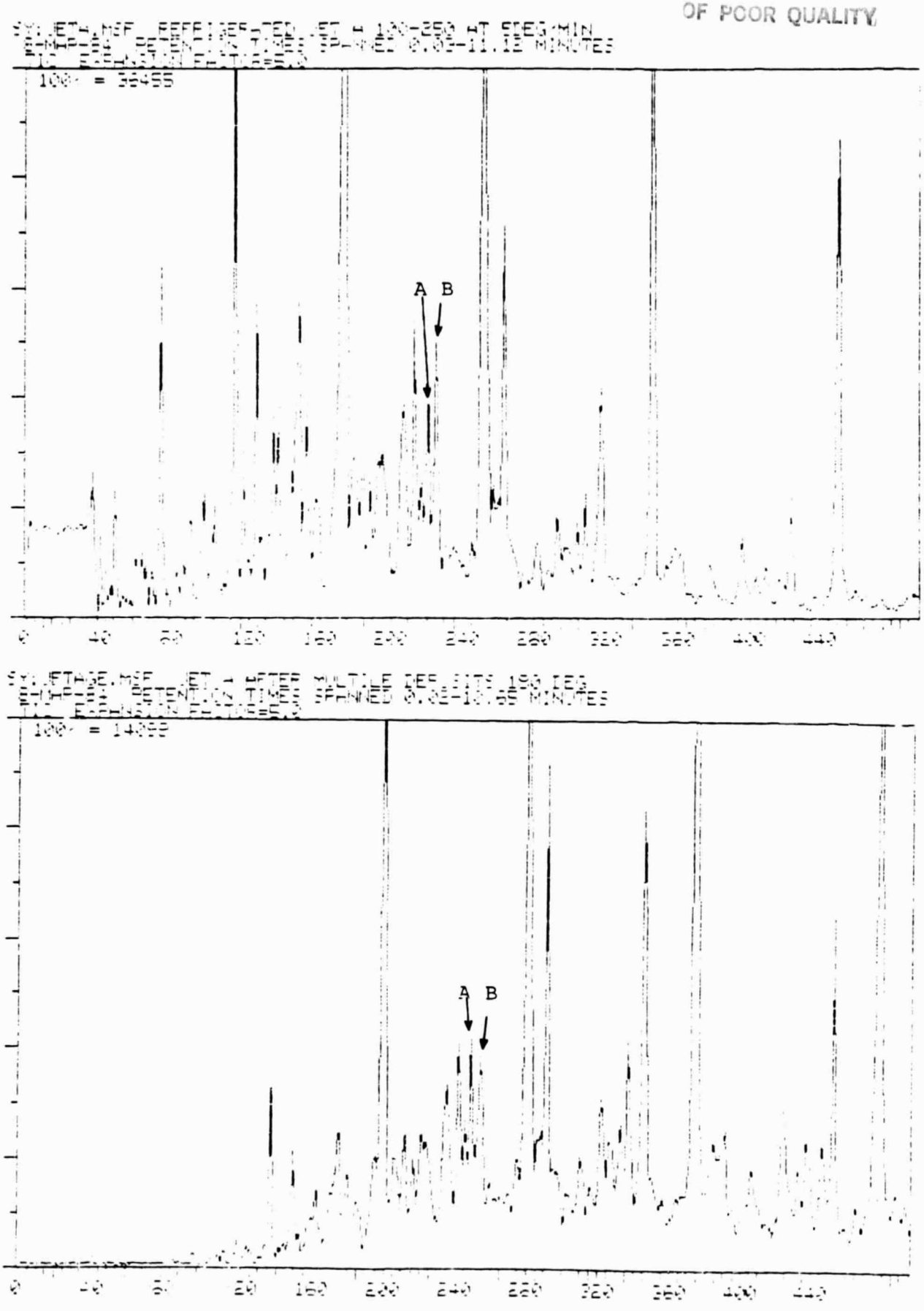

FIGURE 11. ION CHROMATOGRAMS - JET A FUEL

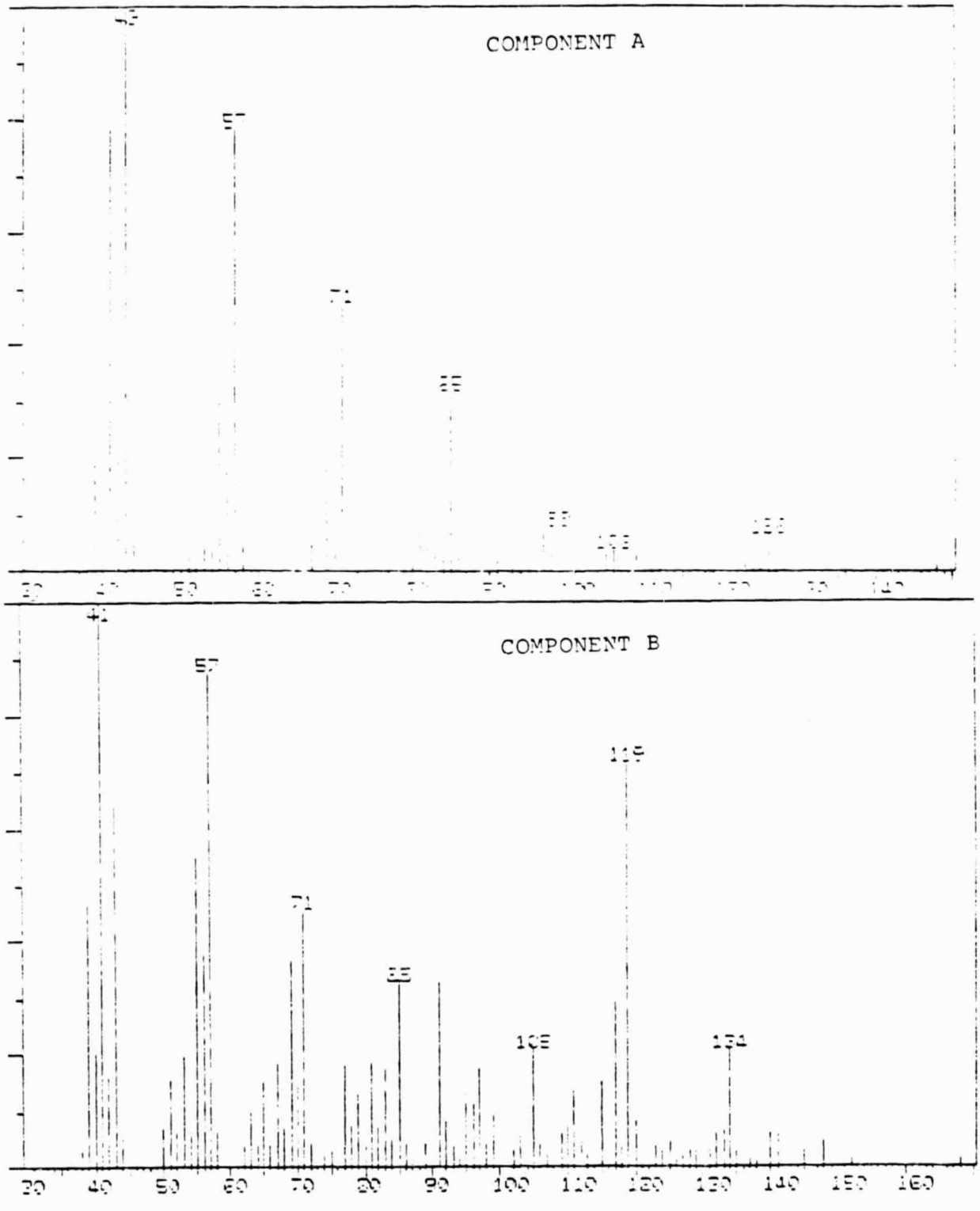

FIGURE 12. MASS SPECTRA - SELECTED COMPONENTS

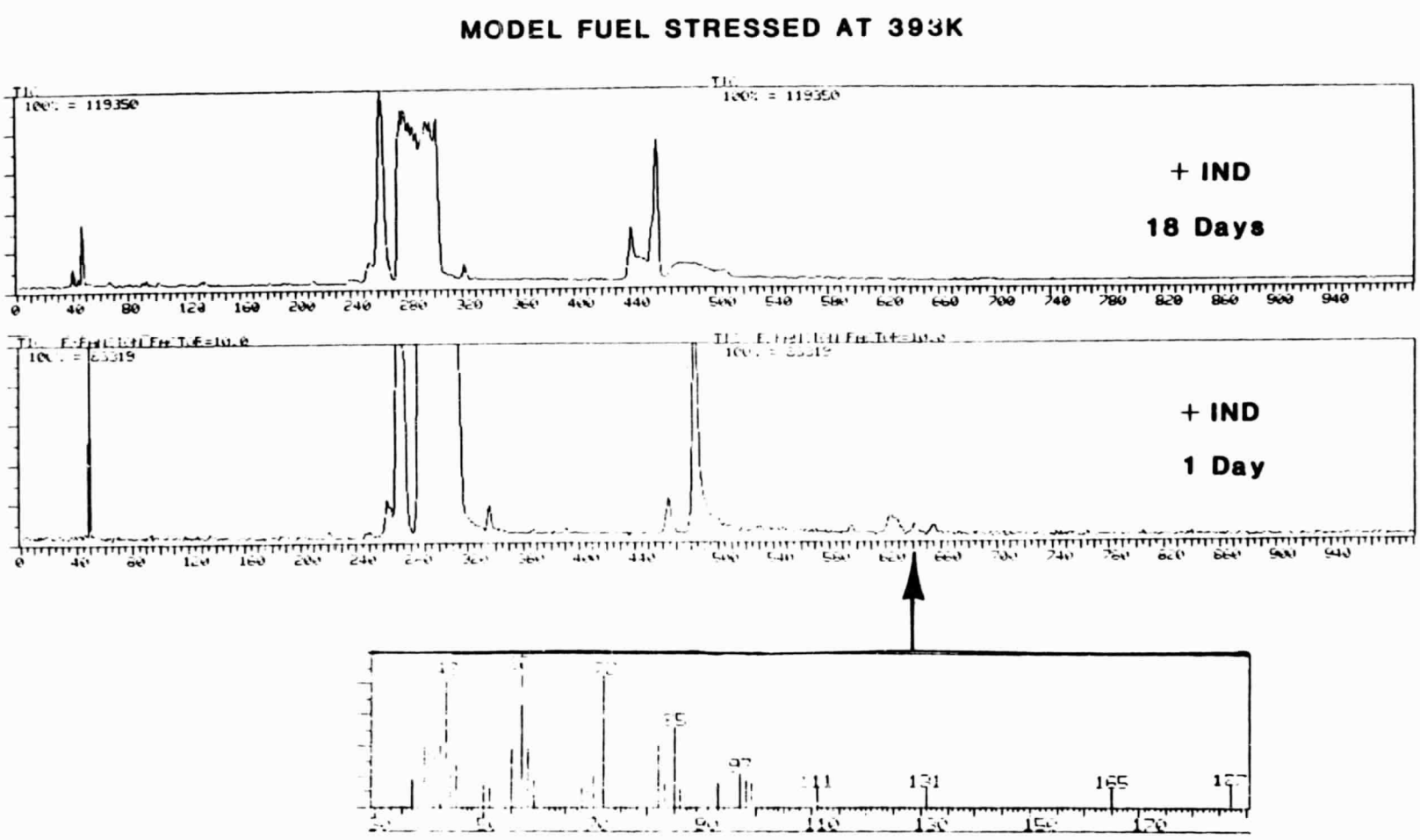

FIGURE 13. TRANSIENT DODECANE DERIVATIVES IN MODEL FUEL DEGRADATION

$(CH_3CH_2CH_2CH_2CH_2)_2S$	dipentylsulfide	DPS
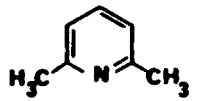	2,6-dimethylpyridine	LUT
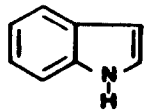	indole	IND
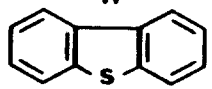	dibenzothiophene	DBT
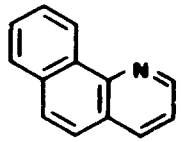	7,8-benzoquinoline	BZQ
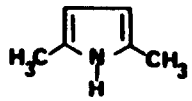	2,5-dimethylpyrrole	DMP

FIGURE 14. HETEROATOMICS ADDED TO FUELS

FIGURE 15.

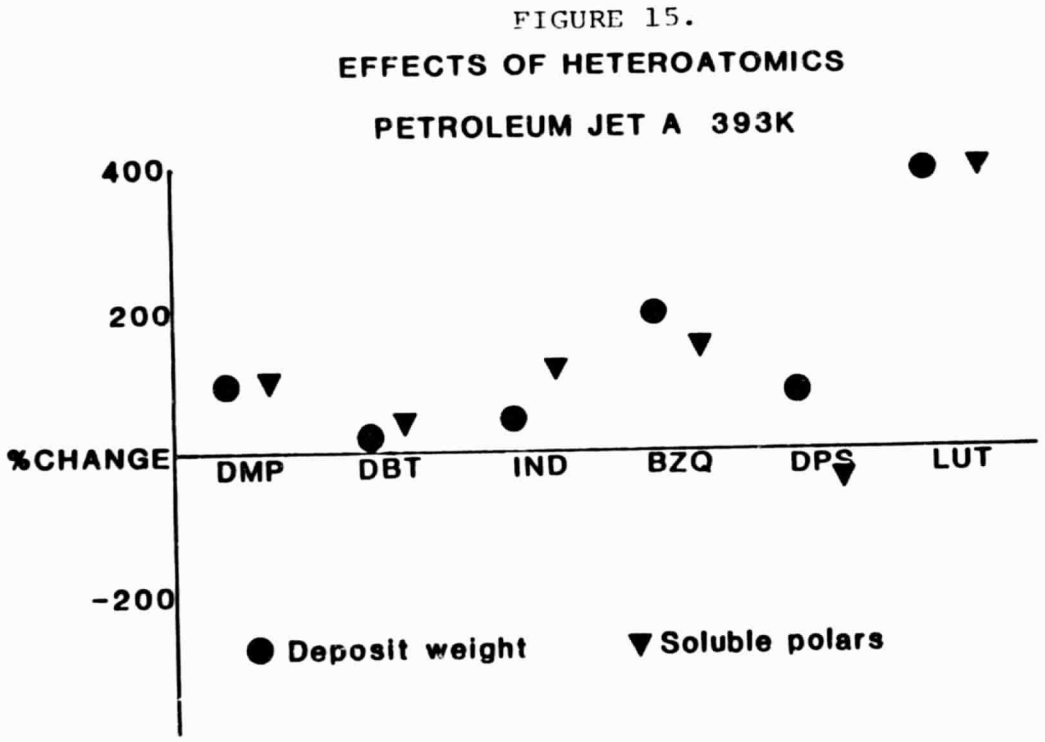
EFFECTS OF HETEROATOMICS
PETROLEUM JET A 393K
400
200
%CHANGE
-200
DMP
DBT
IND
BZQ
DPS
LUT
Deposit weight
Soluble polars

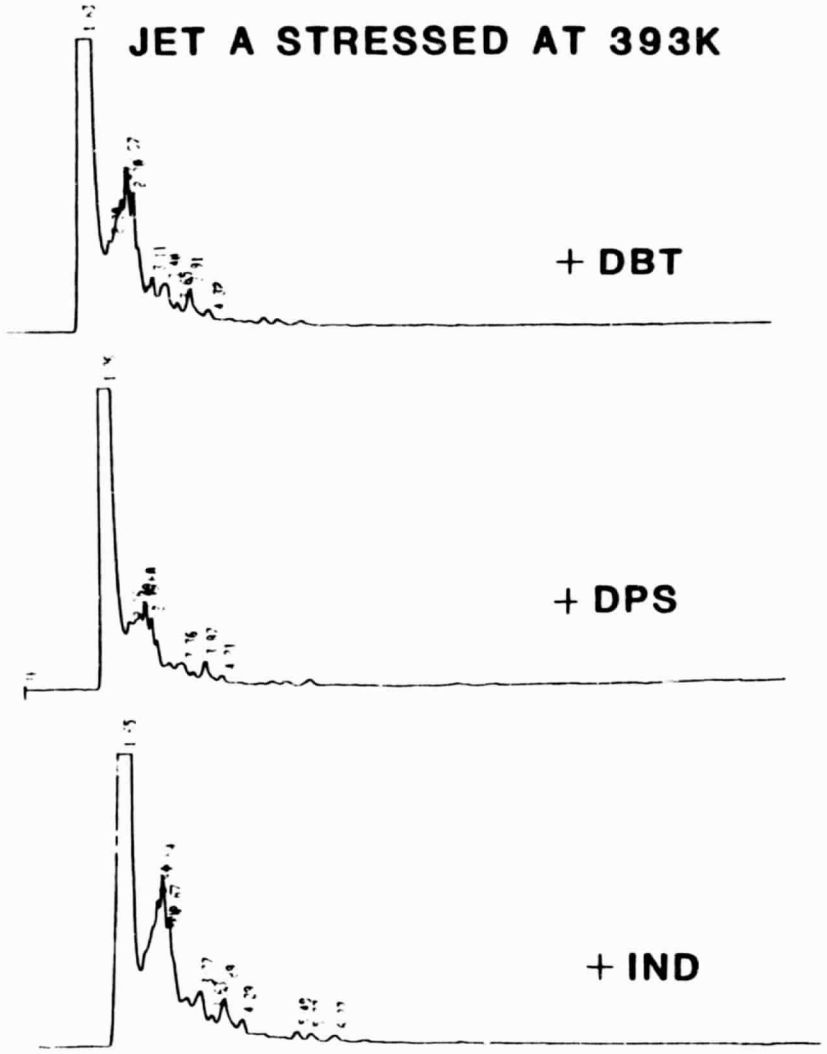

FIGURE 16. EFFECT OF HETEROATOMICS ON FUEL-PHASE COMPOSITION

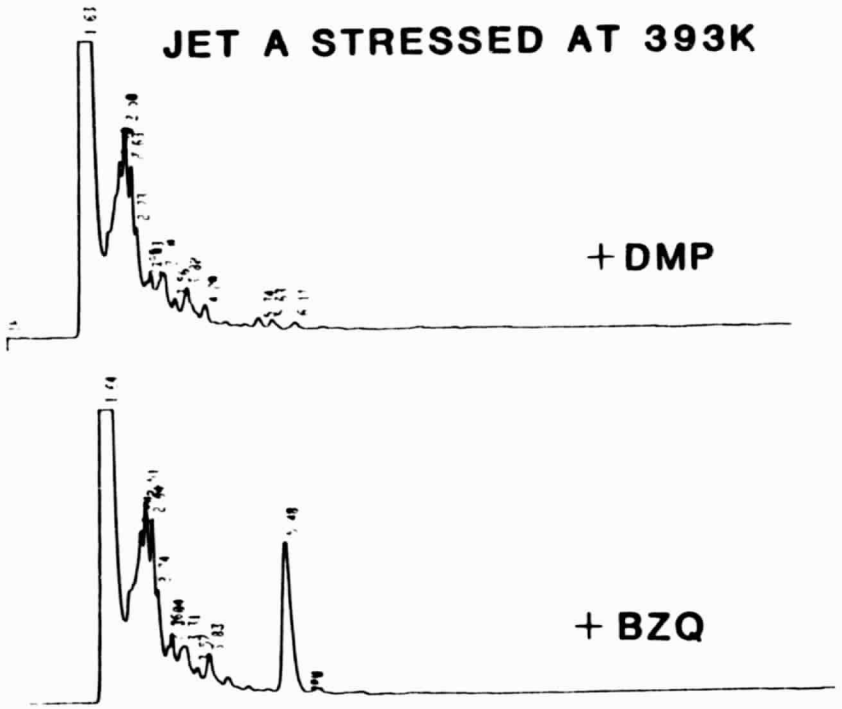

FIGURE 17. EFFECT OF HETEROATOMICS ON FUEL-PHASE COMPOSITION (CON.)

FIGURE 18.

EFFECTS OF HETEROATOMICS

SHALE JP-5 393K

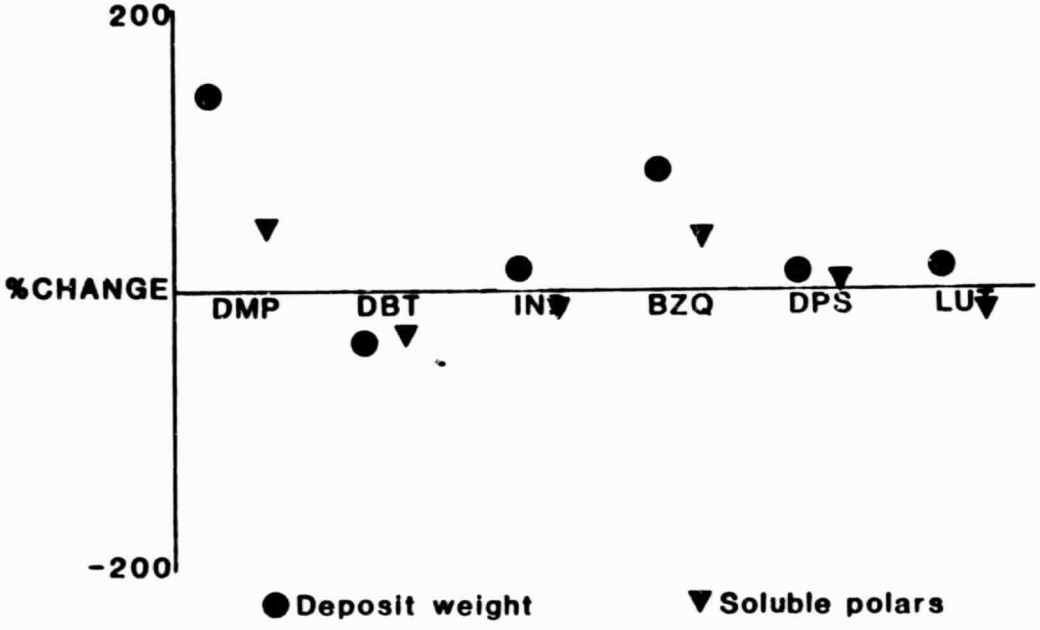

FIGURE 19.

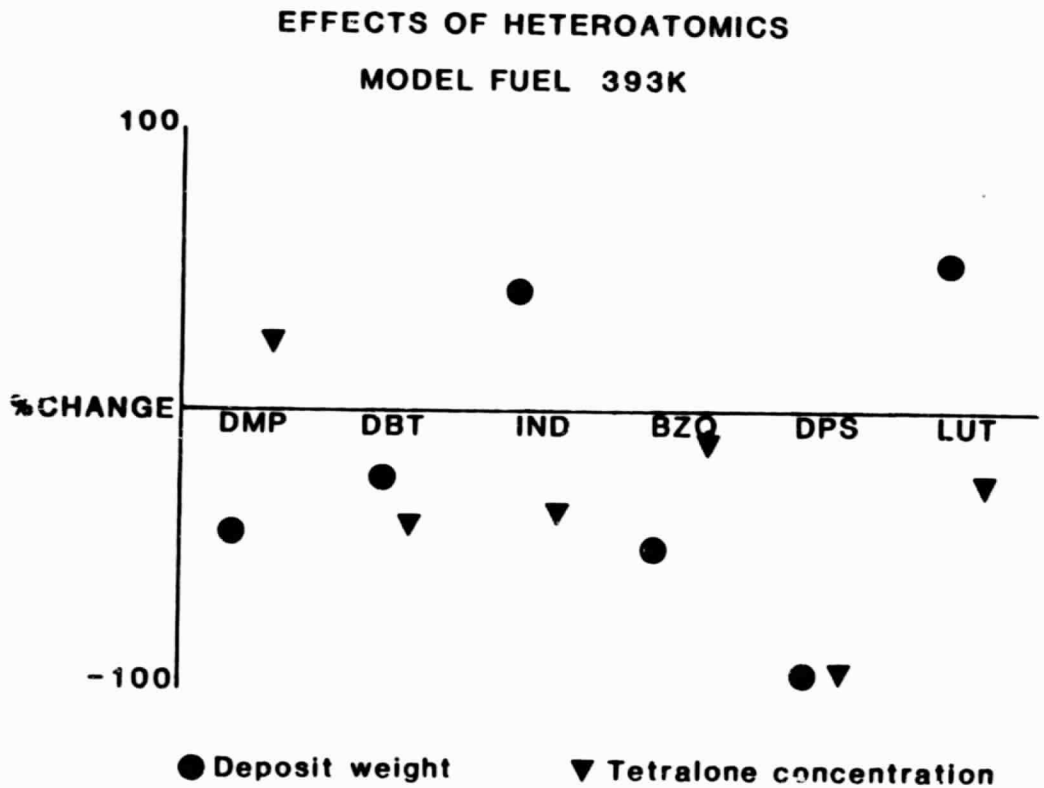
EFFECTS OF HETEROATOMICS
MODEL FUEL 393K
100
%CHANGE
-100
DMP
DBT
IND
BZO
DPS
LUT
Deposit weight
Tetralone concentration

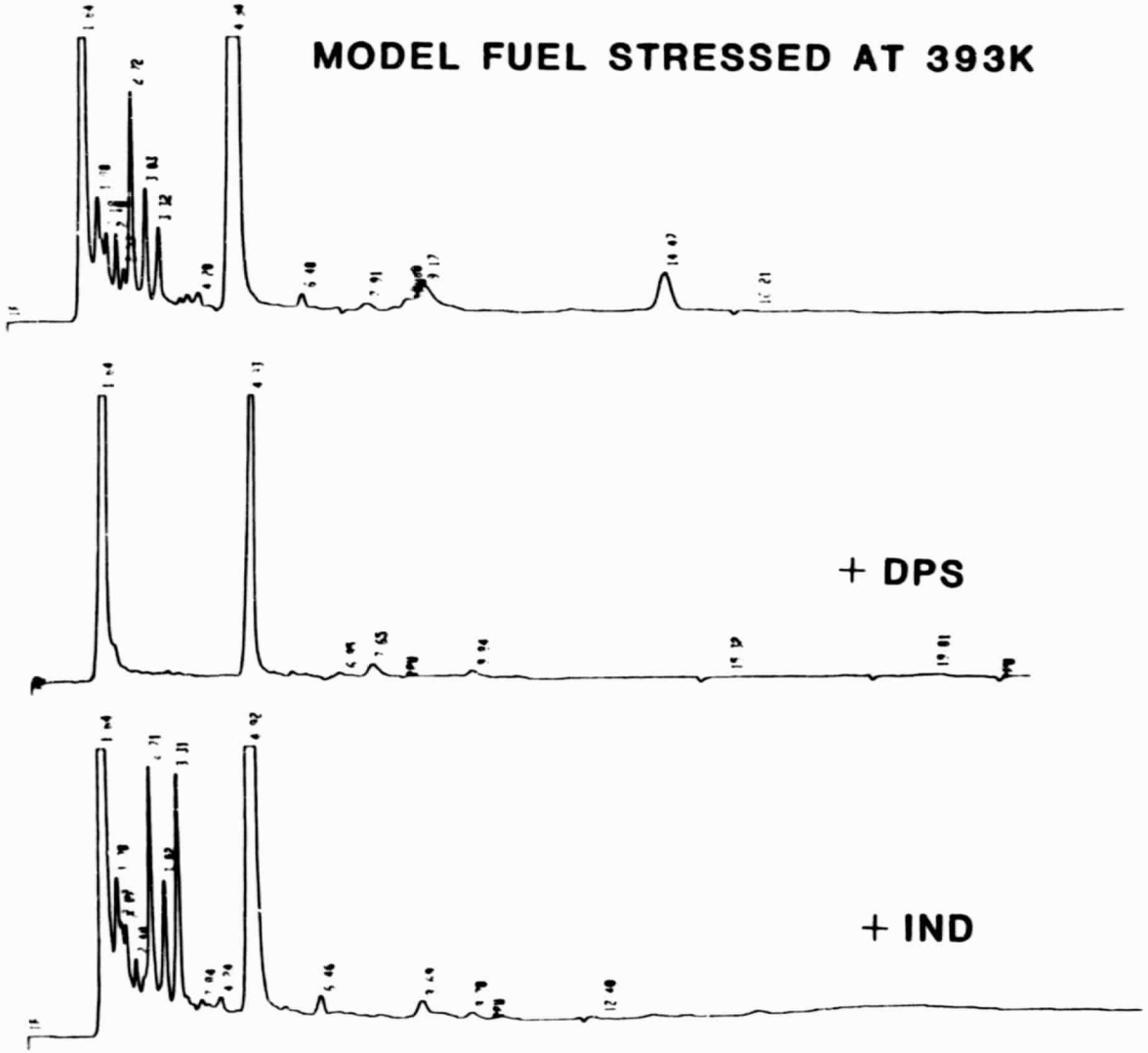

FIGURE 20. EFFECT OF HETEROATOMICS ON LIQUID-PHASE COMPOSITION

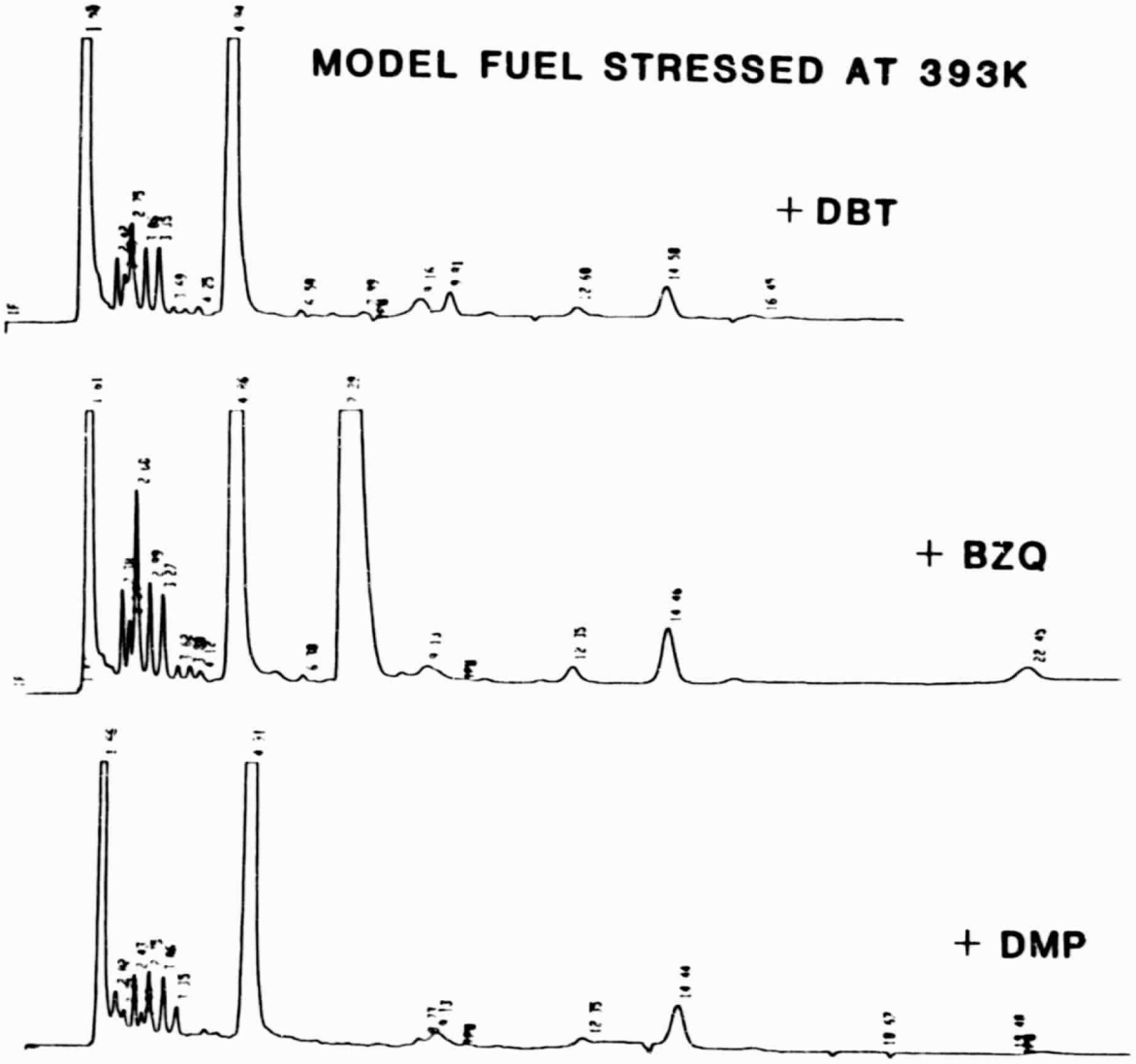

FIGURE 21. EFFECT OF HETEROATOMICS ON LIQUID-PHASE COMPOSITION (CON.)

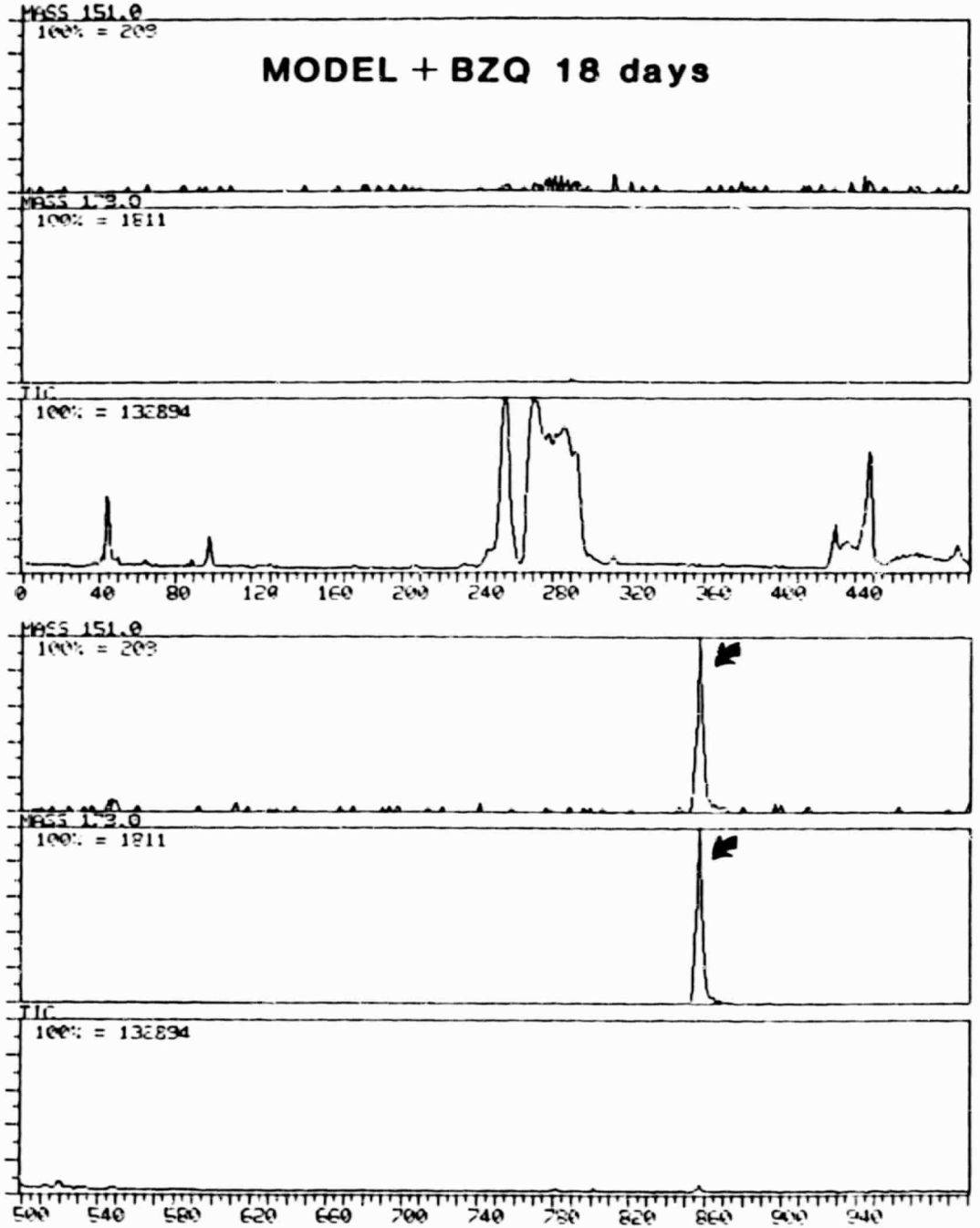

FIGURE 22. FATE OF BENZOQUINOLINE IN STRESSED MODEL FUEL

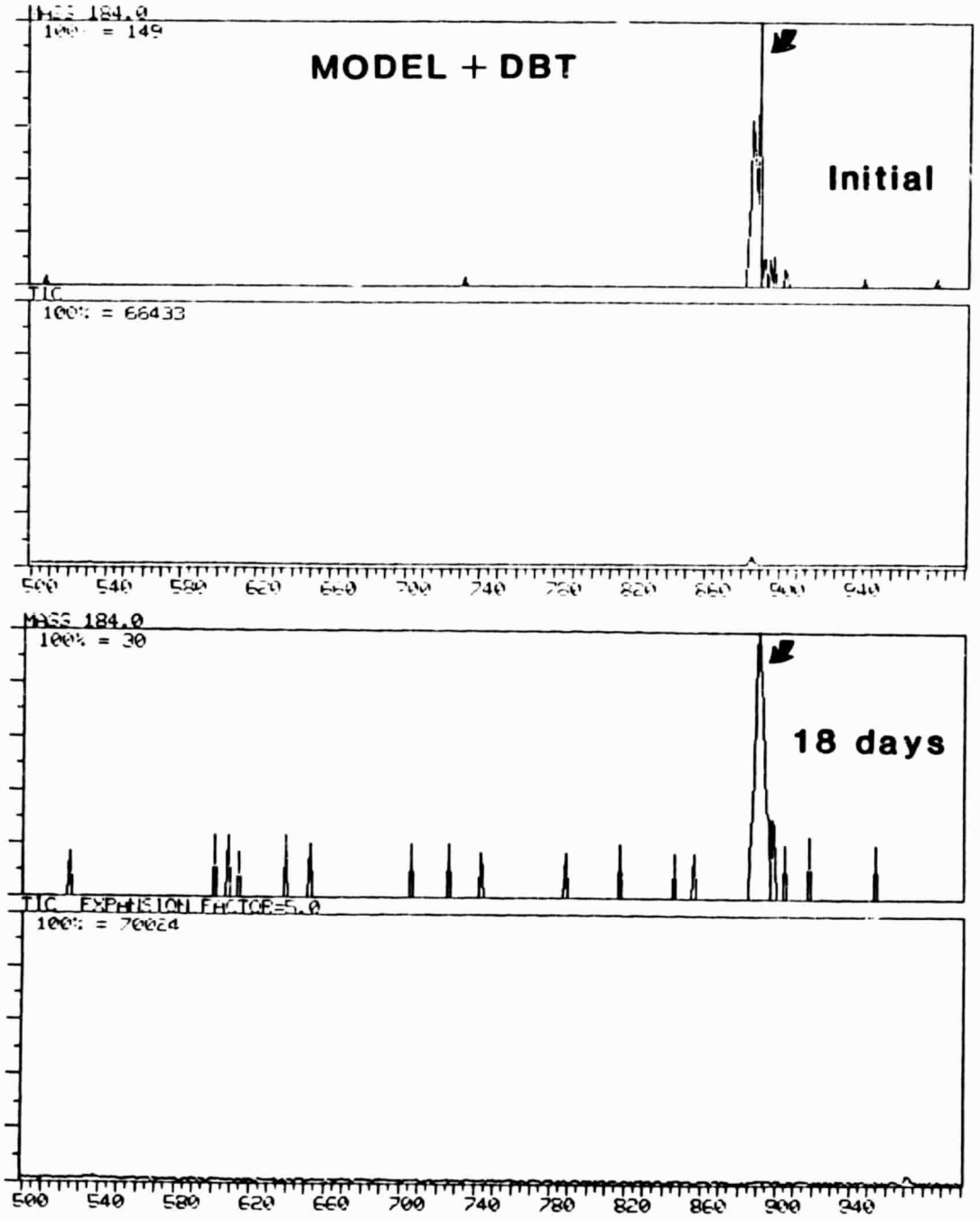

FIGURE 23. FATE OF DIBENZOTHIOPHENE IN STRESSED MODEL FUEL

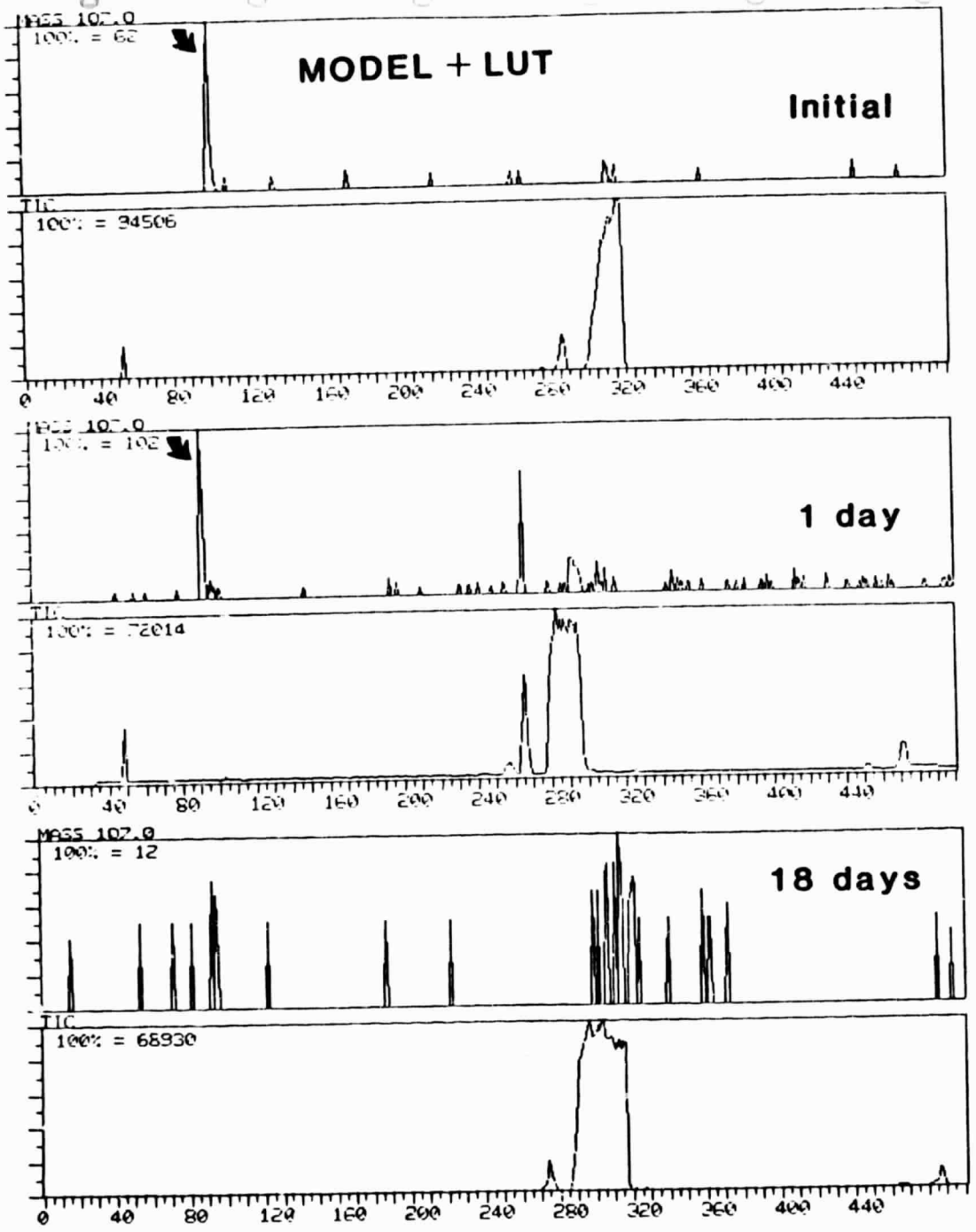

FIGURE 24. FATE OF DIMETHYLPYRIDINE IN STRESSED MODEL FUEL

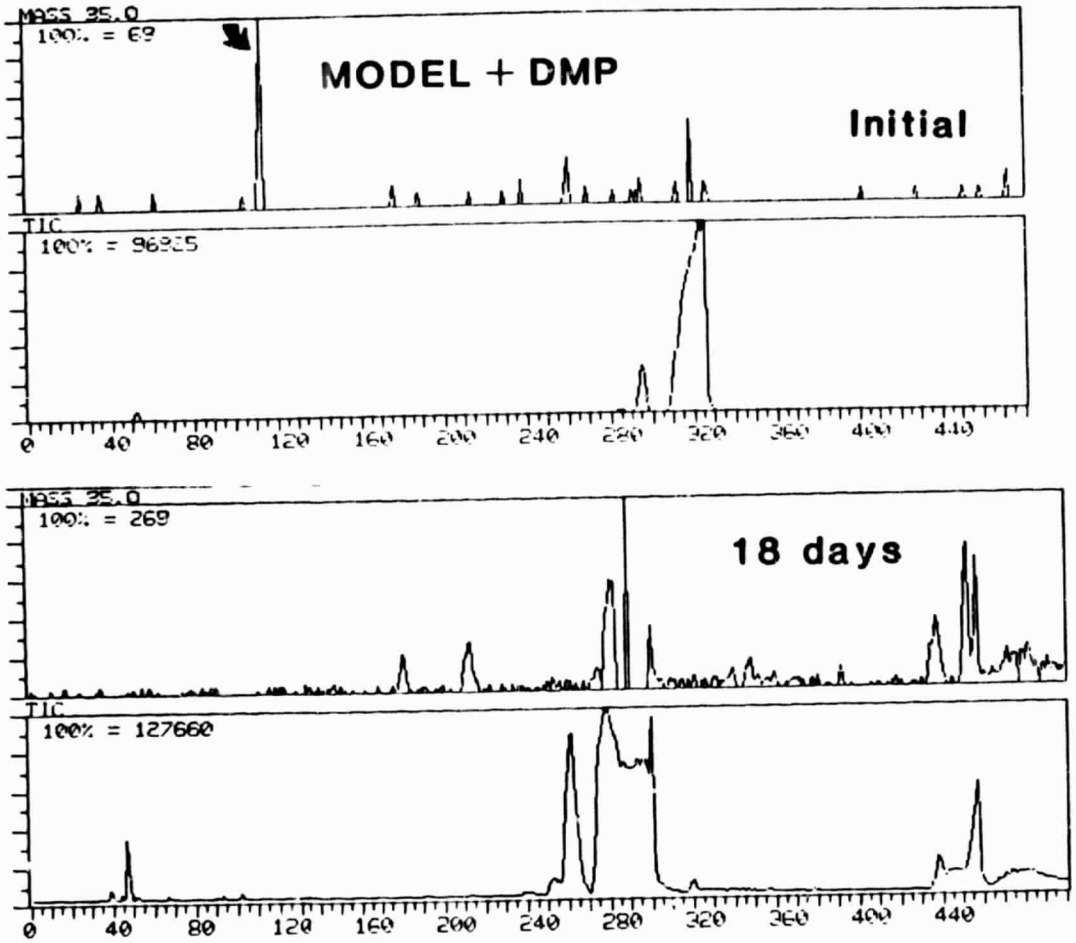

FIGURE 25. FATE OF DIMETHYLPYRROLE IN STRESSED MODEL FUEL

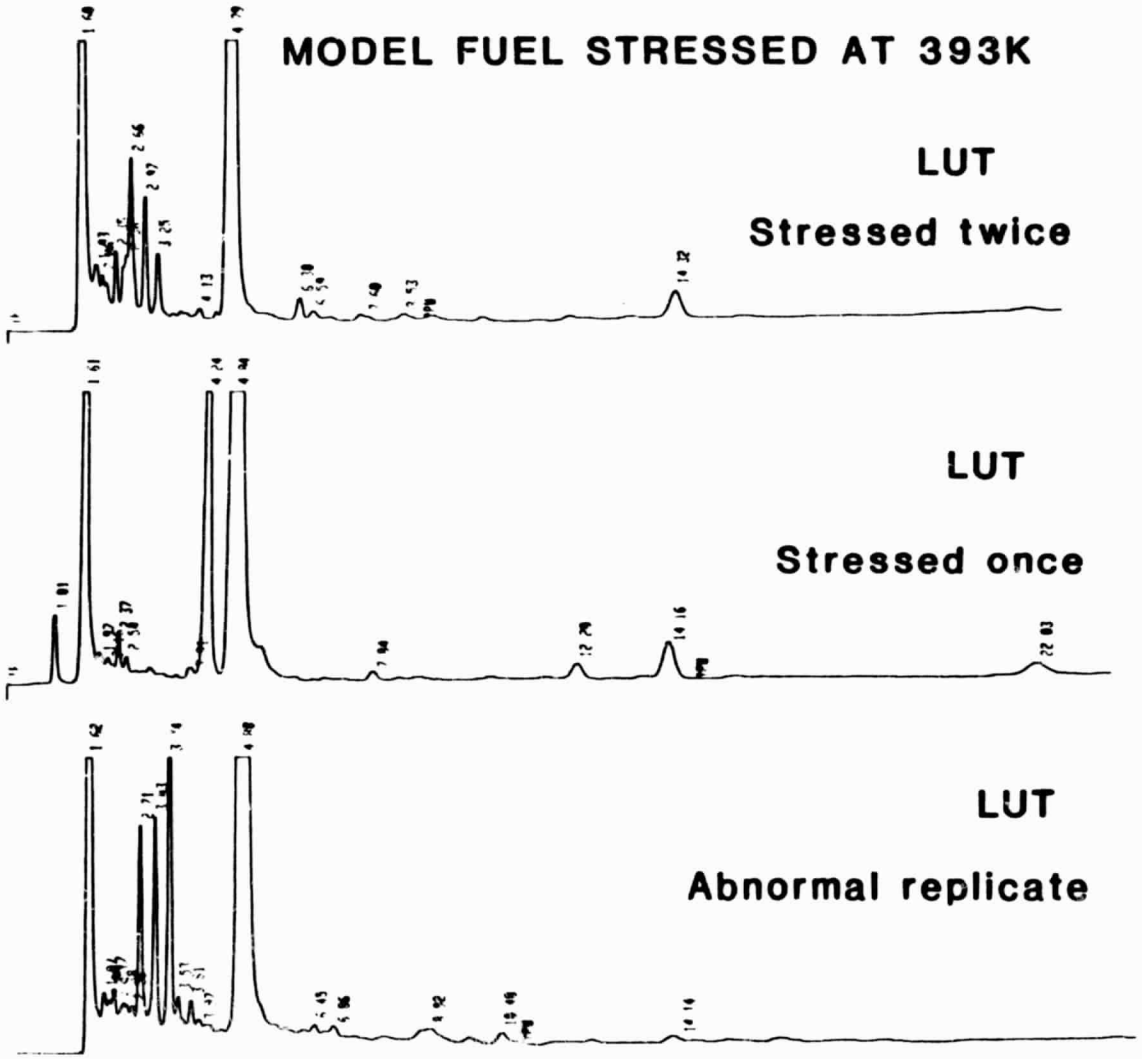

FIGURE 26. EFFECT OF DIMETHYLPYRIDINE ON MODEL FUEL

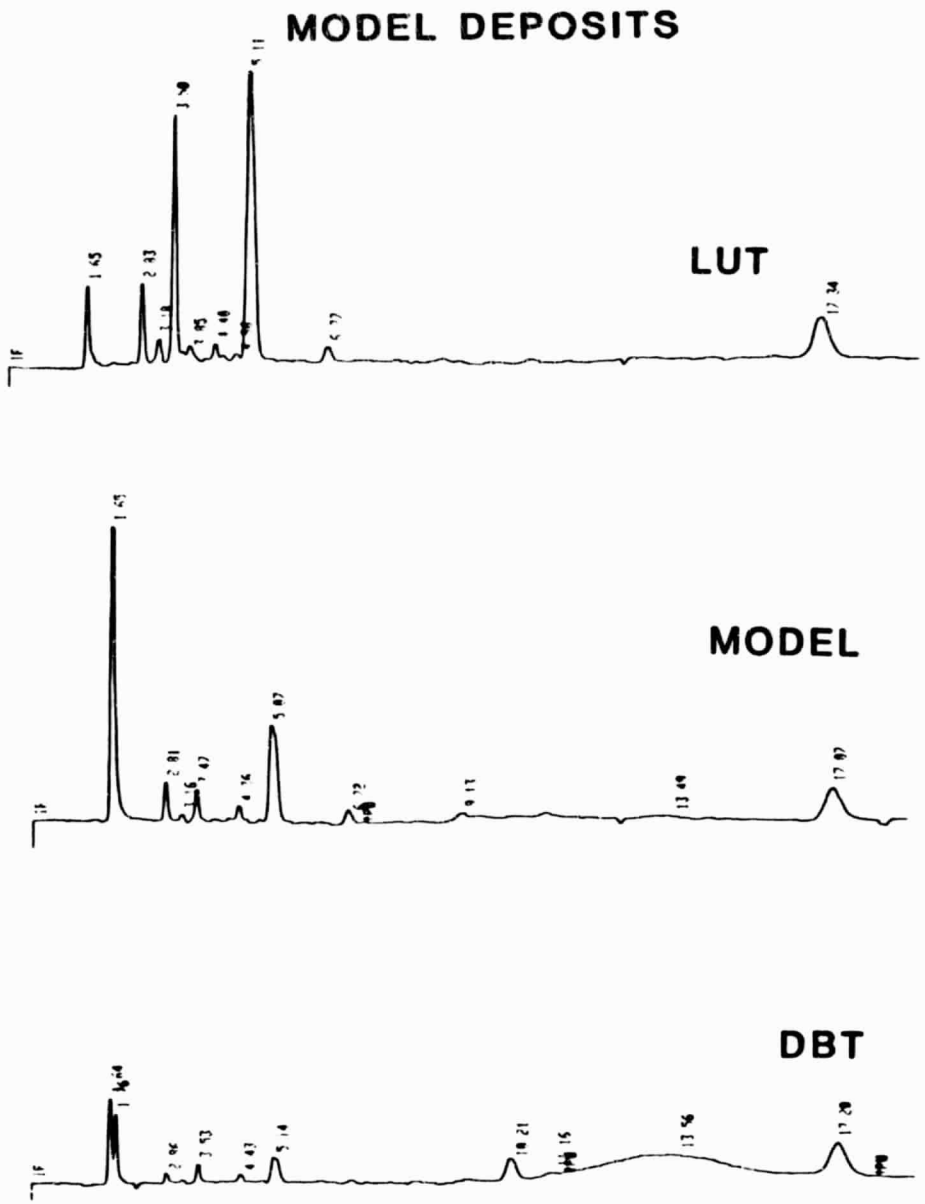

FIGURE 27. HPLC ANALYSES - MODEL DEPOSITS

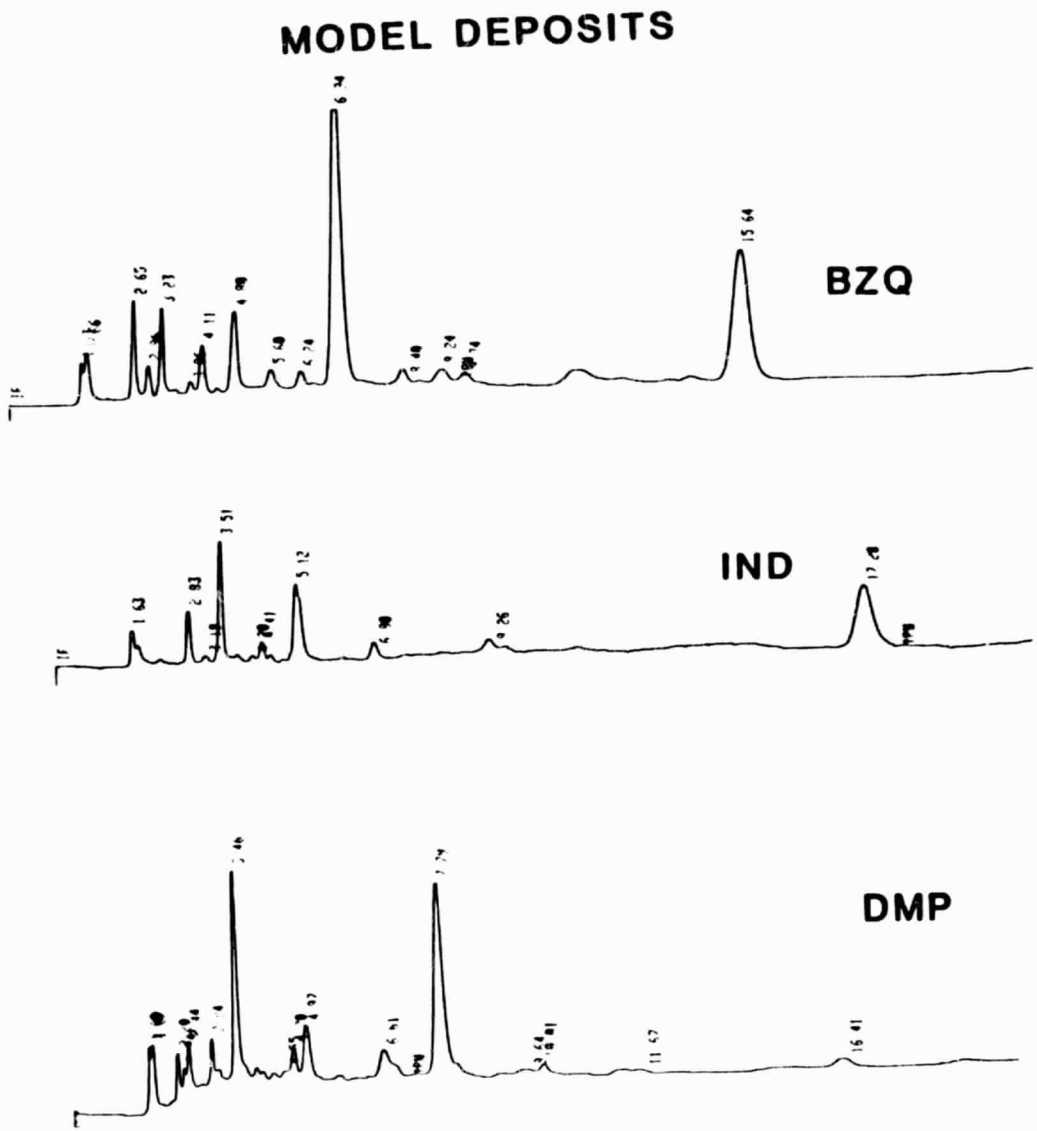

FIGURE 28. HPLC ANALYSES - MODEL DEPOSITS (CON.)

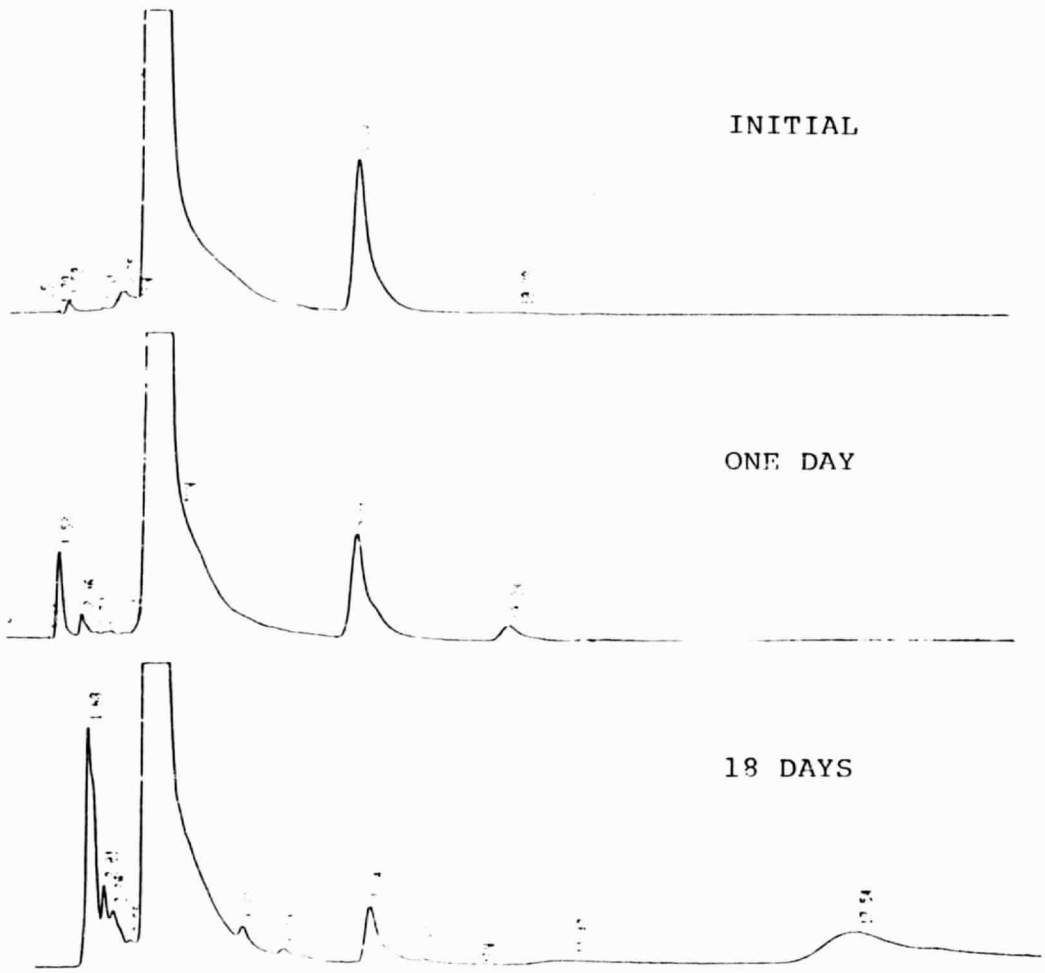

FIGURE 29. HPLC OF TETRALONE-HYDROPEROXIDE REACTION MIXTURE

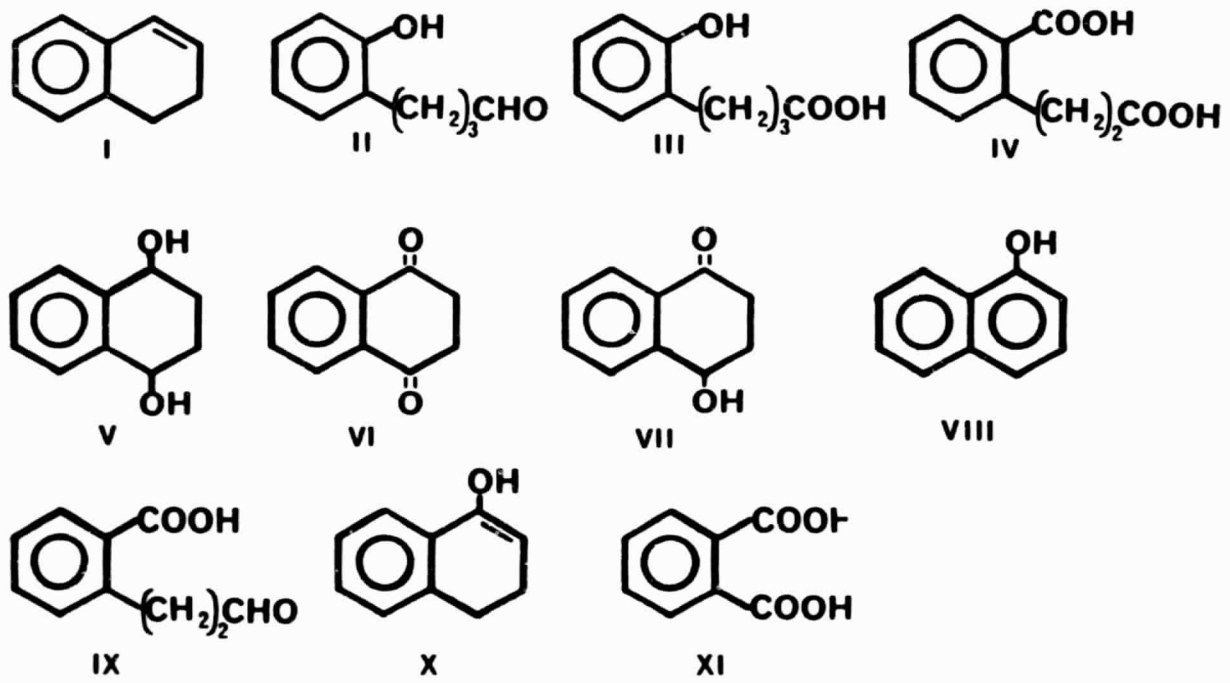

FIGURE 30. SOME OXIDATION PRODUCTS OF 1-TETRALONE

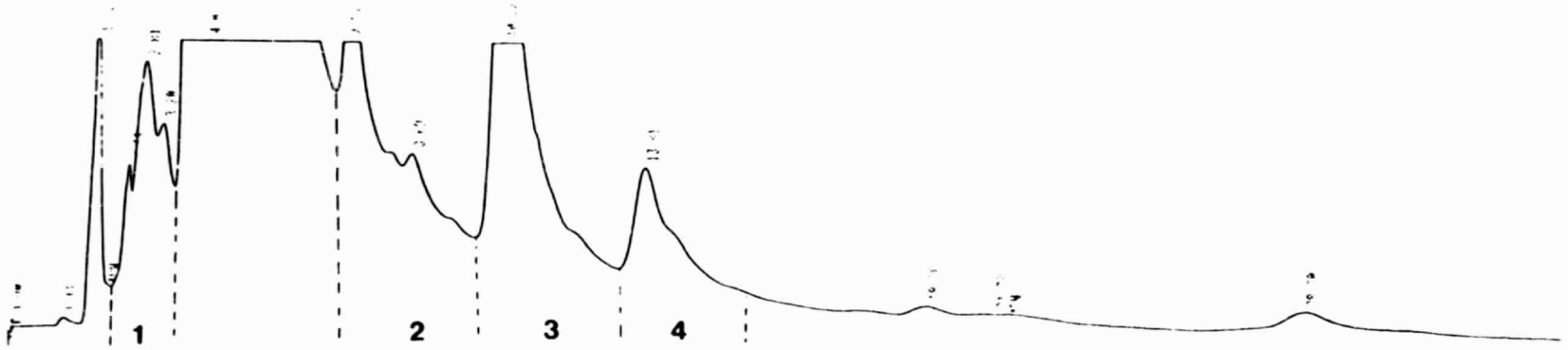

FIGURE 31. HPLC FRACTIONATION OF OXIDIZED TETRALONE

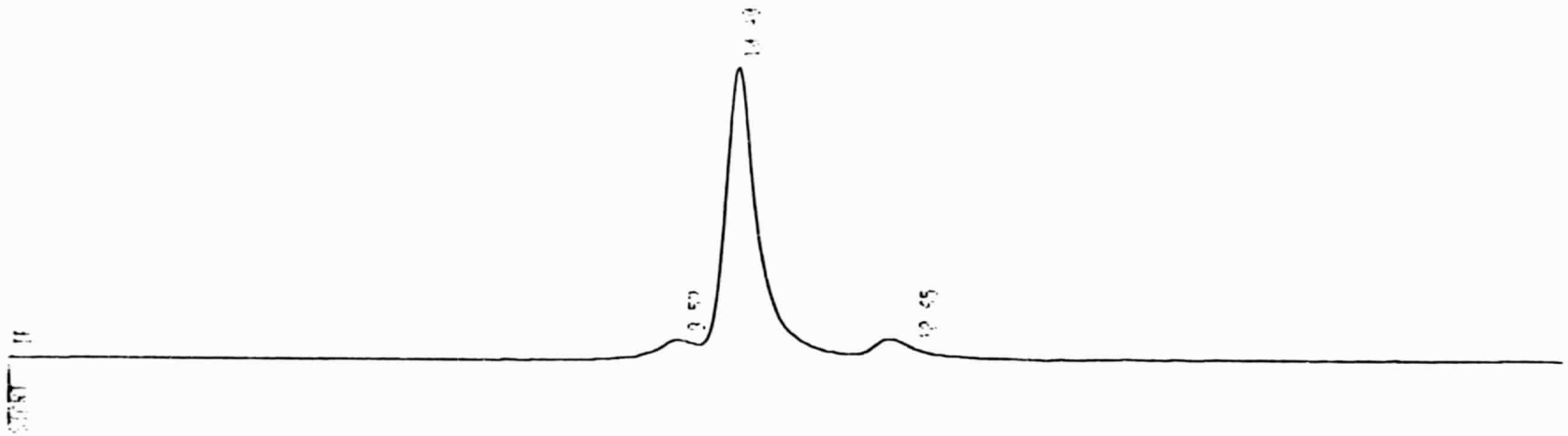

FIGURE 32. GEL PERMEATION CHROMATOGRAM OF OXIDIZED TETRALONE

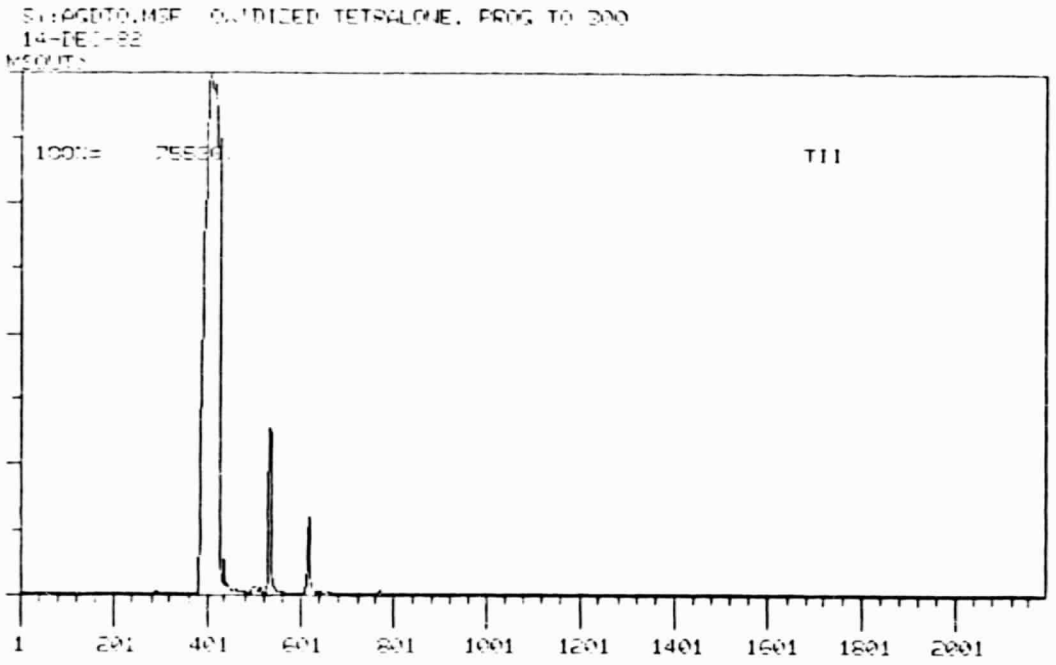

FIGURE 33. TOTAL ION CHROMATOGRAM - OXIDIZED TETRALONE

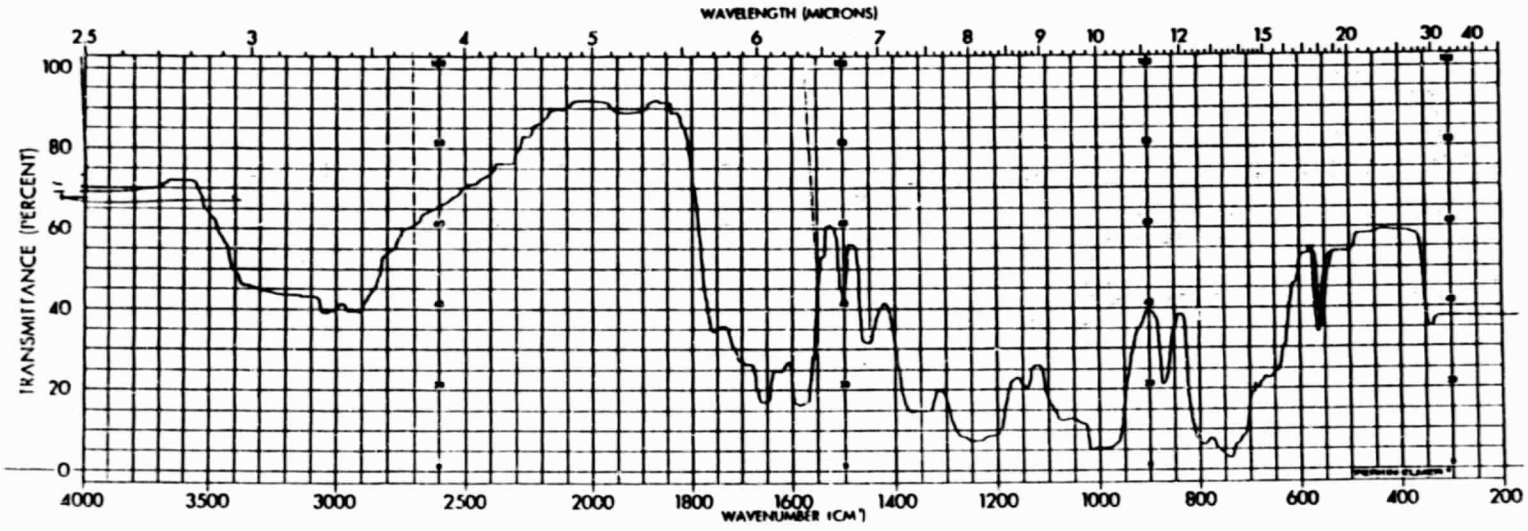

FIGURE 34. MIR - BASE-SOLUBLE FRACTION OF OXIDIZED TETRALONE

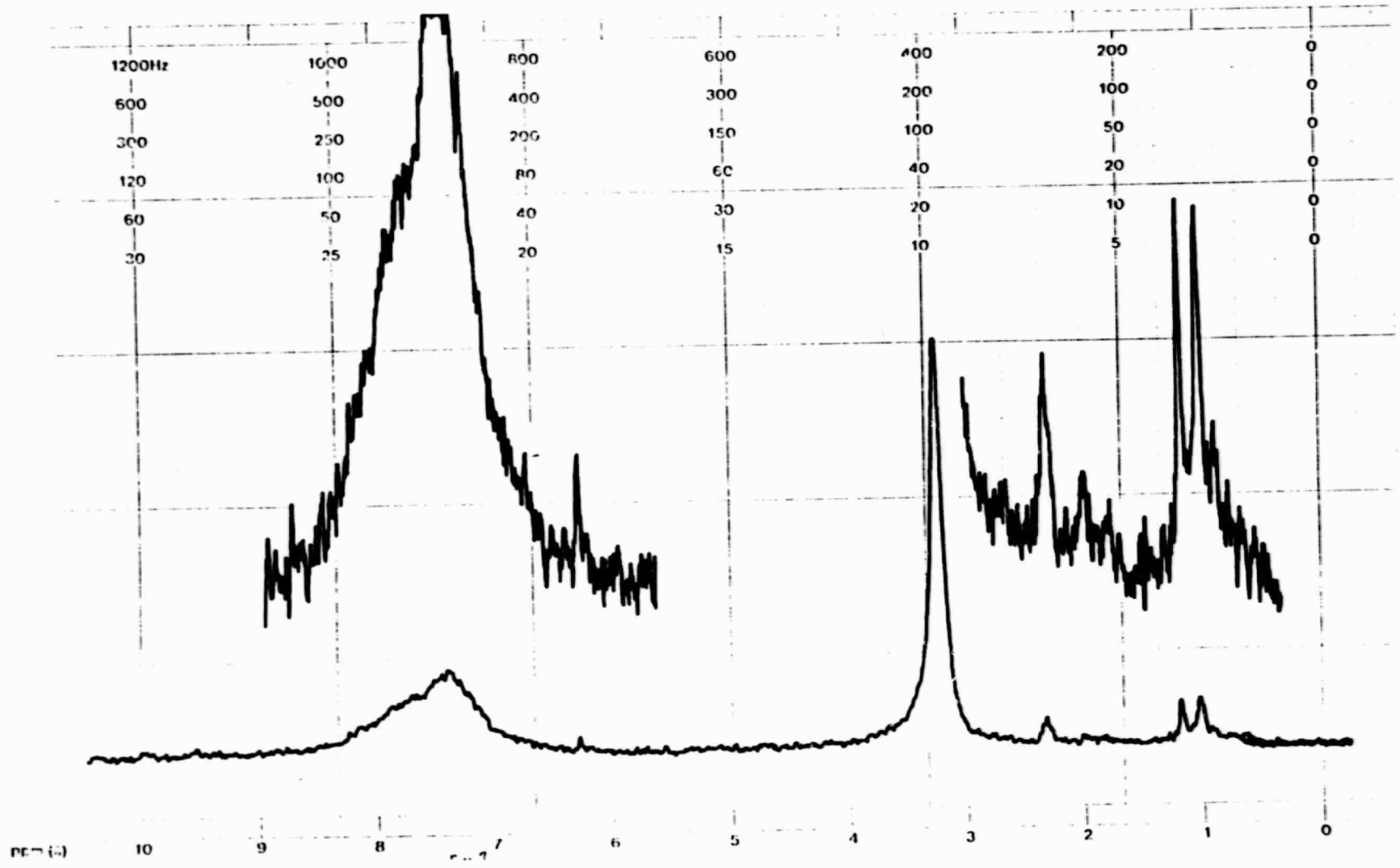

FIGURE 35. ^{1}H NMR - BASE-SOLUBLE FRACTION OF OXIDIZED TETRALONE

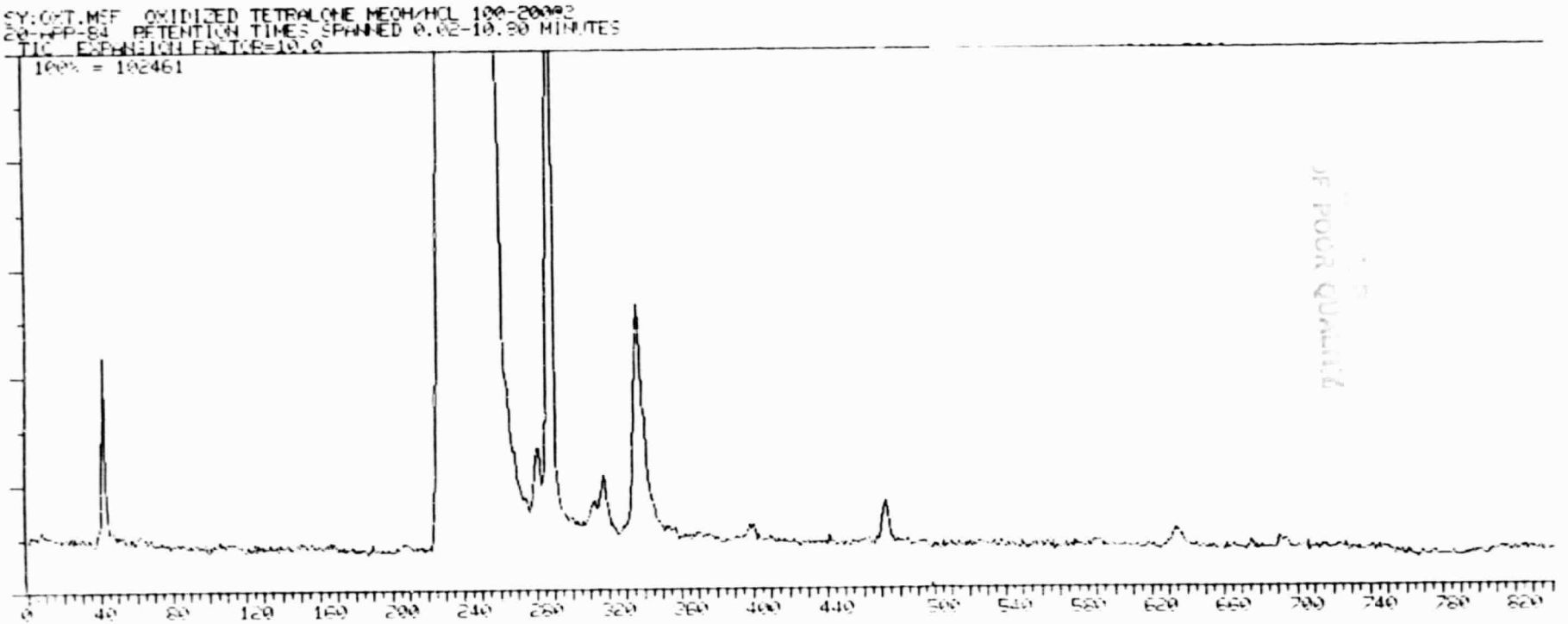

FIGURE 36. TOTAL ION CHROMATOGRAM - METHYLATED OXIDIZED TETRALONE

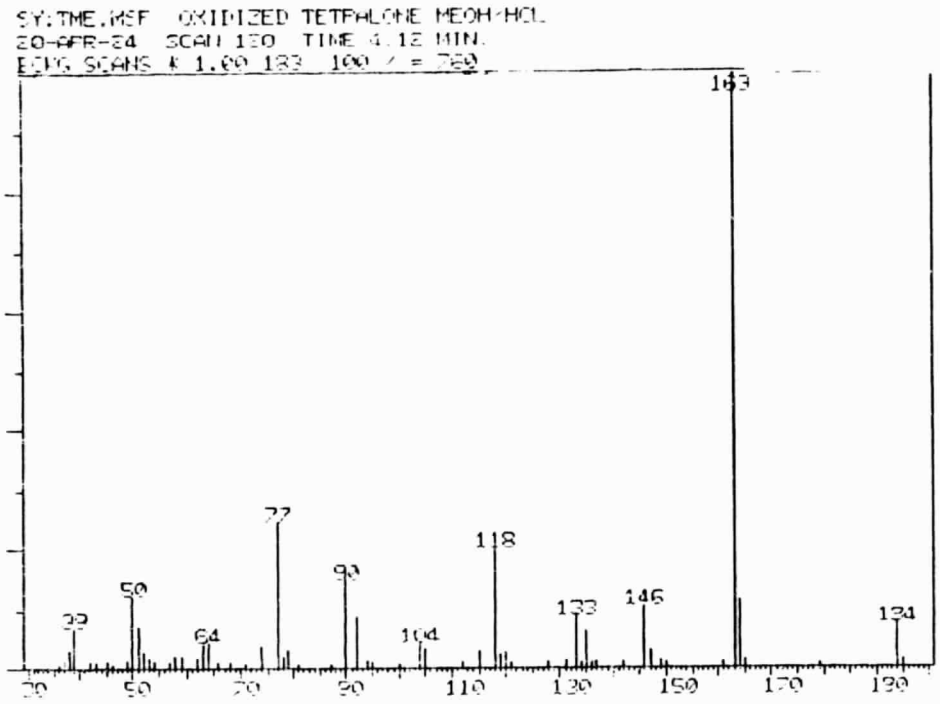

FIGURE 37. DIMETHYLPHTHALATE IN METHYLATED OXIDATION PRODUCTS

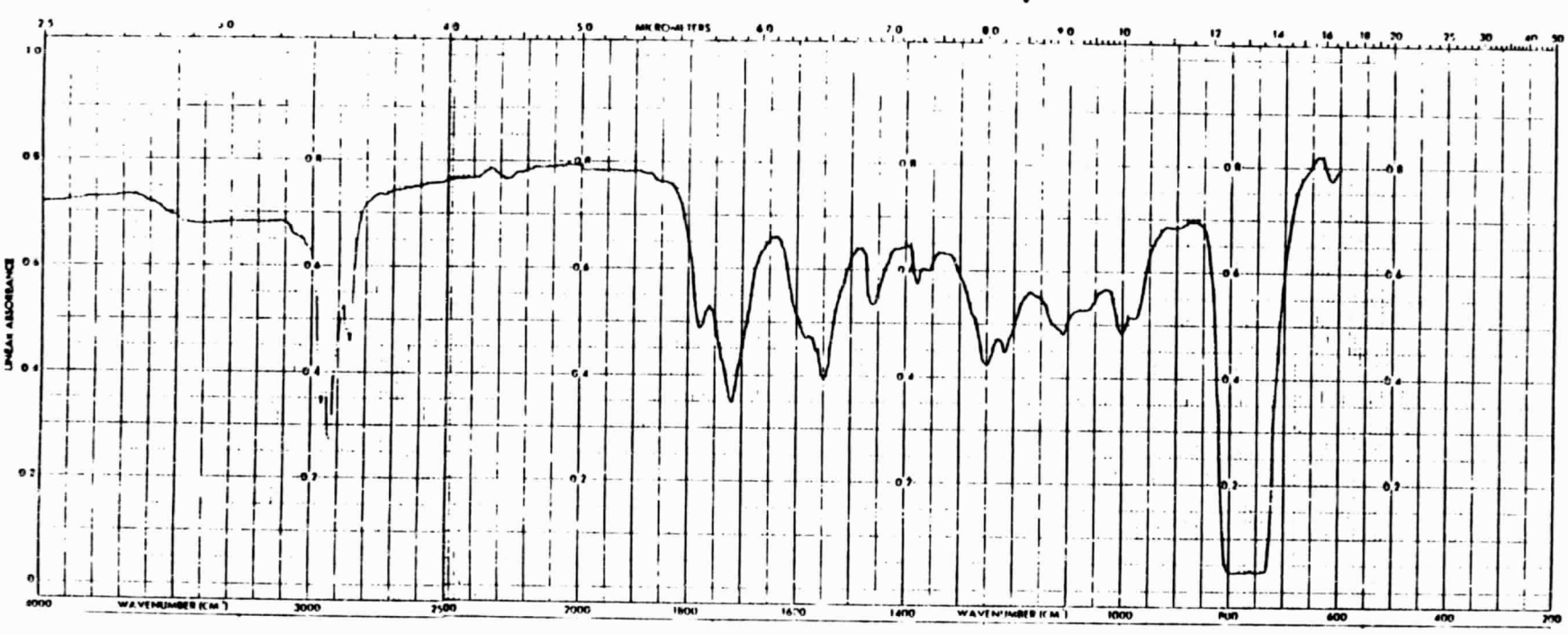

FIGURE 38. IR SPECTRUM - JP5 DEPOSIT

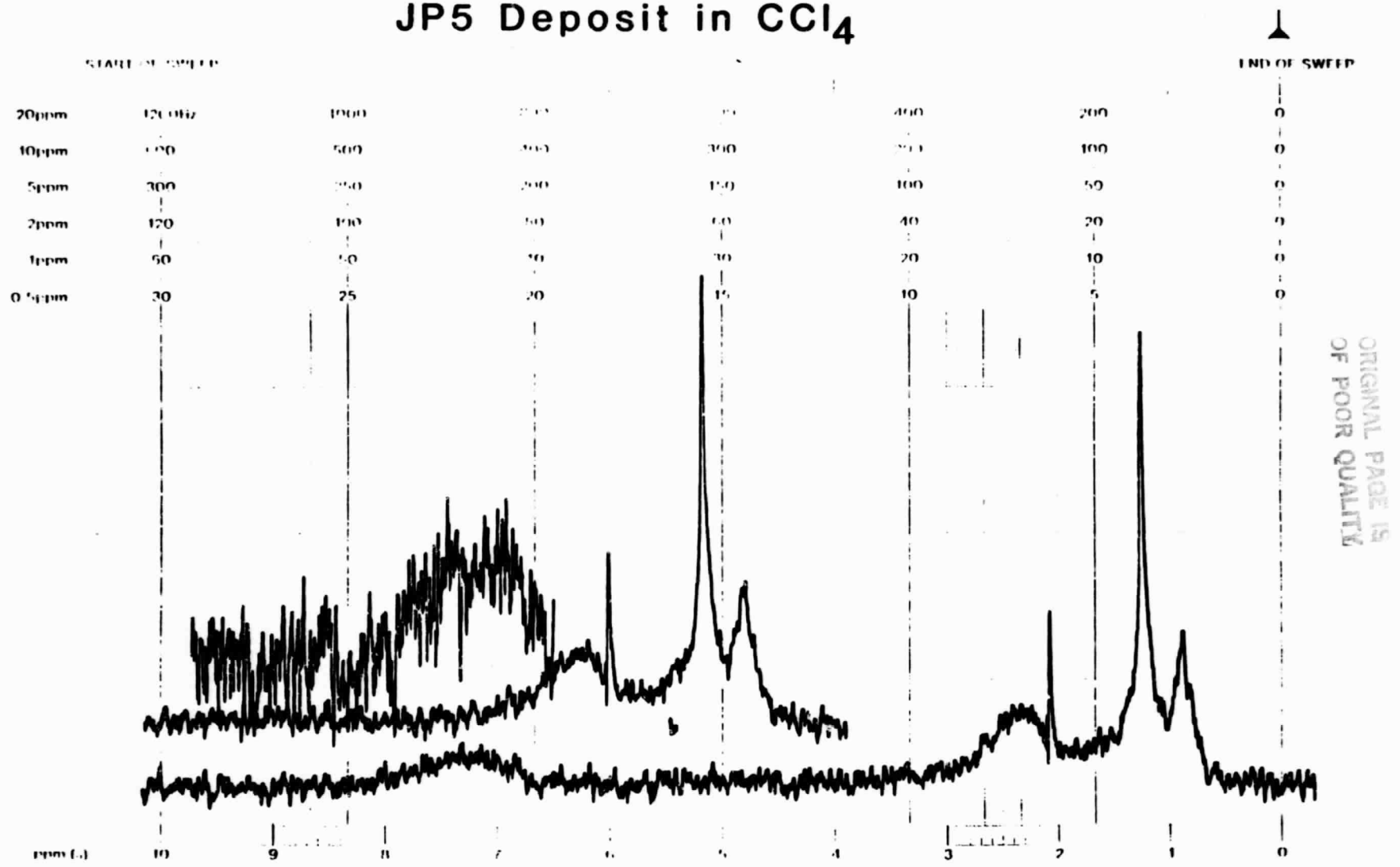

FIGURE 39. ^{1}H NMR SPECTRUM - JP5 DEPOSIT

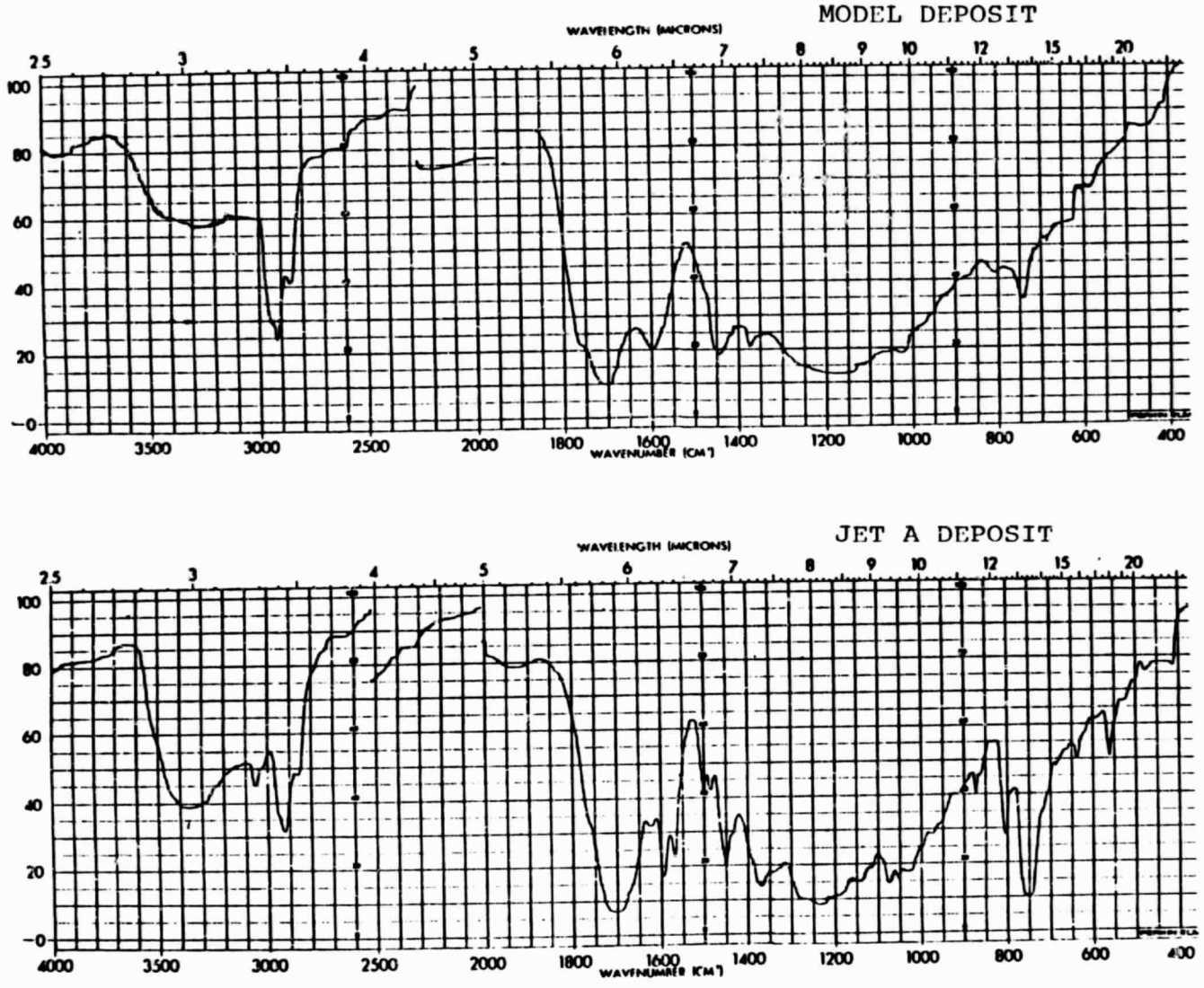

FIGURE 40. MIR SPECTRA - FUEL DEPOSITS

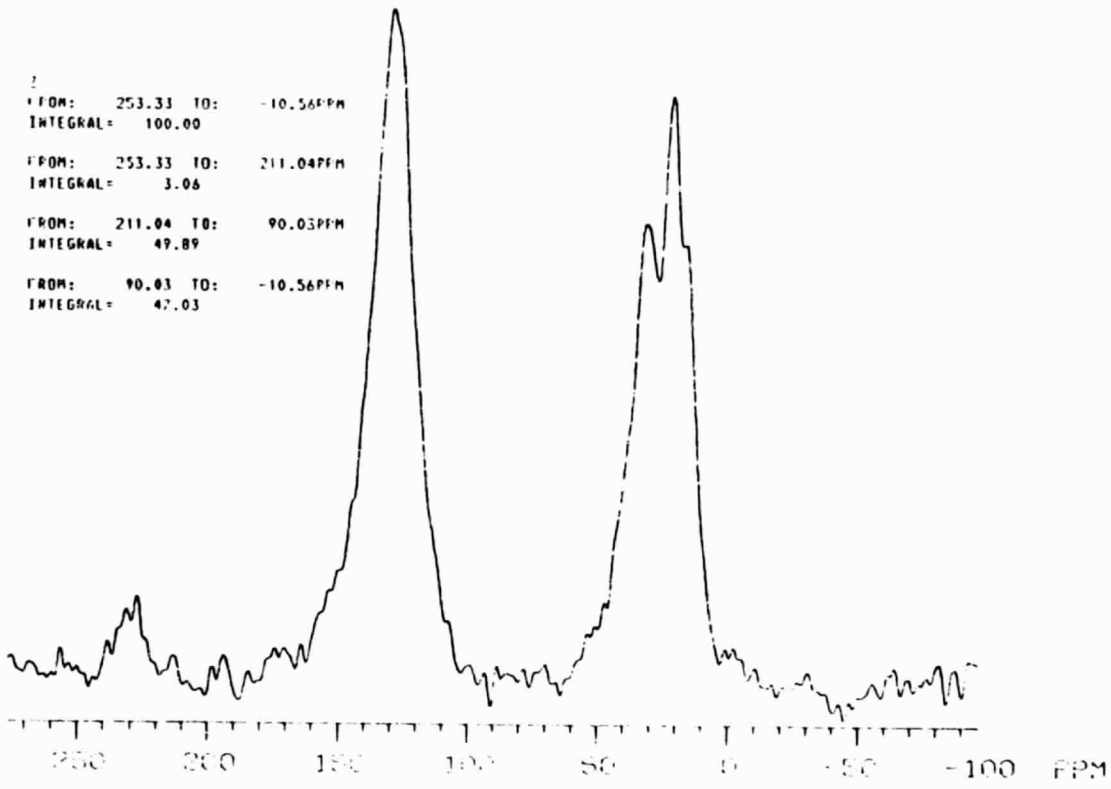

FIGURE 41. CP/MAS SPECTRUM - JET A DEPOSIT

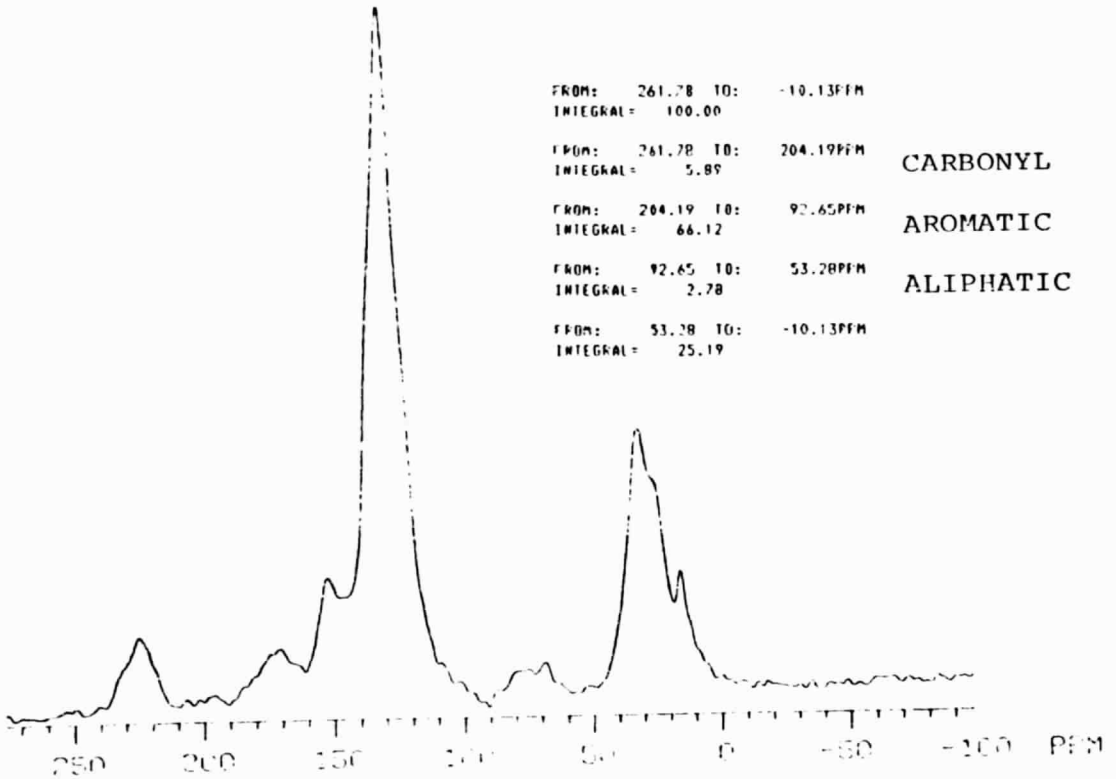

FIGURE 42. CP/MAS SPECTRUM - MODEL DEPOSIT

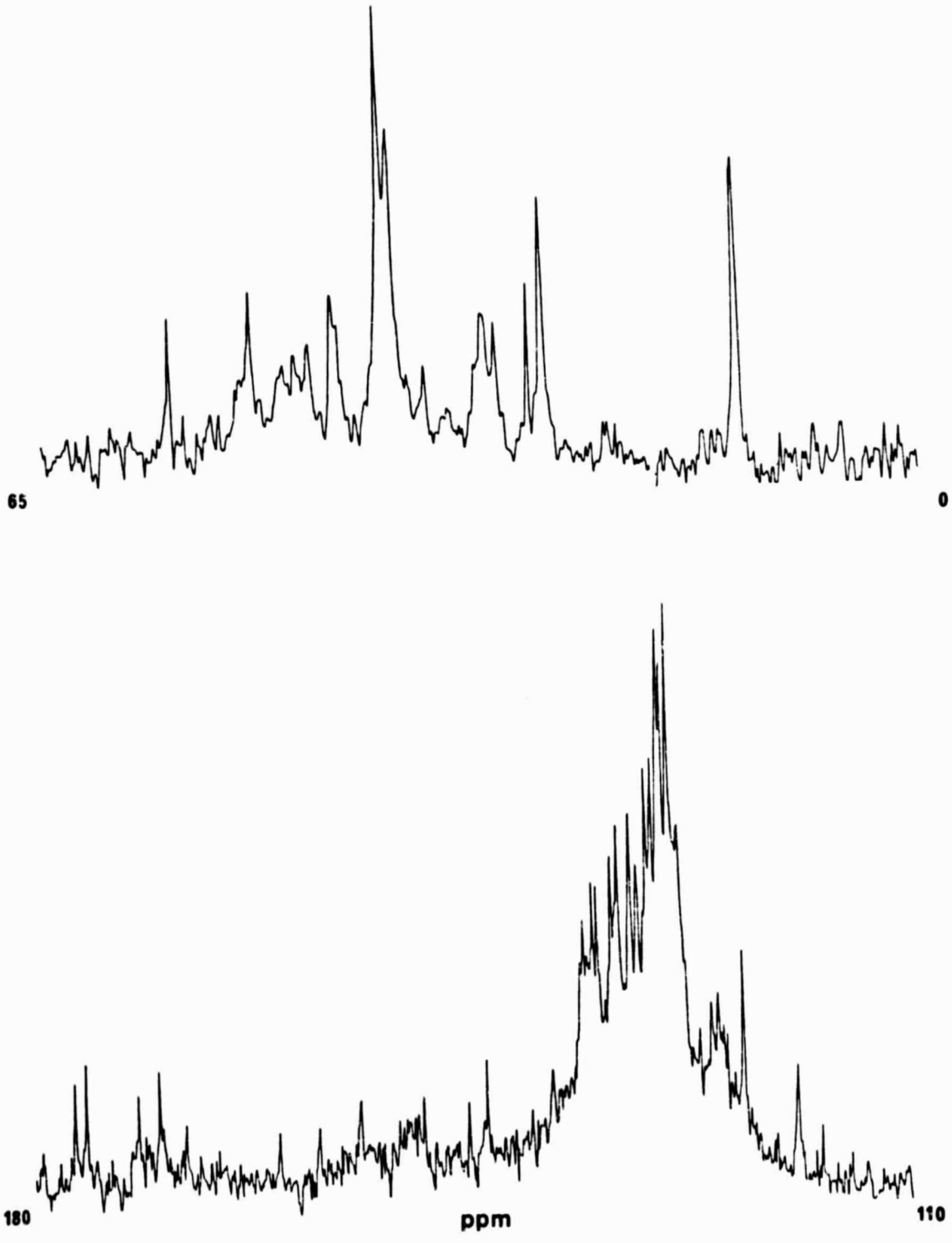

FIGURE 43. SOLUTION-PHASE ^{13}C NMR SPECTRUM - MODEL DEPOSIT

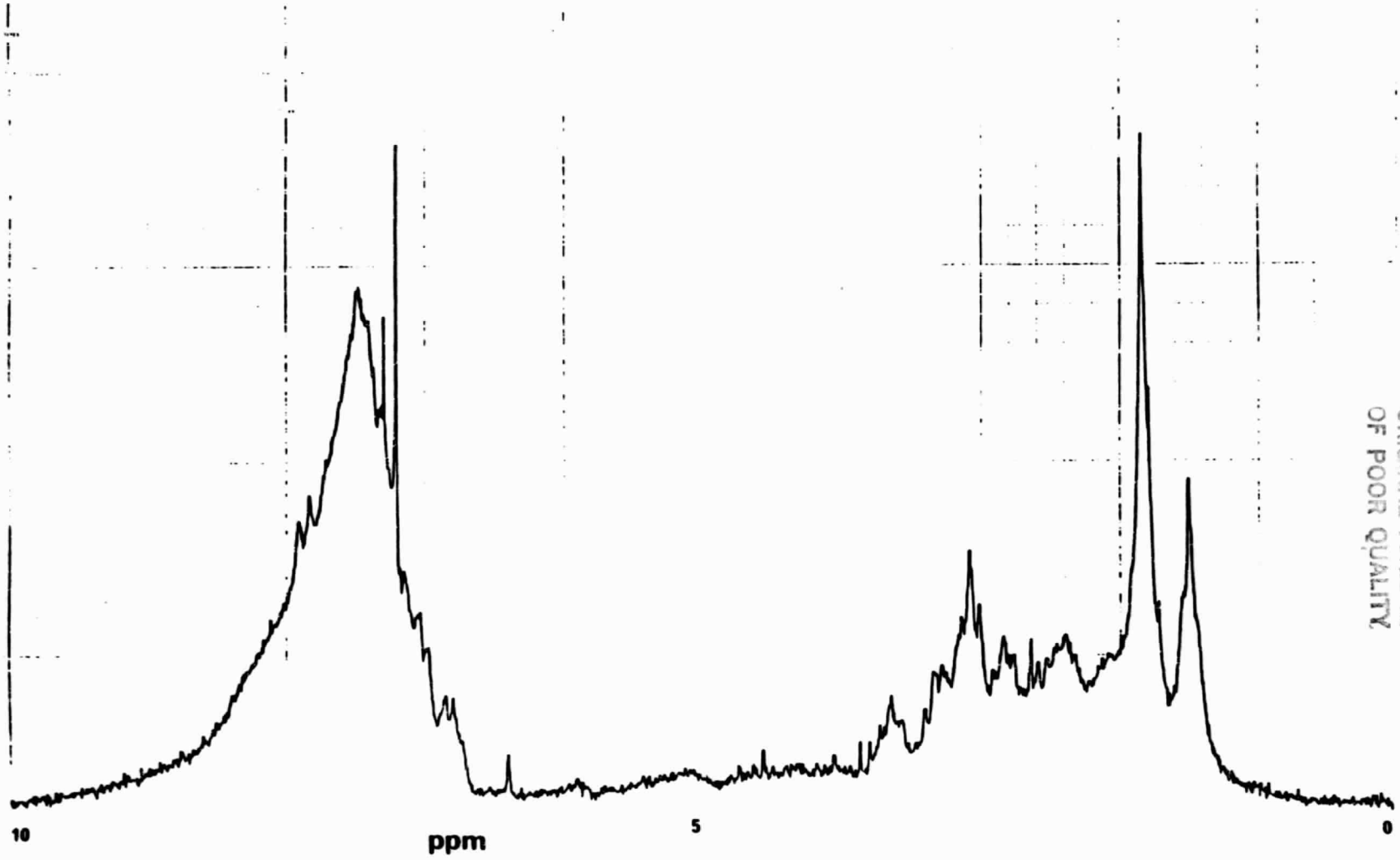

FIGURE 44. ^{1}H NMR SPECTRUM - MODEL DEPOSIT

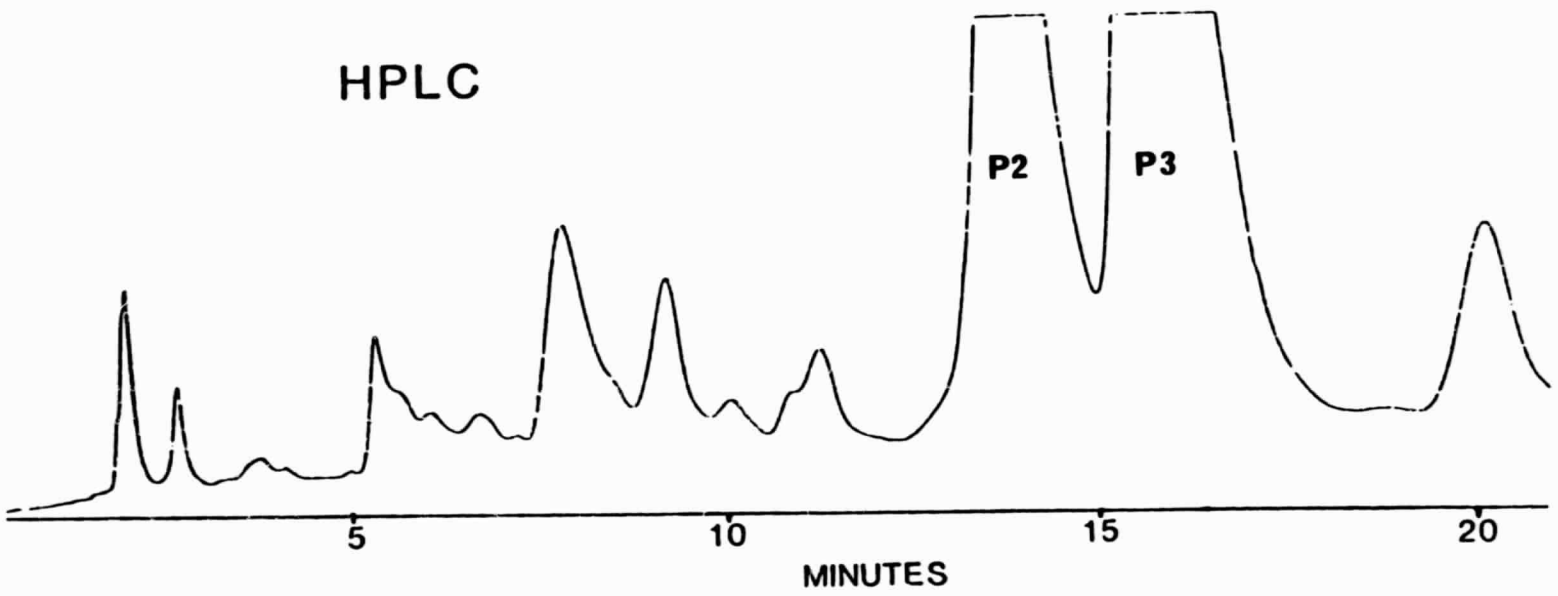

FIGURE 45. HPLC FRACTIONATION - MODEL DEPOSIT

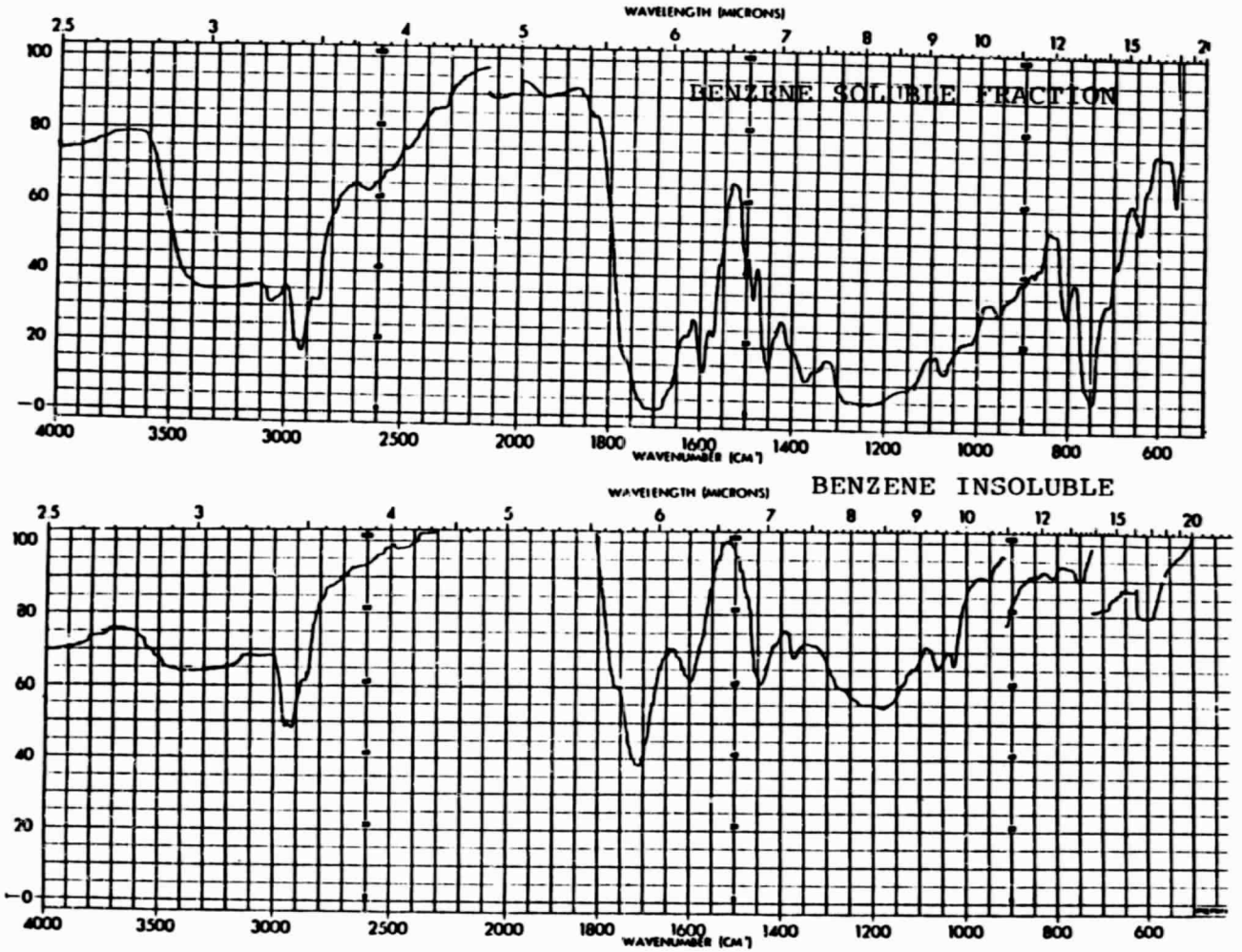

FIGURE 46. MIR SPECTRA - MODEL DEPOSIT FRACTIONS

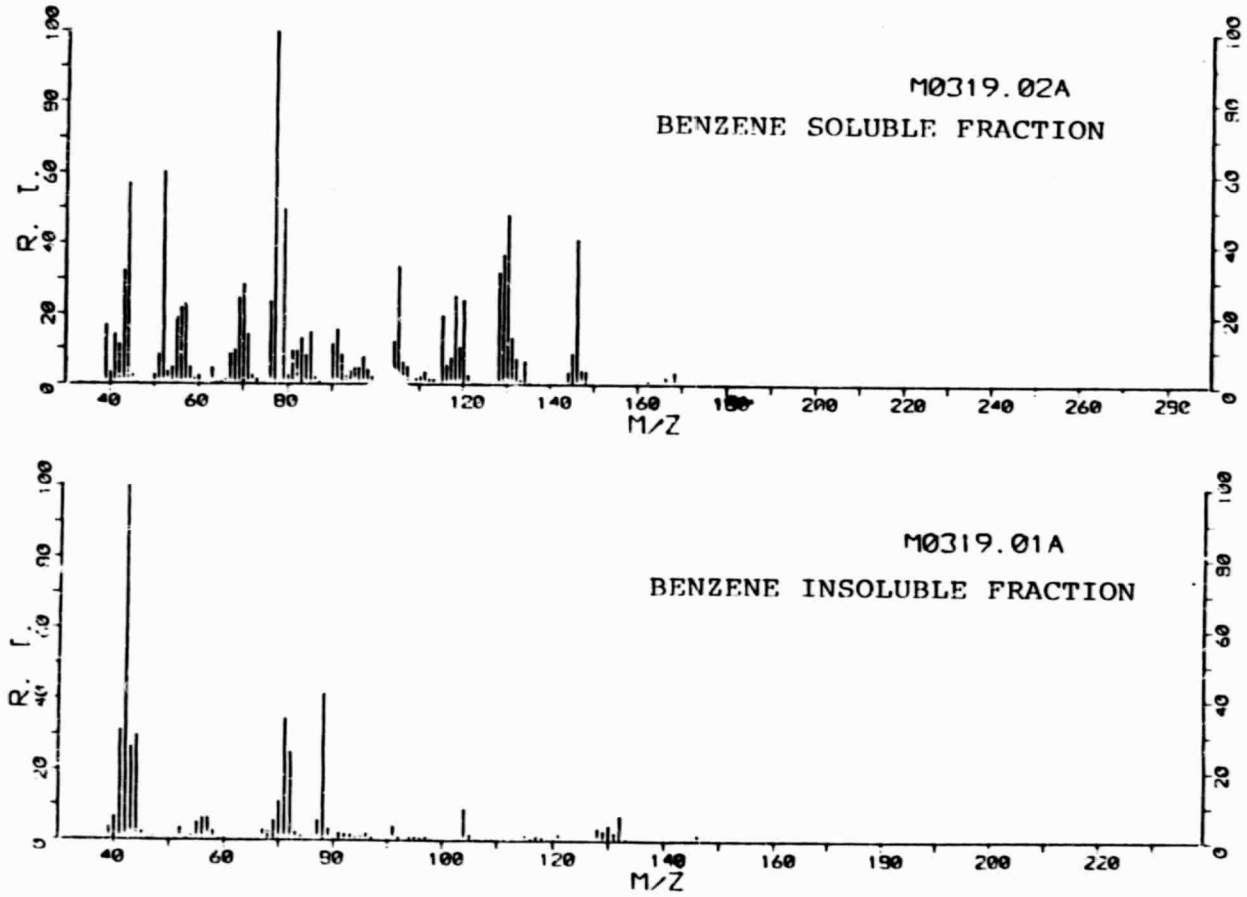

FIGURE 47. py/MS SPECTRA - MODEL DEPOSIT FRACTIONS

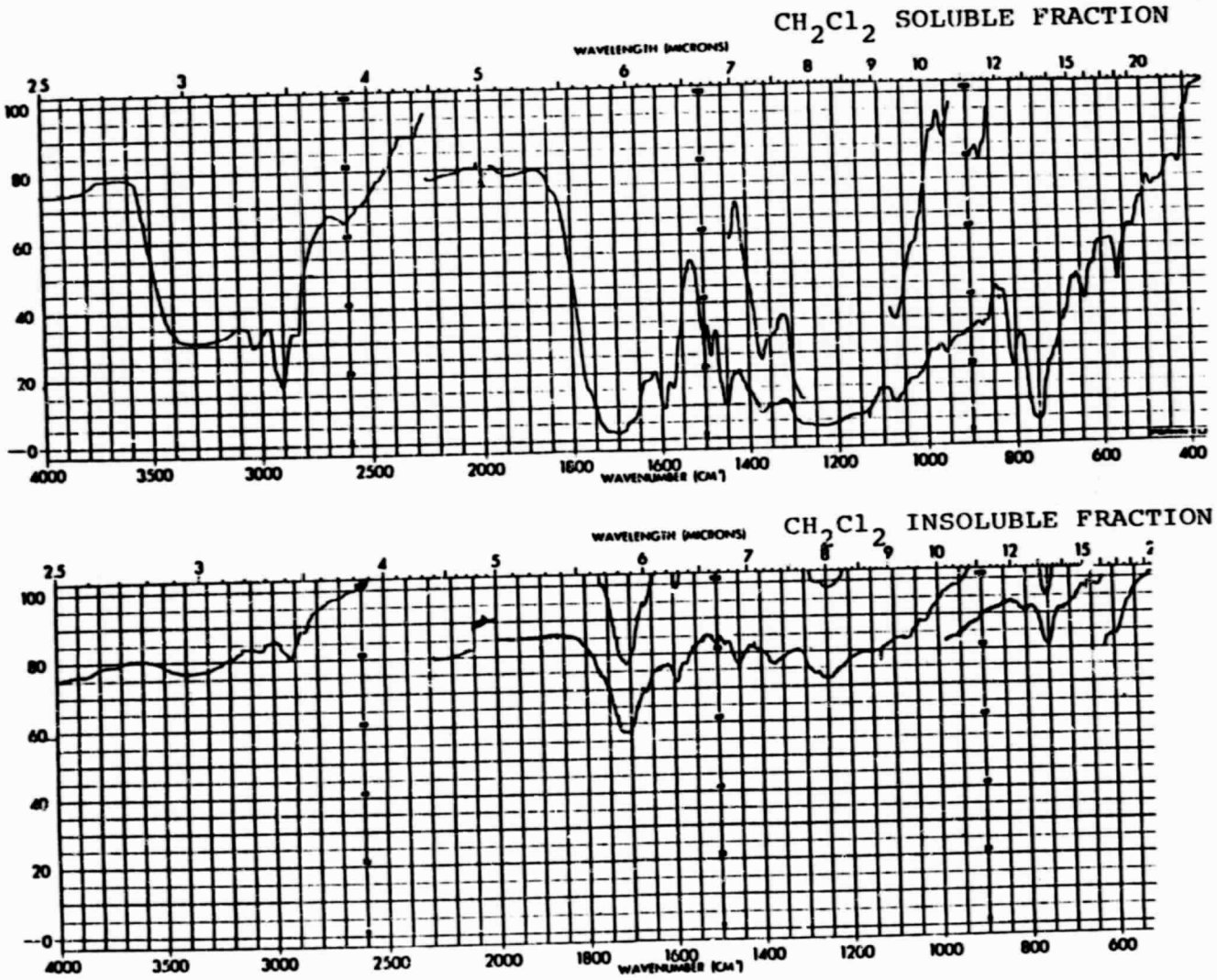

FIGURE 48. MIR SPECTRA - MODEL DEPOSIT FRACTIONS

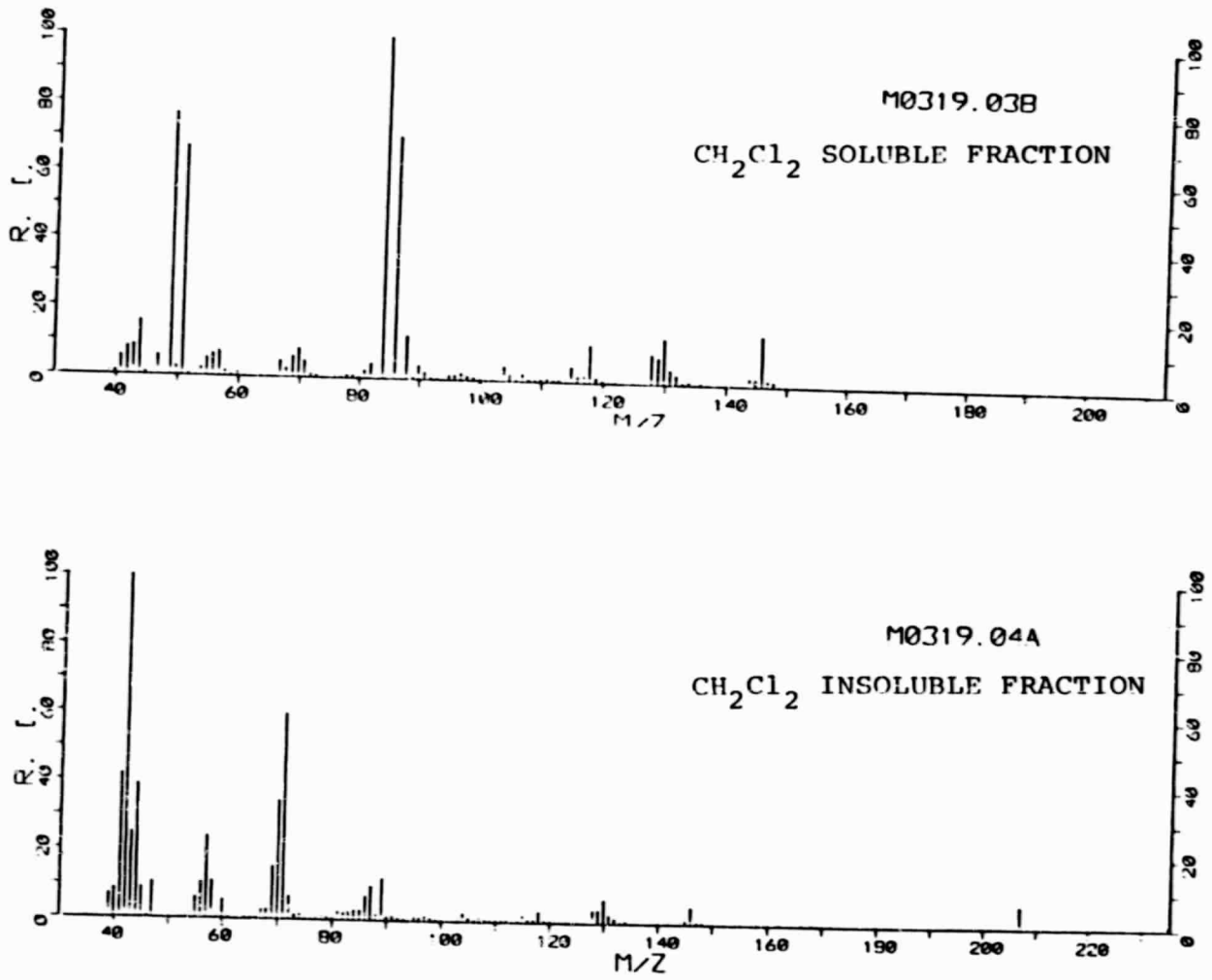

FIGURE 49. py/MS SPECTRA - MODEL DEPOSIT FRACTIONS

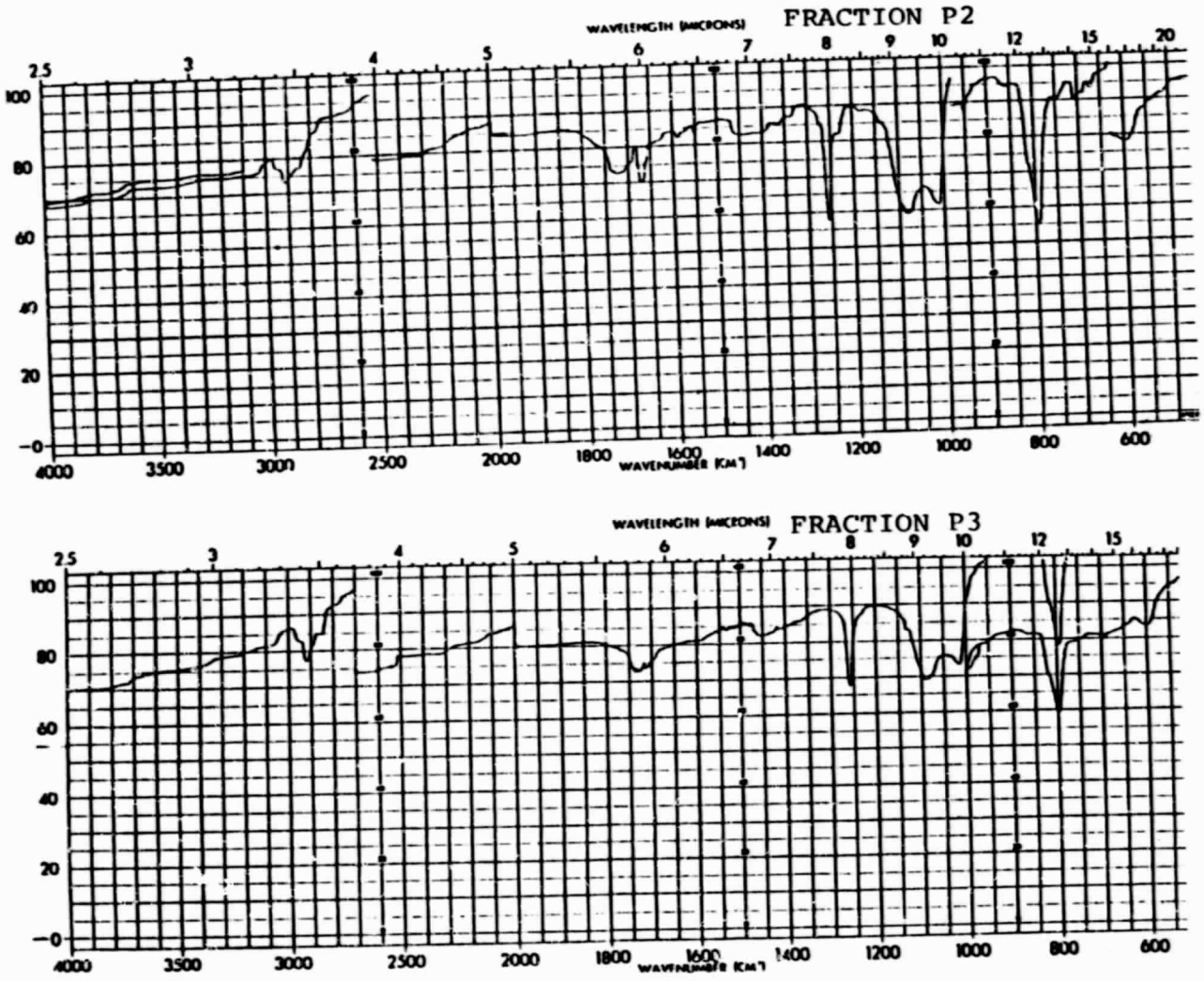

FIGURE 50. MIR SPECTRA - MODEL DEPOSIT HPLC FRACTIONS

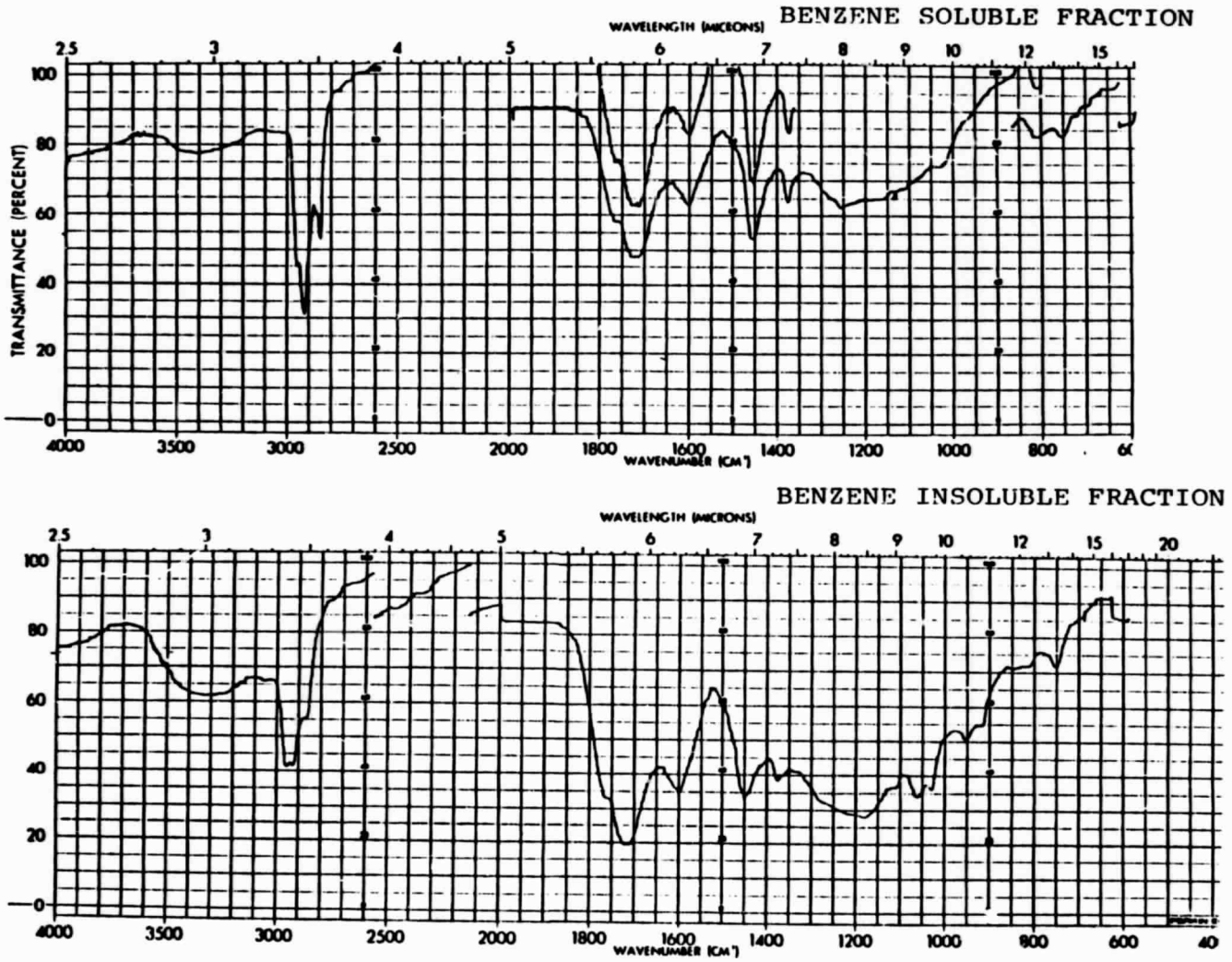

FIGURE 51. MIR SPECTRA - JET A DEPOSIT FRACTIONS

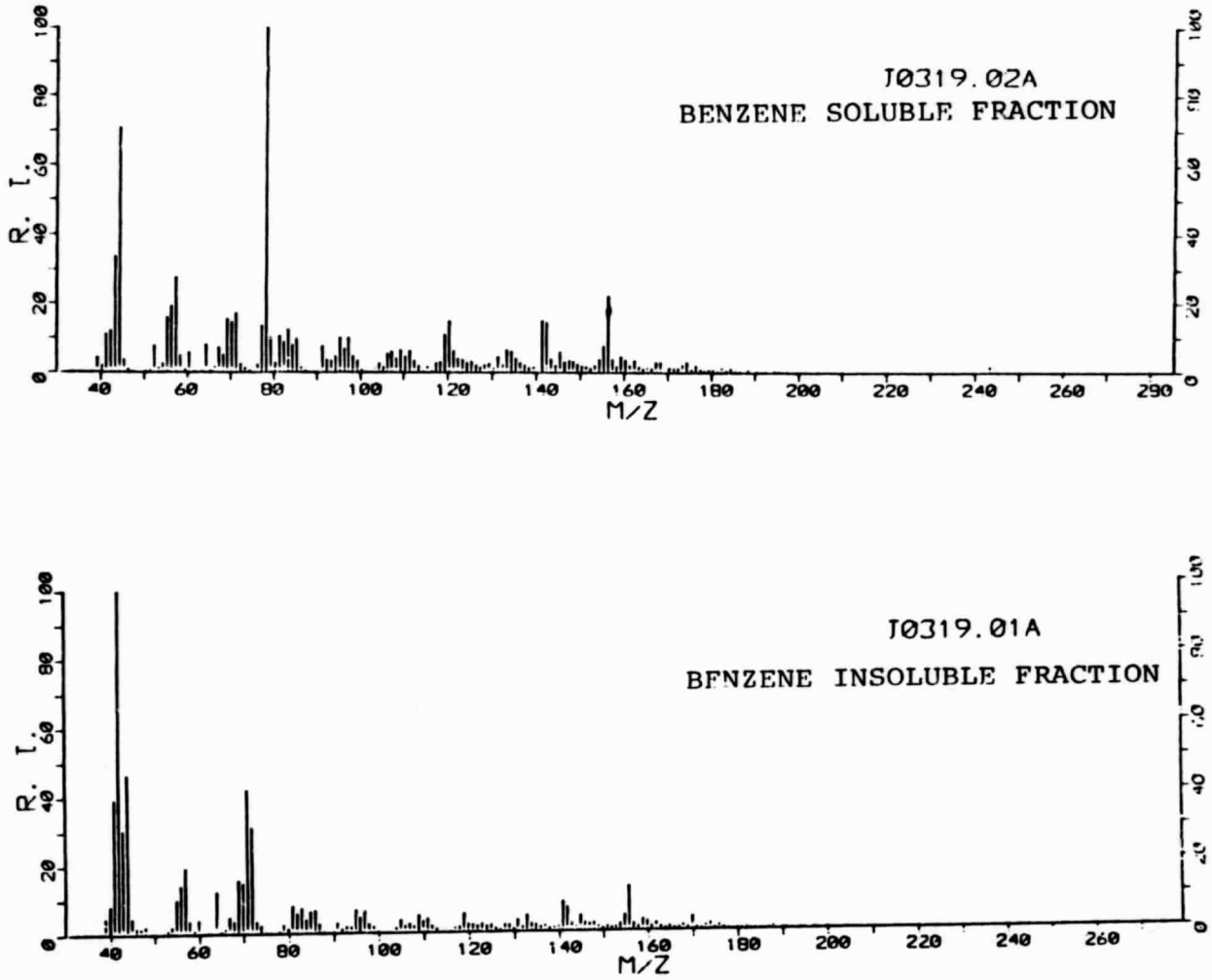

FIGURE 52. py/MS SPECTRA - JET A DEPOSIT FRACTIONS

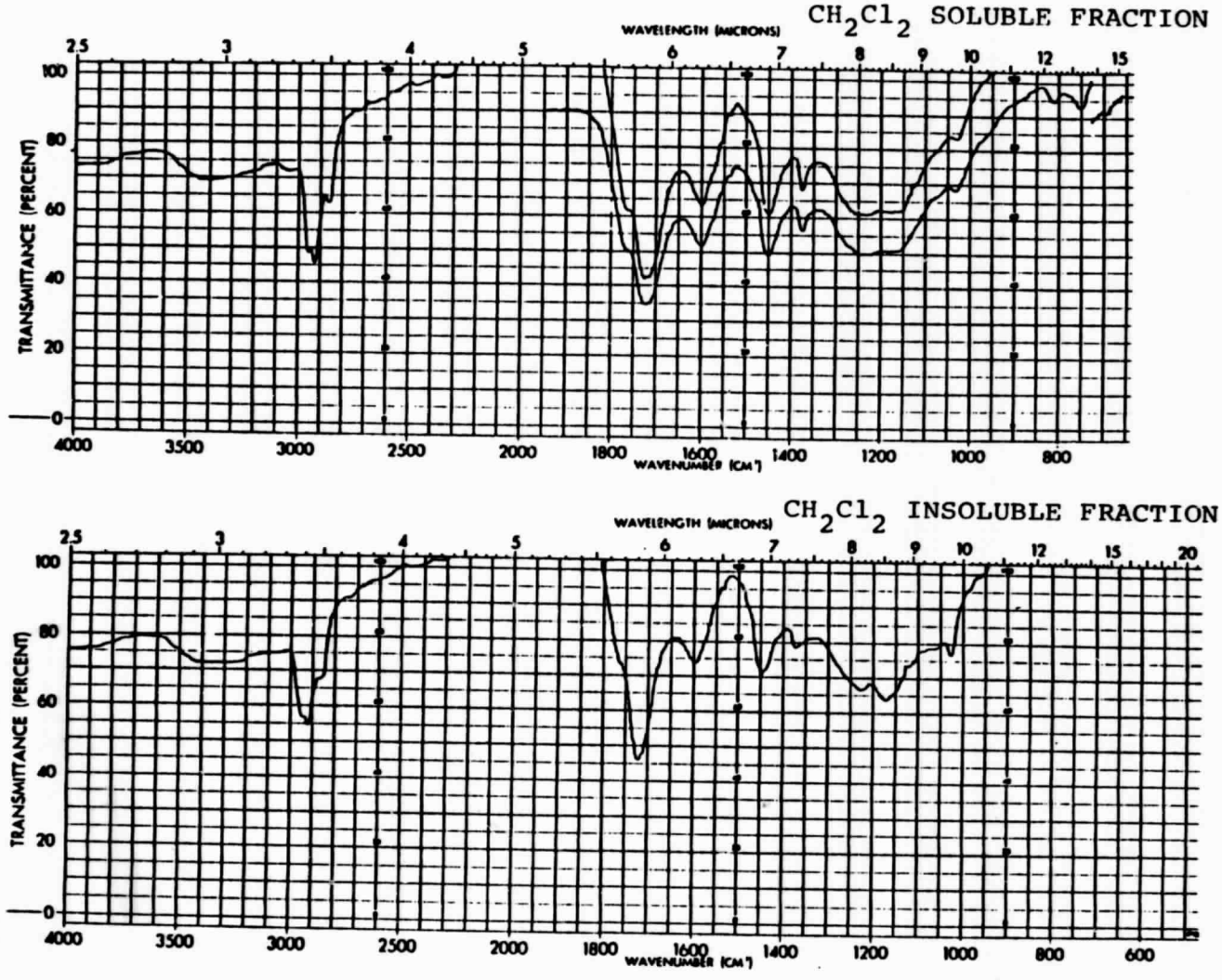

FIGURE 53. MIR SPECTRA - JET A DEPOSIT FRACTIONS

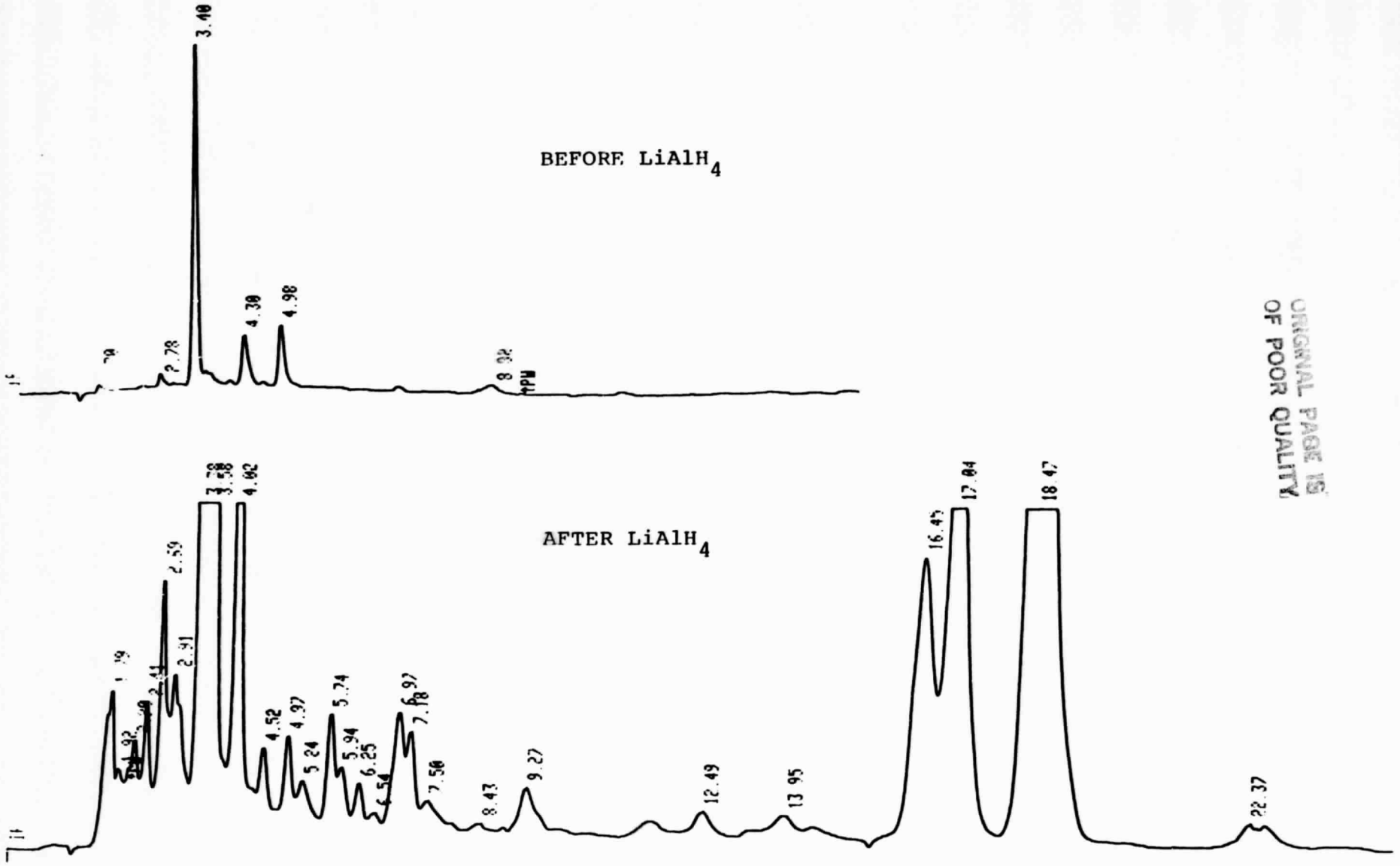

FIGURE 54. HPLC - MODEL DEPOSIT TREATED WITH $LiAlH_4$

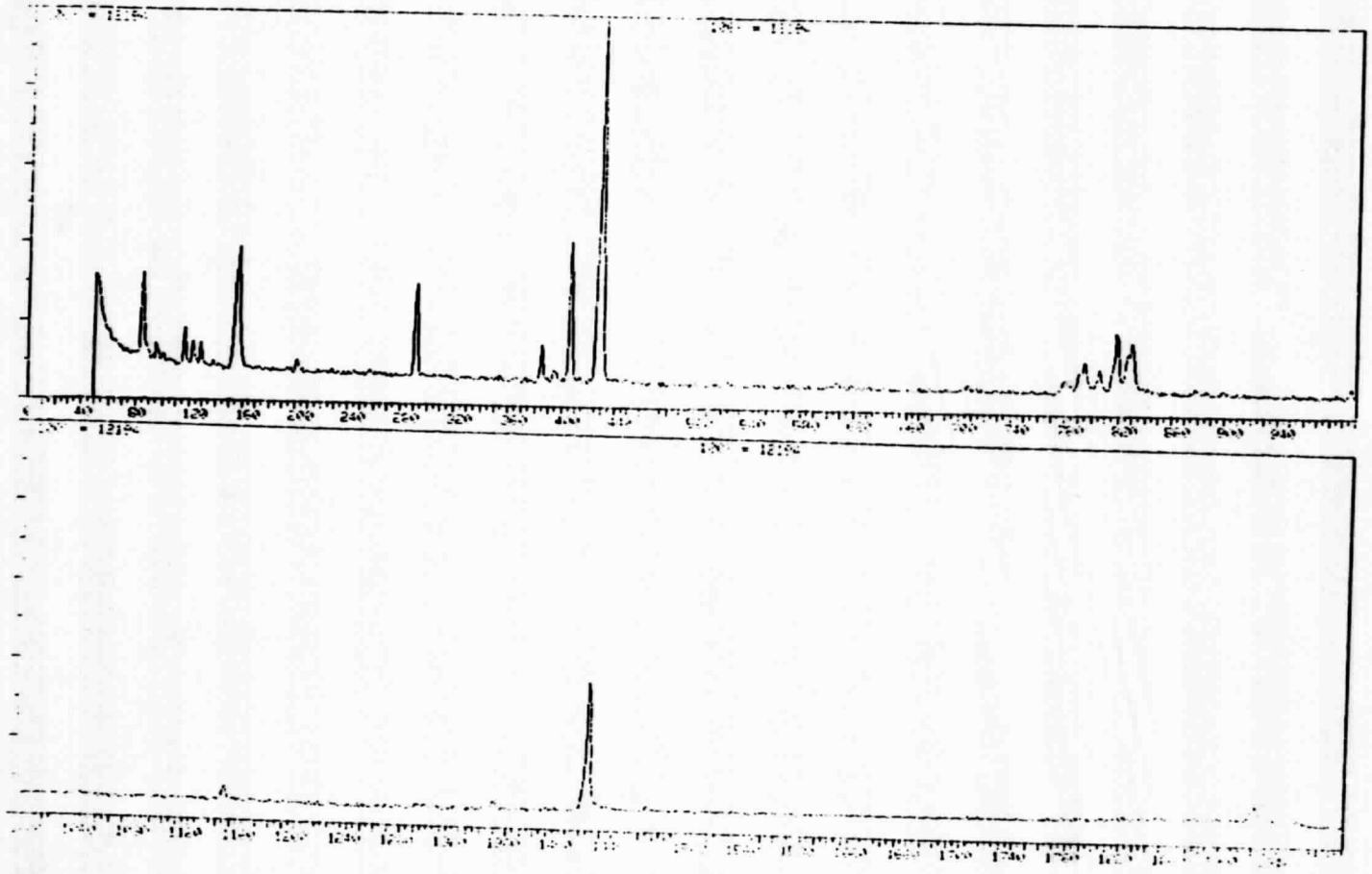

FIGURE 55. TOTAL ION CHROMATOGRAM - $LiAlH_4$ TREATED MODEL DEPOSIT

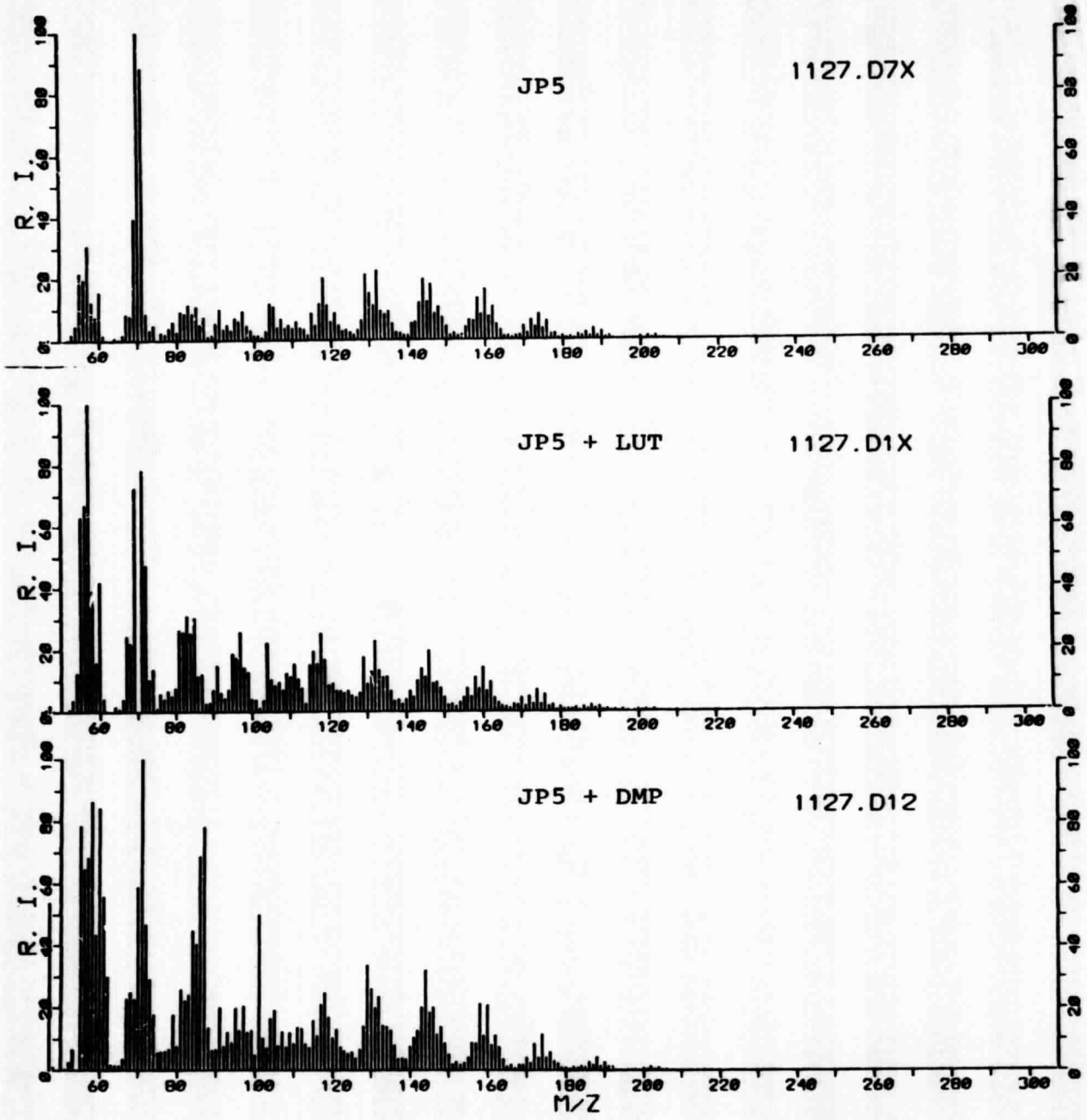

FIGURE 56. py/MS SPECTRA JP5 DEPOSITS

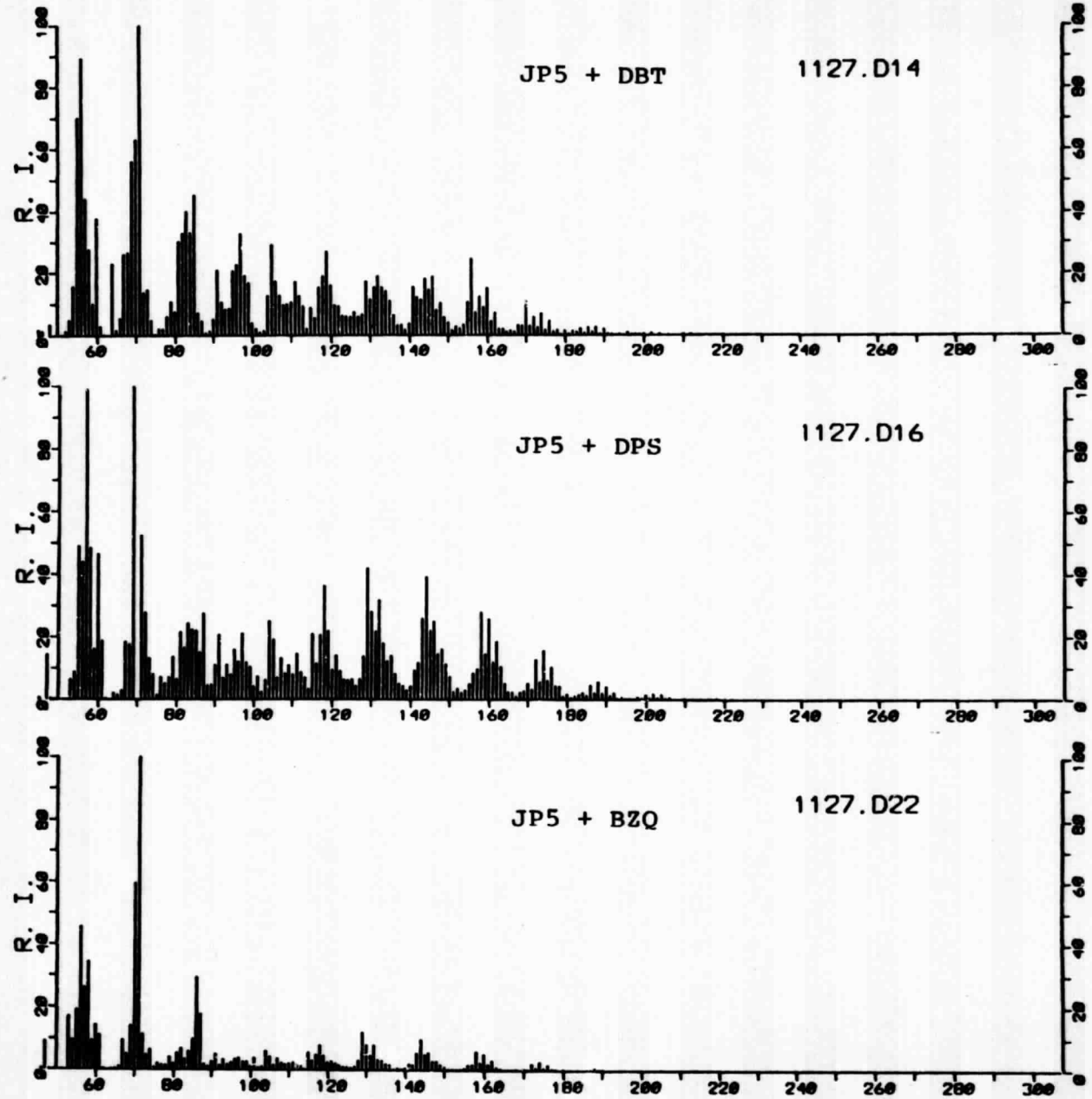

FIGURE 57. py/MS SPECTRA - JP5 DEPOSITS (CON.)